1990

Picosecond Resonance Raman Studies of Solvent Effects on Electron Transfer in Ruthenium-Polypyridine Complexes.

Takahiro Yabe
Louisiana State University and Agricultural & Mechanical College

Order Number 9104183

Picosecond resonance Raman studies of solvent effects on electron transfer in ruthenium-polypyridine complexes

Yabe, Takahiro, Ph.D.

The Louisiana State University and Agricultural and Mechanical Col., 1990

U·M·I
300 N. Zeeb Rd.
Ann Arbor, MI 48106

Picosecond Resonance Raman Studies of Solvent Effects on Electron Transfer in Ruthenium-polypyridine Complexes

A Dissertation
Submitted to the Graduate Faculty of the
Louisiana State University and
Agricultural and Mechanical College
in partial fulfillment of the
requirements for the degree of
Doctor of Philosophy

in

The Department of Chemistry

by
Takahiro Yabe
B.S., Keio University, 1984
M.E., Keio University, 1986
May 1990

ACKNOWLEDGEMENTS

I am very grateful to my advisor, Dr. J.B. Hopkins, for his encouragement, support and training. I also wish to acknowledge the help and encouragement of other members of my research group: Y.J. Chang, D.R. Anderson, L.K. Orman, Xiaobing Xu, Soo-Chang Yu, Robert Lingle Jr., and Dr. C. Veas. Many thanks are in order for Vickie Lyons, Alice Millican and Judith Heintze who typed this manuscript.

TABLE OF CONTENTS

ABSTRACT

Solvent effects in D_3 symmetric ruthenium-polypyridine complexes were studied by using the transient resonance Raman technique. Picosecond laser techniques were used to determine if electron transfer between ligands could be observed in an effort to learn about electron localization in ruthenium-polypyridine complexes. $Ru(bpy)_3^{2+}$ (bpy is 2,2'-bipyridine), $Ru(bpym)_3^{2+}$ (bpym is 2,2'-bipyrimidine), and $Ru(Me_2\text{-}bpy)_3^{2+}$ (Me_2-bpy is 4,4'-dimethyl-2,2'-bipyridine) were investigated in viscous glycerol solution at room temperature and -15°C. The viscosities of glycerol at these temperatures are 1487cP and 66500cP, respectively. It was found that in all three metal complexes investigated the metal-to-ligand-charge-transfer state is already localized on the time scale of less than 30ps in spite of these high viscosities. In addition, it was found that the interligand electron coupling was not strong enough to overcome the vibrational reorganization energy. As a result, delocalization of electron density over all three ligands cannot occur and the solvents do not play a major roll in the MLCT state of those metal complexes. The interpretation of the mechanism responsible for producing this result is presented based on quantum mechanical electron transfer theory. In these metal complexes, it is also known that interligand electron transfer takes place in heteroligand substituted complexes. In order to investigate this kind of interligand electron transfer, $Ru(bym)_2(bpy)^{2+}$ and $Ru(Me_2\text{-}bpy)_2(bpy)^{2+}$ were studied in glycerol and in water at room temperature. It was determined that the former complex has fast interligand electron transfer rate ($k_{ILET} \geq 2 \times 10^{11}$) and the latter

complex has slow interligand electron transfer rate ($k_{ILET} \leq 2 \times 10^6$) in water. By changing the viscosity from 1cP (water at room temperature) to 1487cP (glycerol at room temperature), a solvent dependence of interligand electron transfer was investigated. The result is that in spite of the dramatic change of the viscosity there are no dynamics observed in these metal complexes. These results were interpreted to indicate that interligand electron transfer occurs in the upper electronic states, or singlet metal to ligand charge transfer state.

PREFACE

This dissertation is the result of research I have participated in at John Hopkins' group. Our research is the fruit of our group's efforts, so it is not appropriate to write down all research in my dissertation.(1-7) Therefore I am concentrating on three topics which my contribution was the greatest.

Chapter I discusses about localized and delocalized problem in ruthenium-polypyridine complexes. Then in Chapter II and III interligand electron transfer is discussed in mixed ligand complexes.

REFERENCES

1. Y.J. Chang, L.K. Orman, D.R. Anderson, T. Yabe, and J.B. Hopkins, J. Chem. Phys., 87,3249, 1987
2. L.K. Orman, Y.J. Chang, D.R. Anderson, T. Yabe, X. Xu, S. Yu, and J.B. Hopkins, J. Chem. Phys., 90, 1496, 1989
3. T. Yabe, D.R. Anderson, L.K. Orman, Y.J. Chang, and J.B. Hopkins, J. Phys. Chem., 93, 2302, 1989
4. Y.J. Chang, X. Xu, T. Yabe, S. Yu, D.R. Anderson, L.K. Orman, and J.B. Hopkins, J. Phys. Chem., 94, 729, 1990
5. L.K. Orman, D.R. Anderson, T. Yabe, and J.B. Hopklins, Advances in Chemistry Series No. 226, In Press.
6. T. Yabe, L.K. Orman, D.R. Anderson, and J.B. Hopkins, Submitted to J. Phys. Chem., January 1990.
7. T. Yabe, D.R. Anderson, L.K. Orman, and J.B. Hopkins, To be submitted to Chem. Phys. Lett.

INTRODUCTION

There have been intensive studies in polypyridine complexes of ruthenium and other transition metals (1-5). Ruthenium (II)-polypyridine complexes as shown in Figure 1 have been given special attention for their unusual excited state properties and the potential utility of this complex in solar energy conversion schemes.

For bimolecular reactions, only excited states living longer than $\sim 10^{-9}$s may have a chance to encounter other solute molecules. This estimate is based on simple kinetic arguments since typical diffusion controlled reactions have rate constants in solution on the order of $\sim 10^{9} M^{-1}s^{-1}$. For transition metal complexes like Ru-polypyridine complexes, only the lowest triplet excited state has a lifetime comparable to diffusion time scale. The key to the utility of $Ru(bpy)_3^{2+}$ and its analogues in bimolecular photochemically initiated reactions is the existence of the lowest emitting excited states that are reasonably stable to decomposition.

The energy positions of the metal centered (MC), metal-to-ligand charge transfer (MLCT), and ligand centered (LC) excited states as shown in Figure 2 depend on the ligand field strength, the redox properties of metal and ligands, and intrinsic properties of the ligands, respectively. Thus, in a series of complexes of the same metal ion the energy ordering of the various excited state, and particularly the orbital nature of the lowest excited state can be controlled by a judicious choices of the ligands. In this way it is possible to design complexes having the desired properties. Most Ru(II)-polypyridine

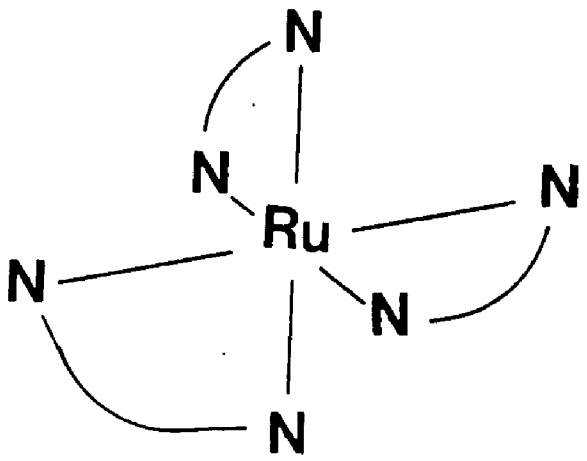

Figure 1. Ruthenium-polypyridine complexes.

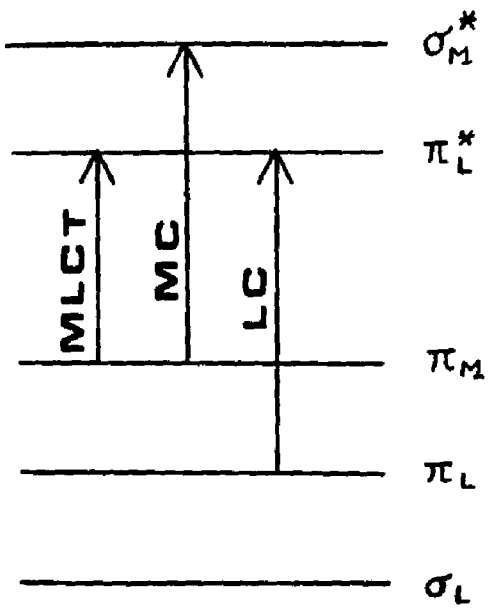

Figure 2. Schematic energy levels.

complexes undergo relatively slow radiationless transitions and thus exhibit long lifetime and intense luminescence emission. These complexes are therefore ideal for these studies.

The literature on $Ru(bpy)_3^{2+}$ photochemistry is quite extensive. No attempt to review it will be made except to point out the features relevant to this discussion. Many of these Ru(II)-polypyridine complexes exhibit strong metal-to-ligand charge transfer (MLCT) absorptions in the 350nm to 550nm region of spectrum. One of the photochemical aspects which has been intensively studied is the fate of the electron following photoexcitation into the MLCT band. For example, $Ru(bpy)_3^{2+}$ has D_3 symmetry. Therefore, the transferred charge can be either delocalized over all three ligands or localized on a single ligand. It is thought that the electron localization process is primarily driven by perturbations such as vibrational distortions and solvent trapping. Metal complexes of this type can therefore be used as excellent models to test electron transfer theory.

Electron localized orbital was suggested by DeArmond et al. from emission studies(6-9). The emission spectra of $Ru(bpy)(py)_4^{2+}$ and $Ru(bpy)_2(py)_2^{2+}$ were nearly identical with those of $Ru(bpy)_3^{2+}$, where bpy is 2,2'-bipyridine and py is pyridine. Moreover localization was observed at 77K. The direct proof for localized orbital was shown by Woodruff et al. by using the nanosecond excited state resonance Raman spectra in 1979 (10). They found out that the vibrational spectra observed necessitated the existence of bpy and bpy^- ligands for their emitting state on the nanosecond time scale. This result is consistent with a localized orbital description of the emitting state species. In this

experiment, excited state frequencies of the $Ru(bpy)_3^{2+}$ MLCT state were compared to ground state frequencies of $Li^+(bpy^-)$, where the electron must be localized on a single ligand in the latter. The similarity of vibrational frequencies observed in the two cases leads to the conclusion that the excited triplet MLCT state of $Ru(bpy)_3^{2+}$ was representative of the charge localized species (bpy^-). Further resonance Raman experiments were performed on the series of Os $(bpy)_n(X)_{3-n}$ where n=3,2,1 and x=$Ph_2PCH=CHPPh_2$. If the electron was delocalized in the MLCT state, the Raman spectrum of $Os(bpy^{-1/3})_3$ should be radically different from the spectrum of $Os(bpy^-)$ $(X)_2$ where the electron is forced to be localized by the asymmetry of the molecule (11). The vibrational frequencies observed showed an invariance to ligand substitution demonstrating that the electron was indeed localized in all complexes including $Ru(bpy)_3^{2+}$. Thus $[Ru(bpy^-)(bpy)_2^{2+}]^*$ is the best description of this excited state.

Some spectroscopic data for dilute and pure single crystals indicates that absorption spectra are best classified within the D_3 symmetry, or delocalized (12-15). The reason for this discrepancy is that absorption spectra monitor singlet MLCT state while resonance Raman and emission spectra monitors triplet MLCT state, or lowest excited state.

In order to develop a full understanding of the nature of the MLCT states it is important to ask whether the apparent localized states are intrinsic to the molecule or induced by an inter or intra molecular perturbation. This problem has been considered theoretically resulting in models of both intrinsically localized and

delocalized configurations. Experimentally, there is evidence from time resolved luminescence and Raman experiments in low temperature glasses that the $Ru(bpy)_3^{2+}$ MLCT states may be initially delocalized (12-15). In the glass, solvent motions can be slowed down to permit more conventional methods of probing the MLCT state prior to solvent reorganization. If the solvent trapping is the major pathway leading from a delocalized to a localized configuration, it should be possible to observe the inter-conversion process in the low temperature glass. It is important to avoid the significant changes of the ground state vibrational populations, because extremely low temperature changes the Boltzmann population in the ground state. A glycerol solvent was chosen since the melting point is 20°C and it is easy to control the viscosity around room temperature.

We have investigated this problem by using picosecond resonance Raman spectroscopy and attempted to clarify and quantify some questions like how electron localizes or how solvent motion acts in localization process. The short time solvent effects on electron transfer for a series of related complexes have been investigated by varying the viscosity of the solvent. Also, the interligand electron transfer (ILET) in tris ligand complexes and mixed ligand complexes has been investigated in terms of tunneling effects.

EXPERIMENTAL

A mode-locked Quantronix 416 cw NdYAG laser generates a 100 MHz train of picosecond pulses (16-17). This beam is coupled into a polarization preserving single mode fiber optics with an 8mm core. Pulse compression occurs in the fiber due to self phase modulation. This chirped pulse has an 80ps linewidth with $2cm^{-1}$ frequency bandwidth. For amplification, the chirped pulse from the fiber is injected into a Quantronix 416 cw NdYAG laser as shown in Figure 3. Electrooptic modulation controls the number of round trips in the regenerative amplifier and also serves to switch out the amplified pulse. Since the system is designed around a cw laser high repetition rates of 1-2kHz can be generated. By controlling the magnitude of the frequency chirp the pulse width can be changed between 10ps to 150ps. A 10ps pulse can be achieved with the addition of grating compression. The pulse width was checked by use of autocorrelator and streak camera (IMACON 500). Pulse energies were limited to between 10 μJ/pulse and 20μJ/pulse at 354.7nm by using an NRC laser power attenuator in a 30ps pulse width. In this way, high average laser powers could be provided at the sample leading to relatively large concentrations of excited state species for interrogation using resonance Raman spectroscopy. Since the viscosity of glycerol is too high to flow the solution, a spinning cell was made of aluminum and quartz tube as specified in Figure 5. This was used under conditions which guaranteed that each laser pulse interrogated a fresh region of sample. In this way local heating of sample and products from

photochemistry can be avoided. This cell was hard to align because of the curvature of the quartz tube. A different kind of cell called rotating cell was designed from aluminum and a quartz window as shown in Figure 6. This cell proved to be a superior optical design if care was taken to rotate the cell using precision ball bearings.

Raman scattering from the sample was picked up at f1.0 and expanded into f7.8 where the image was focused onto the slits of a double 1 meter Instruments SA monochromator. The Raman scattering geometry was close to the back scattering configurations. The detection system consisted of a Hamamatsu R943-02 photomultiplier tube and gated integration (LeCroy 2249SG). Information from every laser pulse (Raman signal and laser power) was separately analyzed by a DEC LSI 11-73 computer system. The laser power is measured using a photodiode. Fluctuations in energy by more than 20% cause the data for that pulse to be discarded. Long term fluctuations are averaged out by recording the spectrum as a series of spectra obtained in rapid succession. The spectra are then added together by the computer.

In all of the experiments for solvent effects, the transient Raman spectra were generated by one color excitation at 354.7nm as shown in Figure 4. Part of the laser pulse excites electrons in the ground state to the MLCT state while the rest of the pulse scatters from the transient MLCT state. The components studied here were carefully chosen to have a transient absorption at 354.7nm in order to utilize resonance Raman signal enhancement. The spectra observed correspond to the characteristics of the transient MLCT state time averaged over the duration of the laser pulse width.

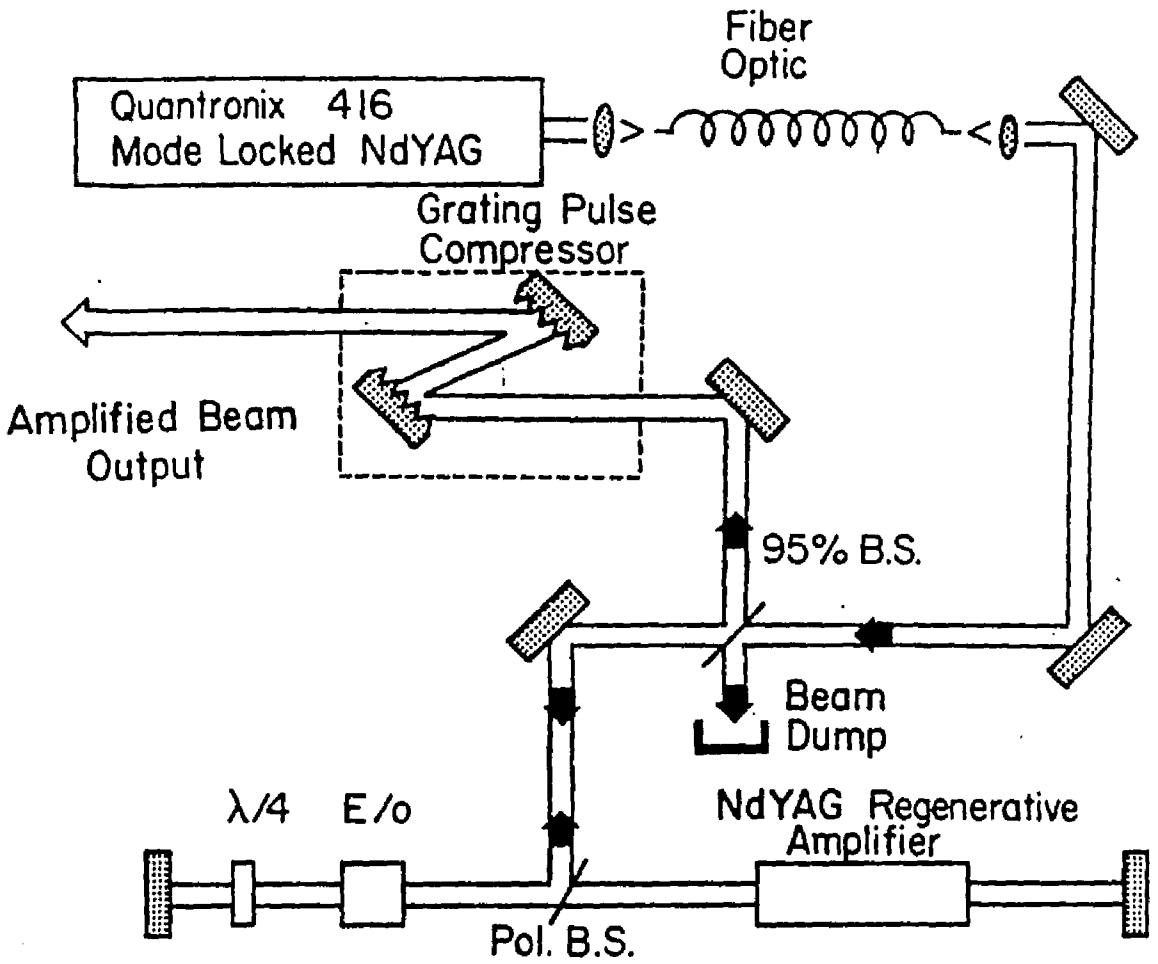

Figure 3. Schematic diagram of 1kHz picosecond laser system.

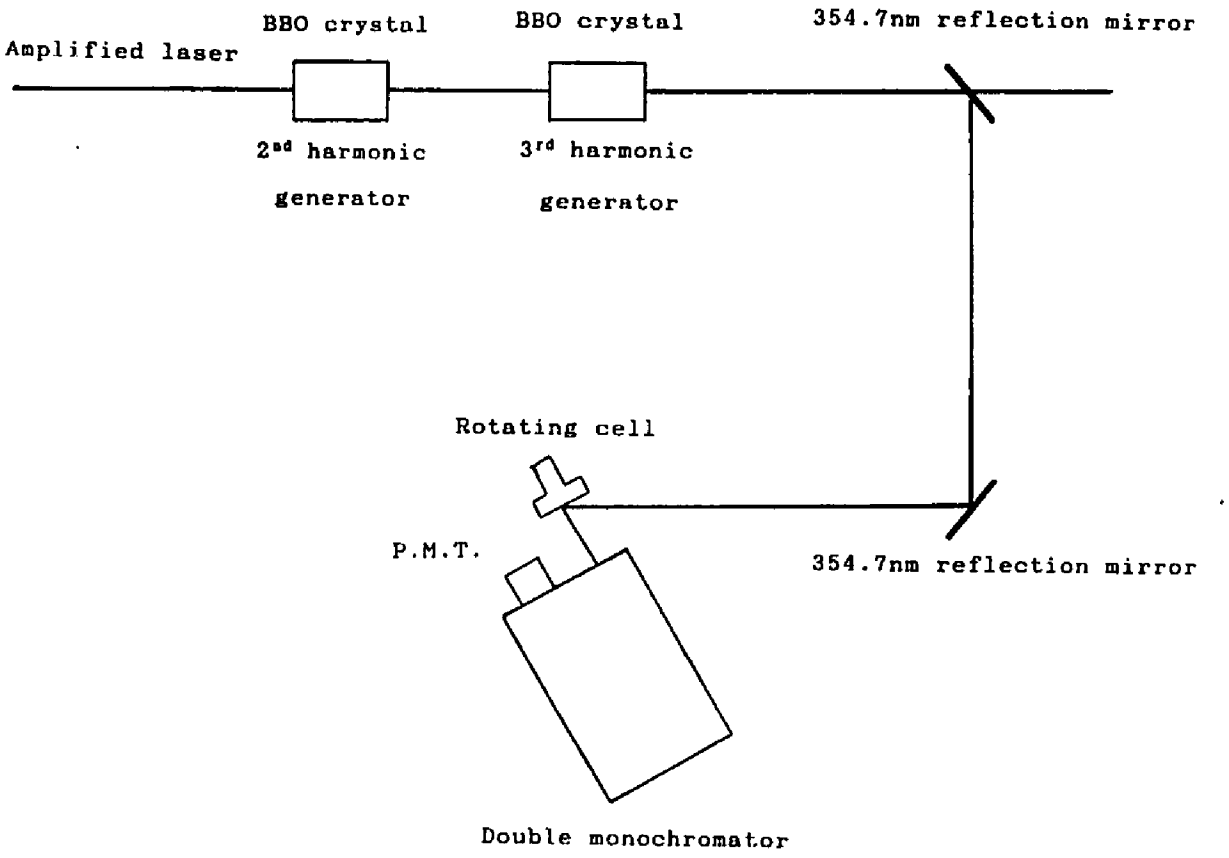

Figure 4. Schematic diagram of excited state resonance Raman experimental apparatus.

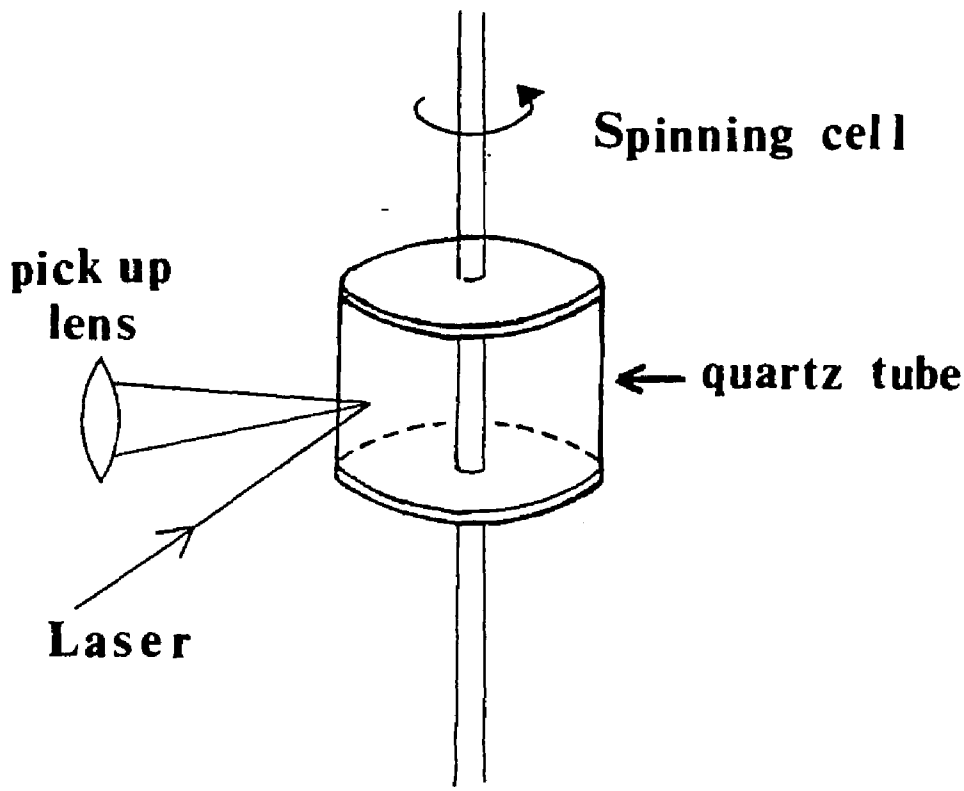

Figure 5. Schematic diagram of spinning cell.

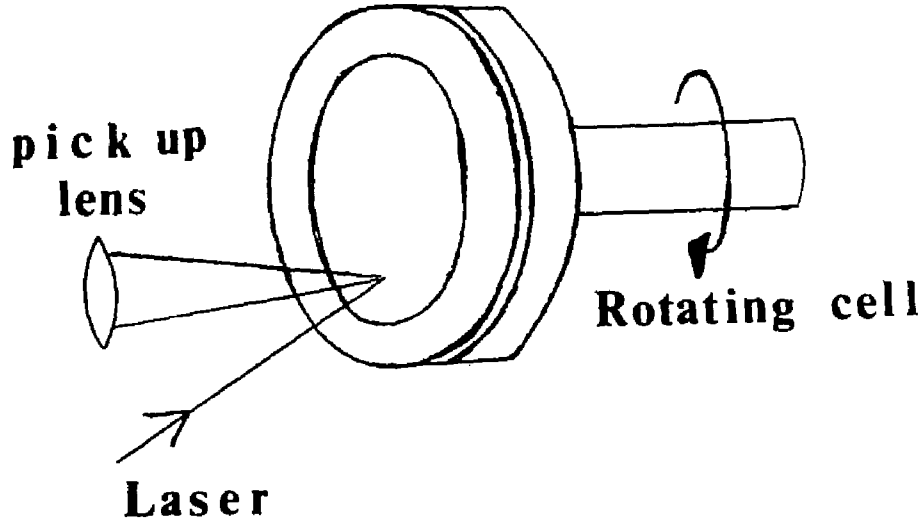

Figure 6. Schematic diagram of rotating cell.

Raman spectra measured over the entire wavelength range of interest were typically generated in a single 10 minute scan. A series of spectra were added together to improve the signal to noise ratio. Accurate Raman band positions were calibrated from the complete Raman spectra which contained a peak from the attenuated Rayleigh line. The sample was cooled by spraying a stream of liquid nitrogen onto the back of the sample cell. Constant temperature was maintained by simultaneously heating the sample with warm air to achieve the desired equilibrium.

$Ru(bpym)_3^{2+}$ was prepared as a chloride salt by modification of a previously published technique (18-19). $Ru(bpy)_3^{2+}$ was purchased from Alpha Products and used as received. $Ru(Me_2\text{-}bpy)_3^{2+}$, was also synthesized as a chloride salt by previous published methods (20-21). All synthesized compounds were purified by repeated recrystalization and chromatography on a Sephadex LH-20 column (Sigma Chemical). Chemical analysis was performed by mass spectroscopic analysis. Glycerol (analytical reagent) was purchased from Mallinckrodt and used as received.

PREPARATION OF COMPOUNDS

Abbreviation

bpy: 2,2'-bipyridine

bpym: 2,2'-bipyrimidine

Me_2-bpy: 4,4'-dimethyl-2,2'-bipyridine

Synthesis of $Ru(bpym)_3$nd $Ru(Me_2\text{-}bpy)_3Cl_2$ (18-21) All tris ligand complexes were prepared by refluxing $RuCl_3xH_2O$ (Aldrich Chemical) or $RuCl_3$ (Sigma Chemical) with five fold excess amount of the desired ligand, bpym (Alfa Products) or Me_2-bpy (Aldrich Chemical), in 2:1 ethanol: water solvent for several hours under the nitrogen atmosphere until the solution changed to reddish solution. This solution was filterated to remove the excess ligand. Then the solution was diluted with ethanol and the solvent was evaporated under reduced pressure. After evaporation, the reddish solid was washed with toluene to remove the excess ligand. The complexes were purified by column chromatography on Sephadex LH-20 (Sigma chemical) by using ethanol as eluent. A small amount of complex was dissolved in a minimum amount of ethanol and loaded into a 1.5 cm x 30 cm column. The bright orange fraction was collected and dried in a desiccator.

Synthesis of $Ru(bpy)Cl_3$(22) 2.103g(1.0mmol) of $RuCl_3xH_2O$ was dissolved in 10.2ml of 1N HCl and then 1.541g(1.0mmol) of bpy was added. This solution was set aside under a nitrogen atmosphere for four days. It was filterated and washed with water. The product was a black powder.

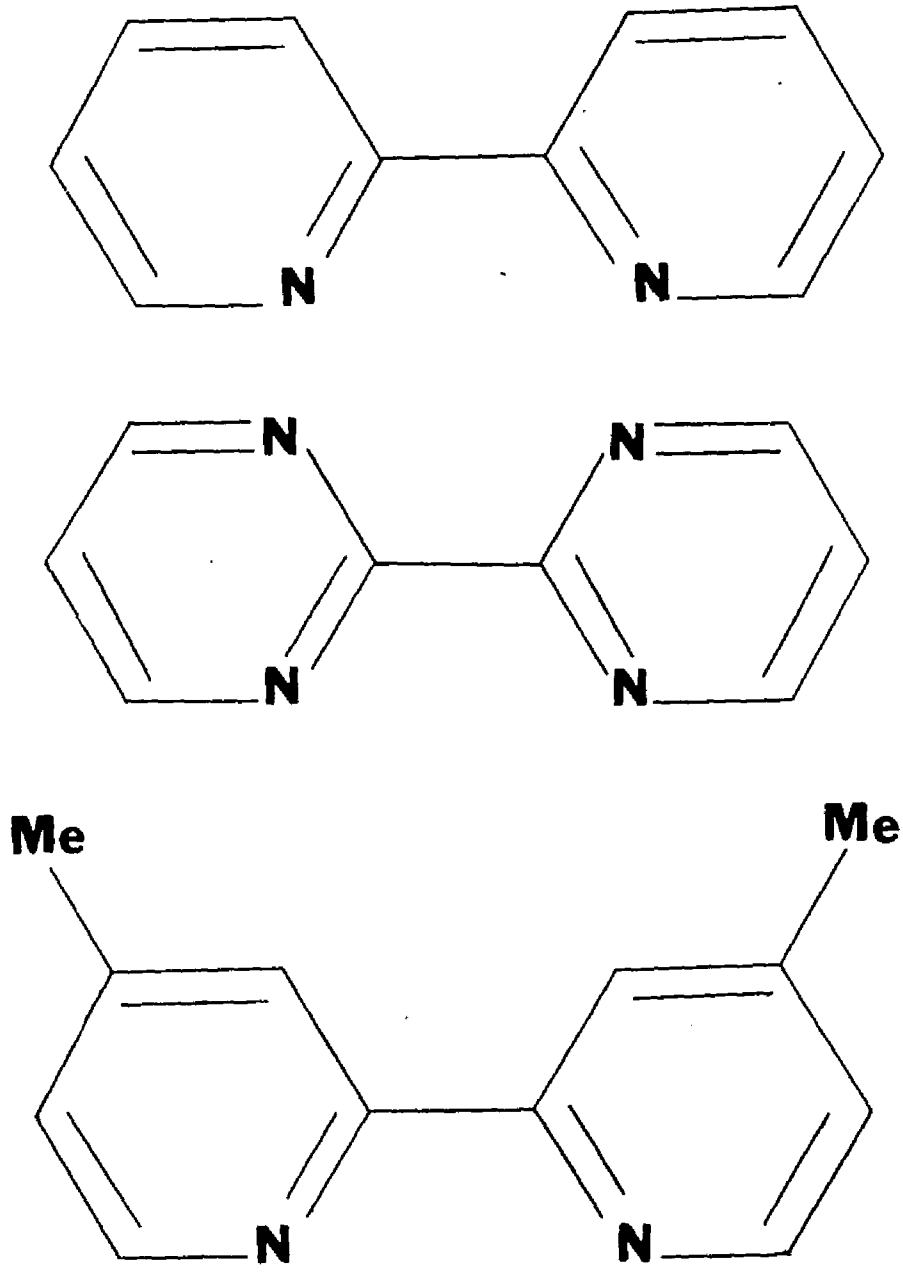

Figure 7. From the top, 2,2'-bipyridine, 2,2'-bipyrimidine, and 4,4'-dimethyl-2,2'-bipyridine.

Synthesis of $Ru(bpym)_2Cl_2 \cdot H_2O$ and $Ru(Me_2\text{-}bpy)_2Cl_2 \cdot H_2O$(23) $RuCl_3$(7.6 mmol), Me_2-bpy(16.3mmol), and LiCl (1.0mmol) were refluxed for 8 hours under nitrogen in 20 ml of dimethylformamide. After the reflux 100 ml of acetone was added. The solution was then refrigerated for several hours. The product was precipitated as fine red black crystals. The crystals were washed with ice cold water and then with cold ethyl acetate. The preparation for the $Ru(bpym)_2Cl_2 \cdot H_2O$ is similar.

Synthesis of $Ru(bpym)_2(bpy)Cl_2$ and $Ru(Me_2\text{-}bpy)_2(bpy)Cl_2$ (23-24) The method is outlined for the preparation of $Ru(bpy)_2(bpym)\ Cl_2$. $Ru(bpy)_2Cl_2$ (Strem Chemicals) and five fold excess amount of bpym ligand were refluxed overnight in 2:1 ethanol:water solvent. The solution was filterated and diluted with ethanol. After the solvent was evaporated under low pressure, the red product was washed with toluene. The product was purified by column chromatography. The same procedure can be used when starting with $Ru(bpy)Cl_3$ and bpym. Either method may be used to prepare $Ru(bpym)_2(bpy)\ Cl_2$ and $Ru(Me_2\text{-}bpy)_2(bpy)\ Cl_2$.

CONCEPTS OF RESONANCE RAMAN

When monochromatic radiation of wavenumber ν_o is incident on gases, liquids, or solids, most of the incident light is transmitted without change, but some scattering of the radiation occurs (25-27). The scattered radiation contains not only incident wavenumber ν_o but also the wavenumbers of the type $\nu' = \nu_o \pm \nu_m$. These new shifted wavenumbers are called Raman lines, or bands. Raman bands at higher energy than the Rayleigh line are called anti-Stokes bands, and those at lower energy than the Rayleigh line are called Stokes bands. In general, the intensity of Rayleigh scattering is about 10^{-3} of the intensity of the incident light and the intensity of strong Raman bands is about 10^{-3} of the intensity of Rayleigh scattering.

The normal Raman effect is produced when the intermediate state is far below the excited electronic state. When the excitation wavenumber is tuned within the absorption continuum, the intensity of the Raman vibrational modes, corresponding to the excited chromophore in the molecule, can be enhanced by several orders of magnitude. This effect is called the resonance Raman effect. Normal Raman scattering is a weak effect, so it is often desirable to increase the sensitivity by using resonance Raman enhancement. Resonance Raman can be performed all the way down to low concentrations on the order of 10^{-7}M.

THEORY OF ELECTRON TRANSFER

Photoinduced electron transfer reactions in condensed phase is one of the most important processes in basic photochemistry. Understanding of the mechanism and dynamics is very important not only in photochemistry but also photobiological reactions - photosynthesis, and development of photo functional materials. In general, electron transfer rate is controlled by the following factors(29).

1. Magnitude of electron interactions between donor and acceptor
2. Energy gap between initial state and final state.
3. Reorganization energy of surrounding solvents of donor and acceptor.
4. Interaction between solvent and donor or between solvent and acceptor.

Schematic diagram of electron transfer in the weak interaction case is shown in Figure 8. In normal region, rate is getting faster as $-\Delta G^{\circ}$ increases. Maximum rate is obtained at the point where potential intersects bottom of the potential. Then after this point rate is getting slower as $-\Delta G^{\circ}$ increases in inverted region. Excited state electron transfer (ET) theory in the metal complexes has been reviewed in the literature.(30-37) So this will be the summary of the ET theory to predict ET rate law. In general, the ET rate constant k_{et} is equals to $\nu_n \kappa_{el} \kappa_n$ where ν_n is a nuclear frequency, κ_{el} is an electronic factor and κ_n is a nuclear factor. Classically the frequency of the vibration which destroys the activated complex corresponds to a nuclear frequency ν_n. The electronic term is given by

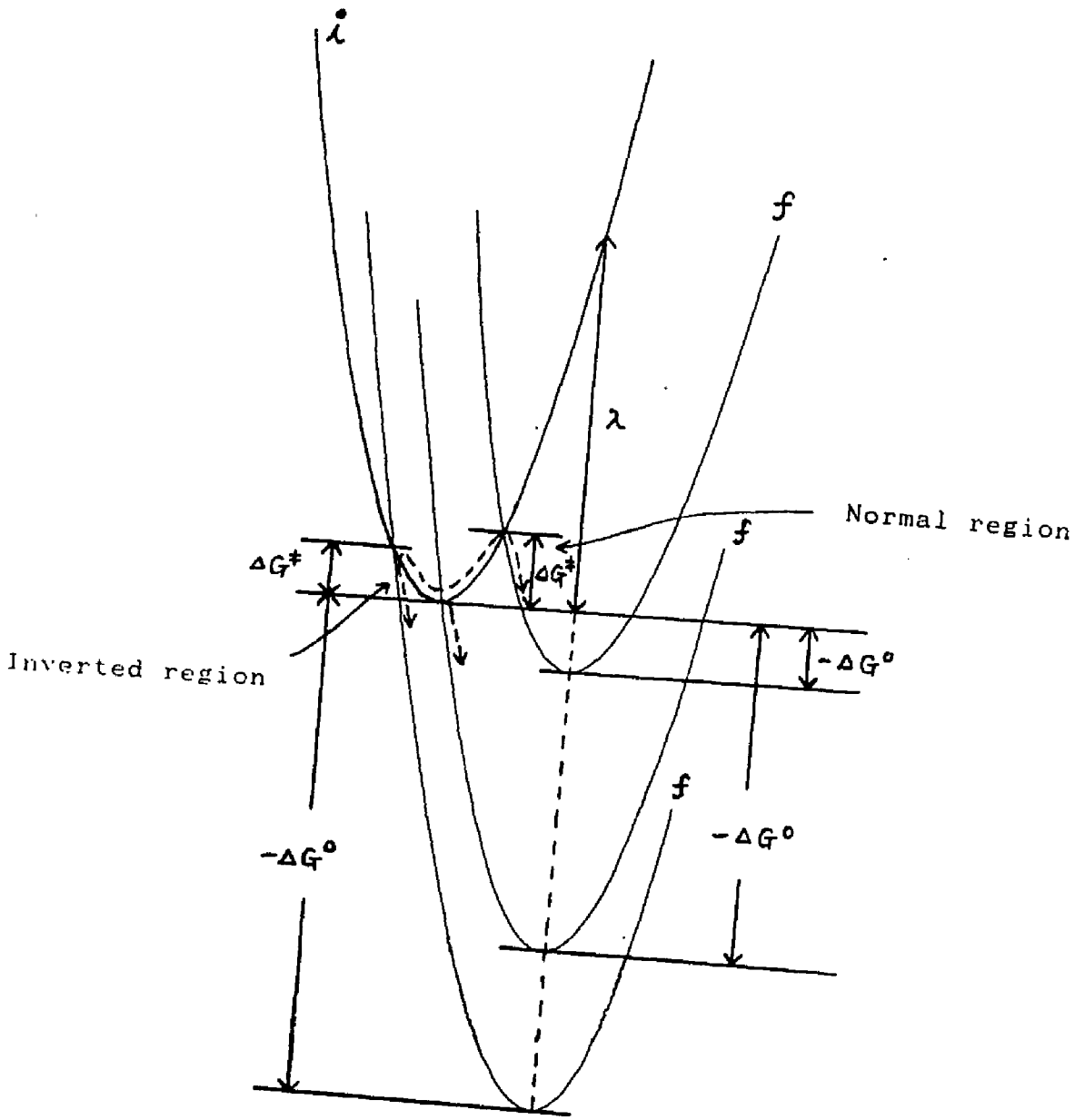

Figure 8. Schematic potential for electron transfer.

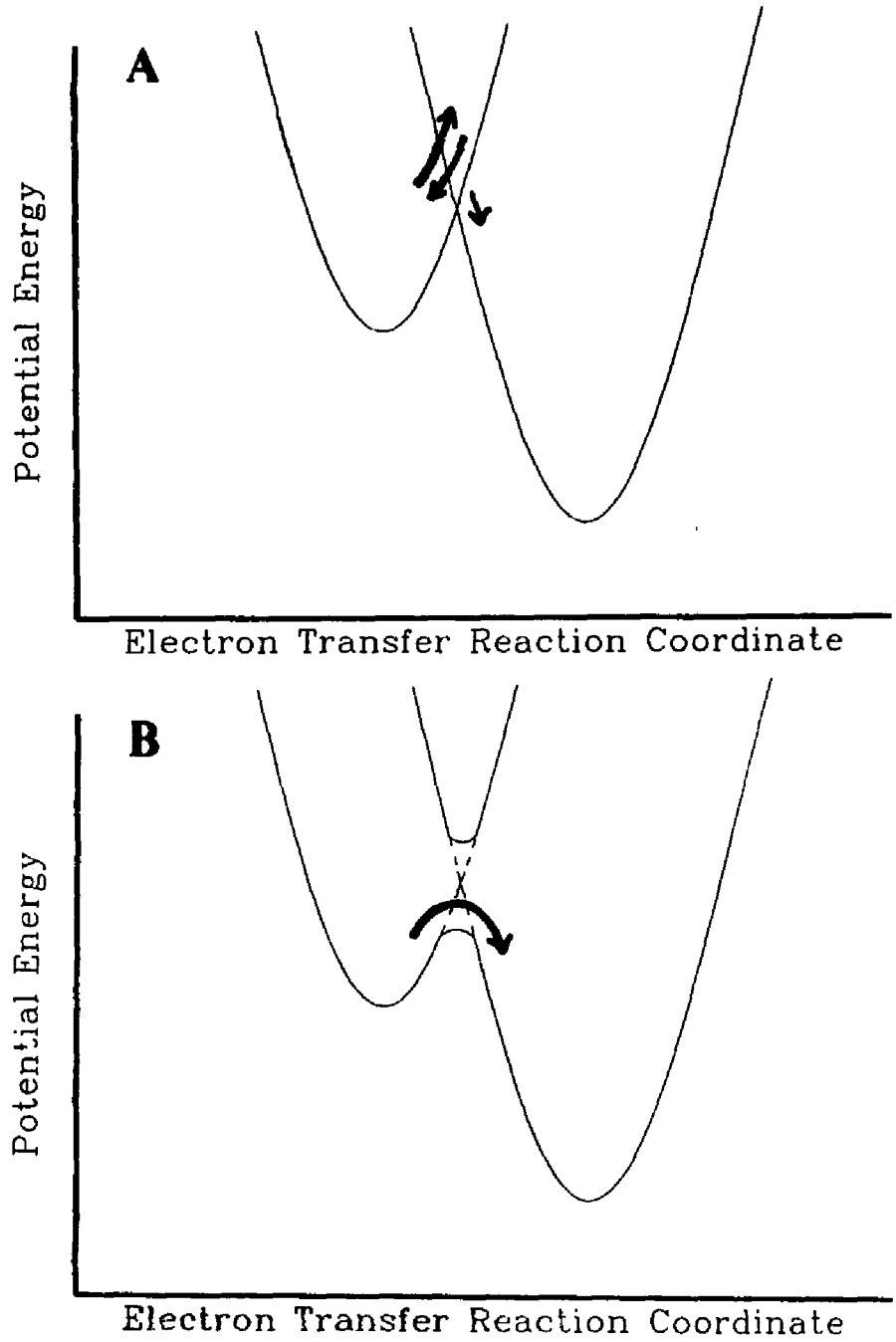

Figure 9. (A) Weak interaction. (B) Strong interaction.

$$\kappa_{el} = \frac{2[1-\exp\{-\nu_{el}/2\nu_v\}]}{2-\exp\{-\nu_{el/2}\nu_n\}}$$

where

$$\nu_{el} = \frac{2H_{ab}^2}{h}\left[\frac{\pi^3}{E_\lambda RT}\right]^{1/2}$$

E_λ is the reorganization energy which is a sum of the energies required for the solvent and vibrational coordinates to adjust the product configuration of the reaction. There are two limits to κ_{el}.
Case. 1: Adiabatic or the high coupling limit where $\nu_{el} >> 2\nu_n$ in this case $\kappa_{el} = 1$ and $k_{et} = \nu_n\kappa_n$. The electronic coupling H_{ab}^2 between ligands is large in comparison to the reorganization free energy E_λ. In this limit the reaction coordinate follows an adiabatic pathway.
Case 2: Nonadiabatic or the low coupling limit where $\nu_{el} << 2\nu_n$ in this case $k_{el}<<1$. The electronic coupling H_{ab}^2 is small. In this limit the rate of ET is dominated by an electronic rather than a nuclear frequency term.

The effect of H_{ab} on the shape of the classical barrier height is shown in Figure 10. The top view represents the non-adiabatic limit for two wells in a D_3 symmetry complex. The bottom view of Figure 10 illustrates the adiabatic limit. In this case, the classical barrier height is reduced in energy from the high degree of electronic mixing.

In order for the MLCT state to appear to be a delocalized state on the time scale of the picosecond resonance Raman experiment the rate of ET has to be much faster than the 30ps interrogation time. It is

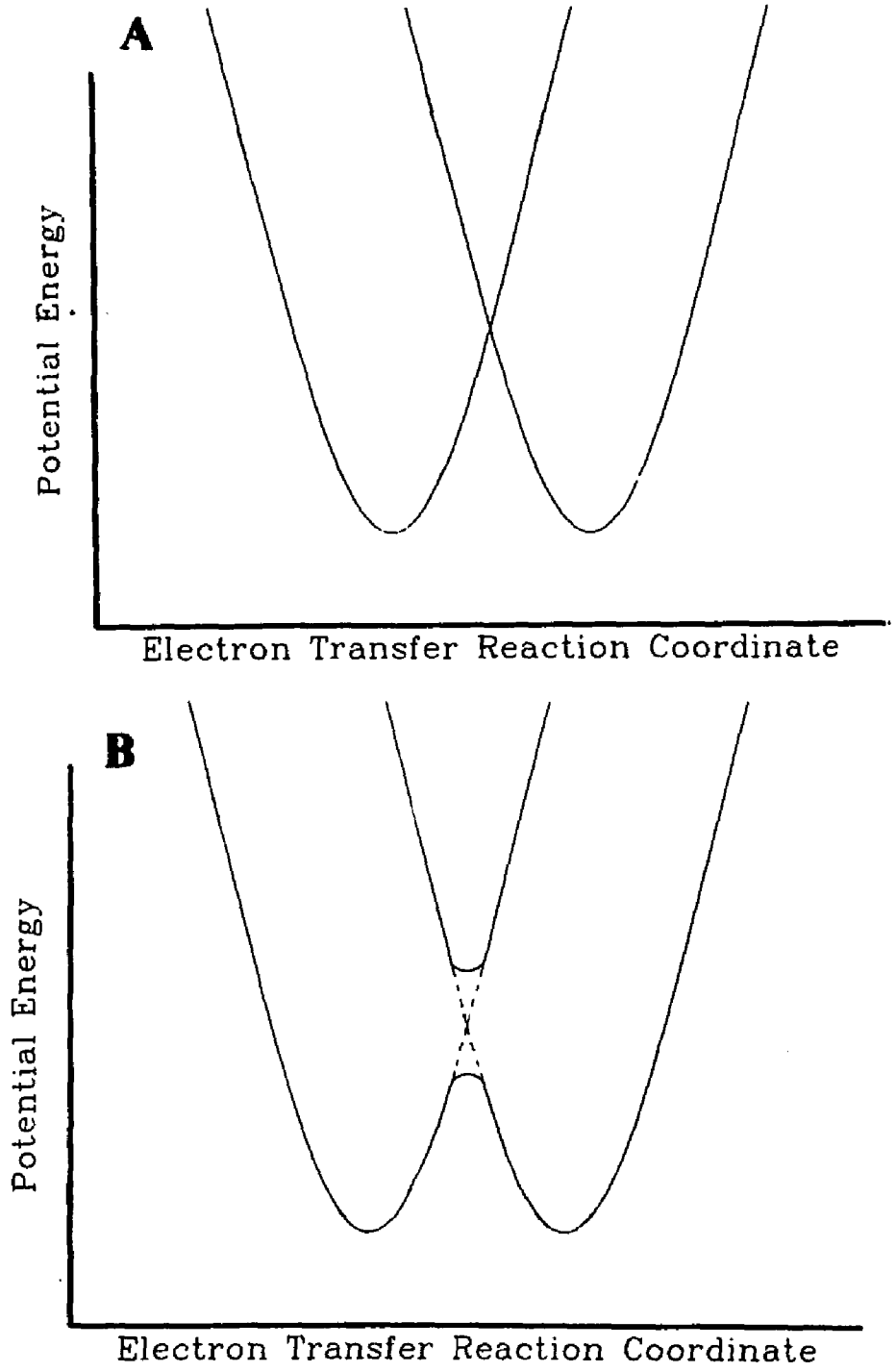

Figure 10. (A) Low coupling limit. (B) High coupling limit.

assumed that the existence of a delocalized potential implies that ET occurs above the classical barrier. In the adiabatic limit $k_{et} = \nu_n$ above the barrier in which case ET occurs on the vibrational time scale. When H_{ab}^2 is small as in the non-adiabatic limit the rate of ET above the intersection region is predicted to be:

$$\frac{2.3 \times 10^{10} cm^{3/2} H_{ab}^2}{E_\lambda^{1/2}} \quad sec^{-1}$$

In order for the MLCT state to appear delocalized to the picosecond experiment, it must be true that $H_{ab}^2 \geq 10 E_\lambda^{1/2}$. This number therefore represents the lower limit in H_{ab}^2 for the appearance of a delocalized potential. From this discussion it can be seen that an electron delocalized MLCT state arises from the combination of a high interligand electronic coupling in competition with the reorganization energy. Experimental measurements of the reorganization energy place the vibrational barrier height in the $Ru(bpy)_3$ ground state at $1400cm^{-1}$ (38). In order to overcome this barrier, and produce a delocalized state H_{ab}^2 would be on the order of $\geq 375cm^{-1}$ at minimum. This result assumes that the vibrational reorganization energy is also approximately $1400cm^{-1}$ in the excited state.

SPECTROSCOPIC ANALYSIS

TRIS COMPLEXES

As mentioned in the introduction, Krausz et al. have inferred, from Raman and fluorescence data, that the MLCT state is not localized in rigid media.(12-15) They reported the characteristic localized resonance Raman spectrum to change into continuum scattering below the glass transition in 1:1 water/gylcol, indicating no localization. They argue from luminescence spectra that solvent reorganization stops below the glass temperature in 4:1 ethanol/methanol and in other glass formers. However, photoselection experiments have been interpreted to indicate localization in frozen rigid environments.(9) If localization in $Ru(bpy)_3^{2+}$ MLCT state is a solvent driven effect, localization requires significant excited state solvation. The solvent reorganization time can be controlled by changing the viscosity of solvent.

The transient Raman spectrum of $Ru(bpy)_3^{2+}$ in water at room temperature, in glycerol at room temperature, and in glycerol at -15°C are shown in Figure 11, Figure 12, and Figure 13, respectively. The transient spectrum in water agrees completely with previously published nanosecond resonance Raman spectra (7,39,-40). The assignments of Raman bands of the ground and excited MLCT state have been worked out and carefully reexamined in several publications.(7,39-41) Asterisks are used above all bands assigned to the excited MLCT state. The spectra in glycerol are similar to those in water except the big solvent bands in the middle of the region scanned. Figure 14 shows the neat glycerol spectrum. In spite of these intense

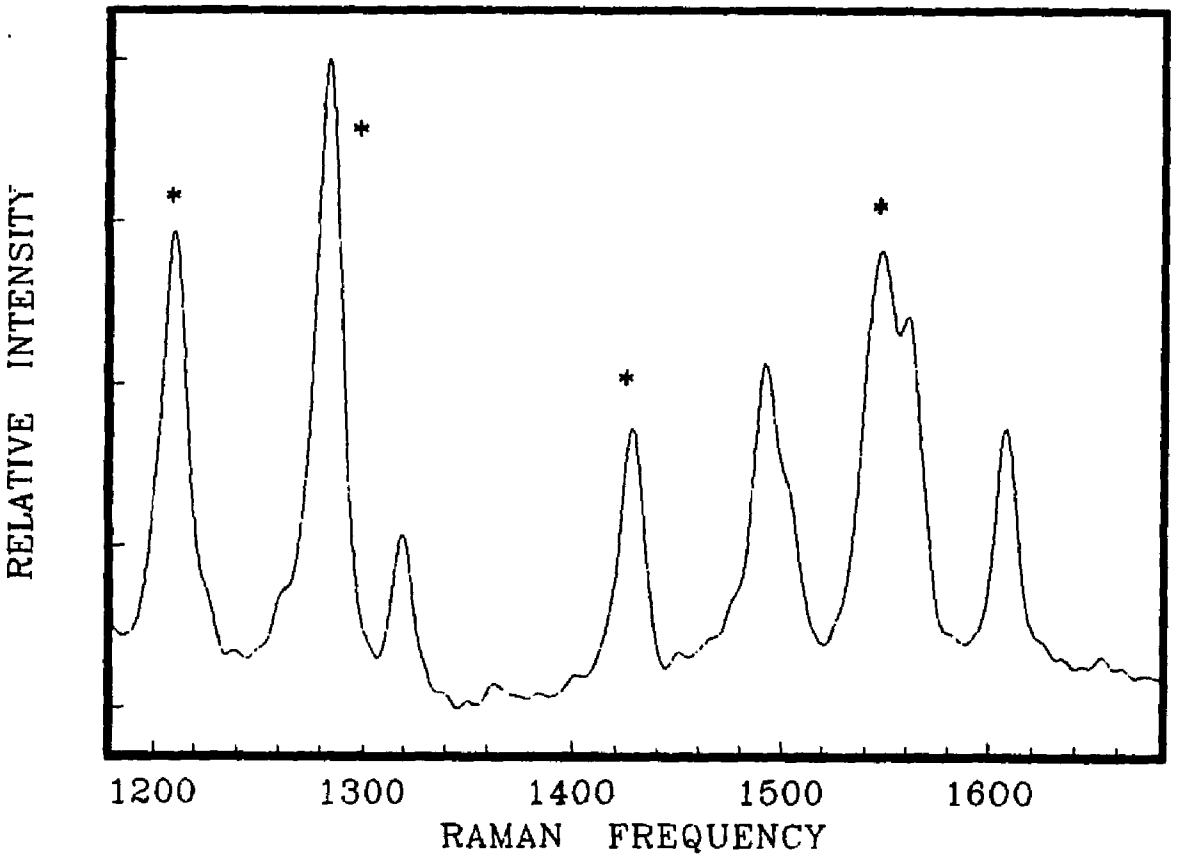

Figure 11. One color transient Raman spectrum of $Ru(bpy)_3^{2+}$ in water at 22°C. Excited state bands have been labeled with an asterisk.

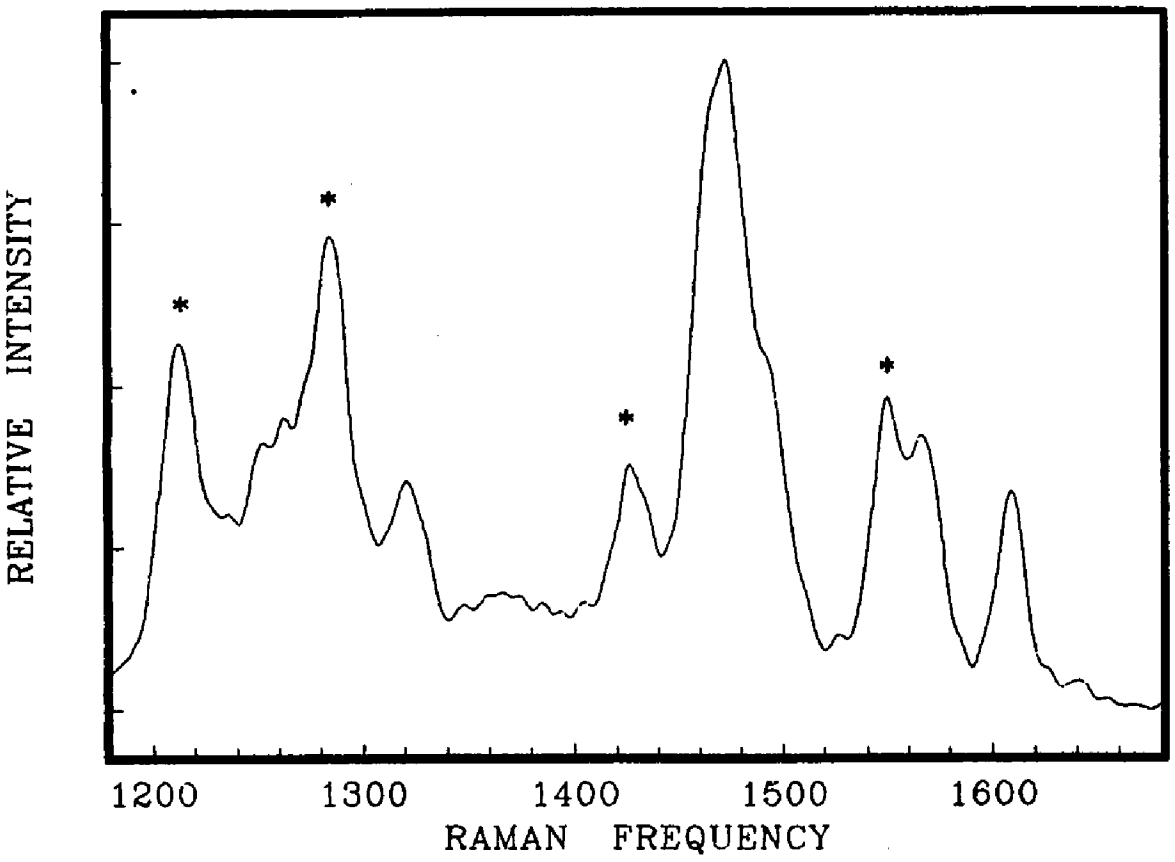

Figure 12. One color transient Raman spectrum of $Ru(bpy)_3^{2+}$ in glycerol at 22°C. Excited state bands have been labeled with an asterisk.

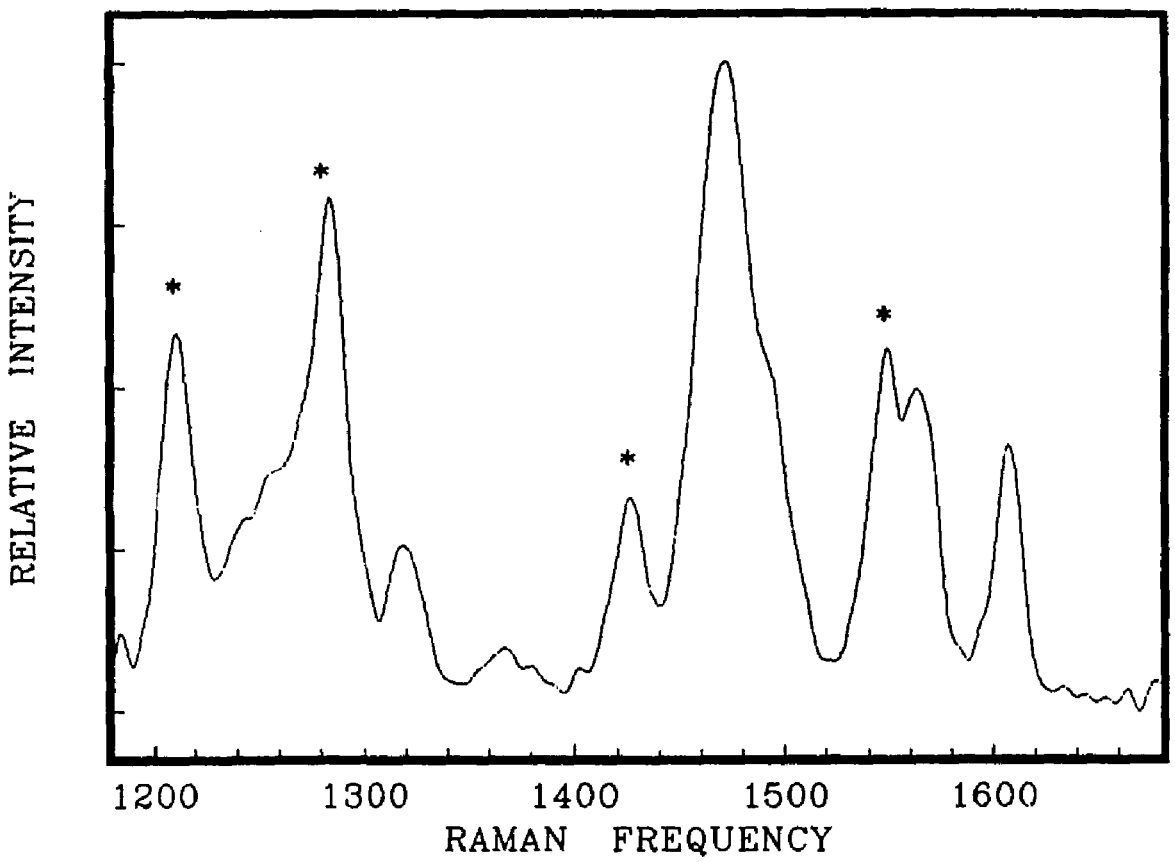

Figure 13. One color transient Raman spectrum of $Ru(bpy)_3^{2+}$ in glycerol at -15°C. Excited state bands have been labeled with an asterisk.

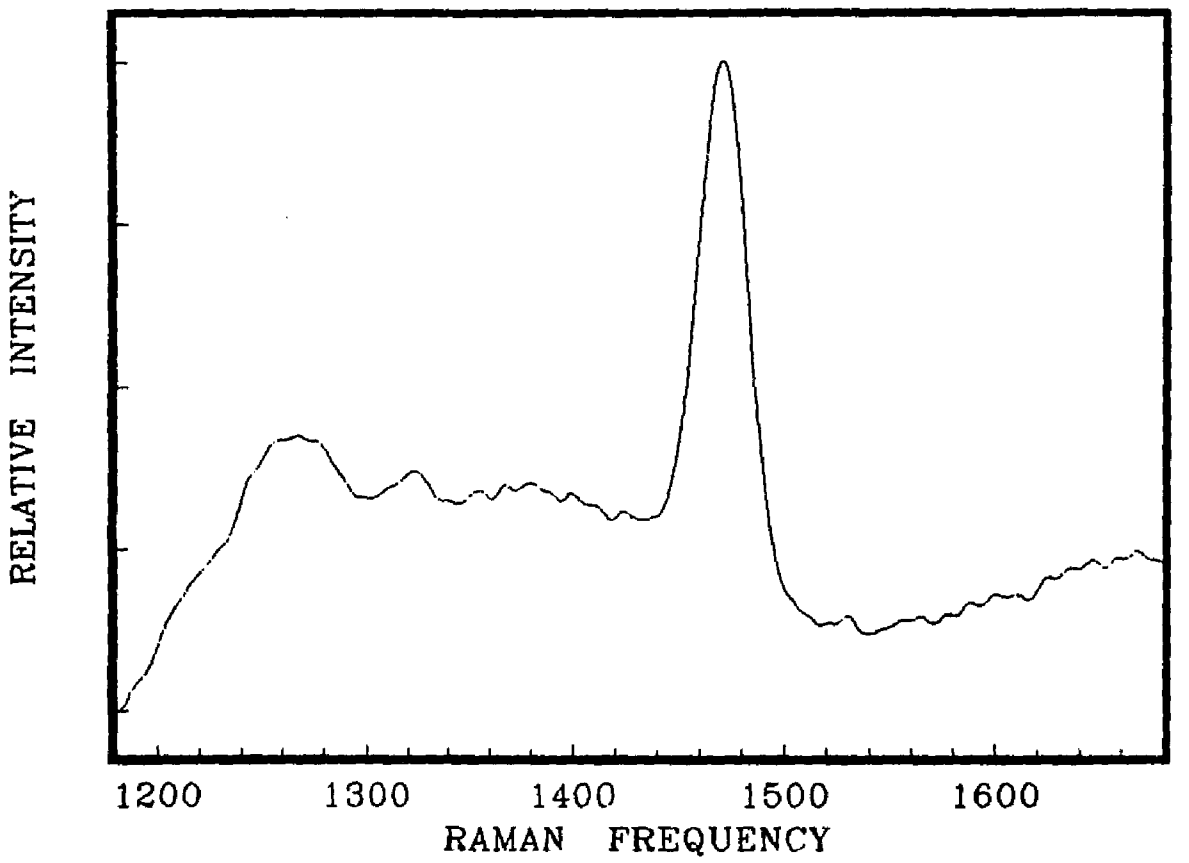

Figure 14. Ground state Raman spectrum of neat glycerol solvent obtained at 354.7nm.

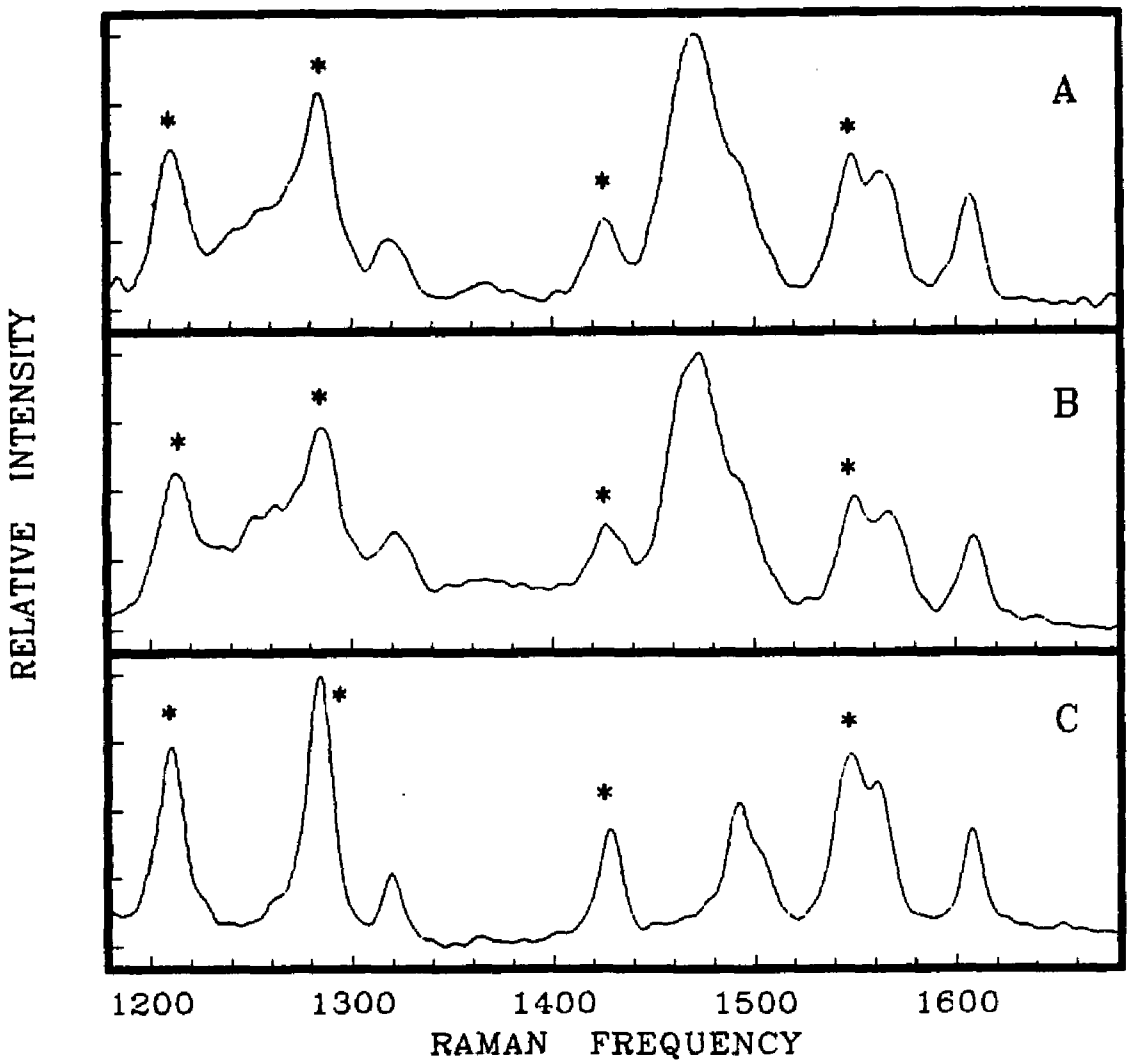

Figure 15. One color transient Raman spectrum of $Ru(bpy)_3^{2+}$. (A) glycerol solution below the glass point at -15°C, (B) glycerol solution above the glass point at 22°C, and (C) water solution at 22°C.

solvent bands, it can be easily seen that the $Ru(bpy)_3^{2+}$ spectrum in glycerol is the sum of the Raman spectrum of aqueous complexes and the solvent. It is concluded from this result that the glycerol solvent has not significantly perturbed the $Ru(bpy)_3^{2+}$ MLCT state under interrogation. The transient Raman spectrum at room temperature and at -15°C are shown in Figure 15. Under these temperatures the viscosities of glycerol are 1487cP and 66500cP respectively. The viscosity change is about a factor of 45. The intensities of the bands are somehow difficult to reproduce because of the inhomogeneity of the rotating frozen solution. However, the inescapable conclusion is that the excited state MLCT spectrum assigned to the electron localized configuration persists both above and below the glass temperature in glycerol in a time scale of less than 30ps. Therefore the solvent does not play a major role in producing the electron localized MLCT configuration. In order to determine whether this result is exceptional to $Ru(bpy)_3^{2+}$ or not, the other D_3 symmetric ruthenium complexes, $Ru(Me_2\text{-}bpy)_3^{2+}$ and $Ru(bpym)_3^{2+}$, have also been examined.

The transient Raman spectrum of $Ru(Me_2\text{-}bpy)_3^{2+}$ in water at room temperatue, in glycerol at room temperature, and in glycerol at -15°C are shown in Figure 16, Figure 17, and Figure 18, respectively. The assignments of the bands of the ground and excited state MLCT state have been previously published (18-19, 42-43). The assignments of the bands of ground and excited MLCT state have been checked by using the laser power dependence of the ground and excited state bands and by two color probe and pump experiments(44-48). The intensity of the excited state Raman bands depends highly on laser

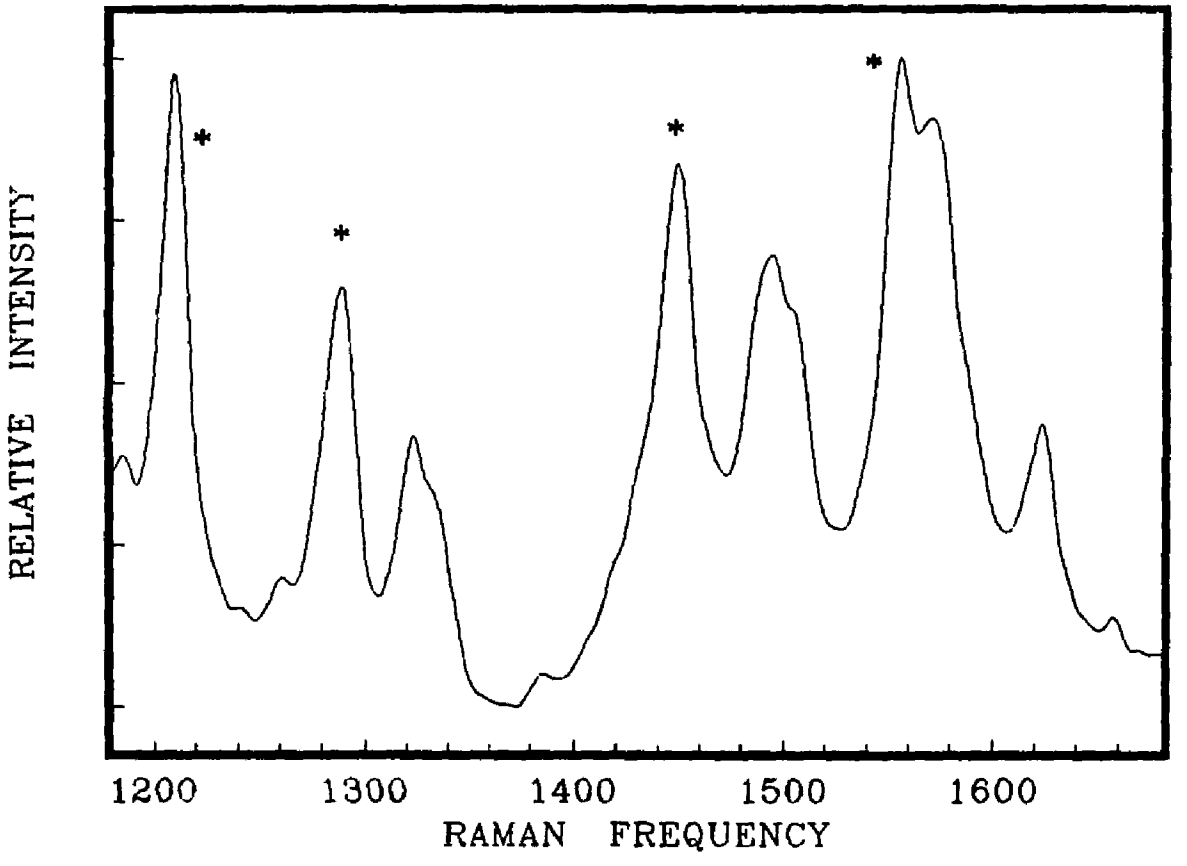

Figure 16. One color transient Raman spectrum of $Ru(Me_2\text{-}bpy)_3^{2+}$ in water at 22°C. Excited state bands have been labeled with an asterisk.

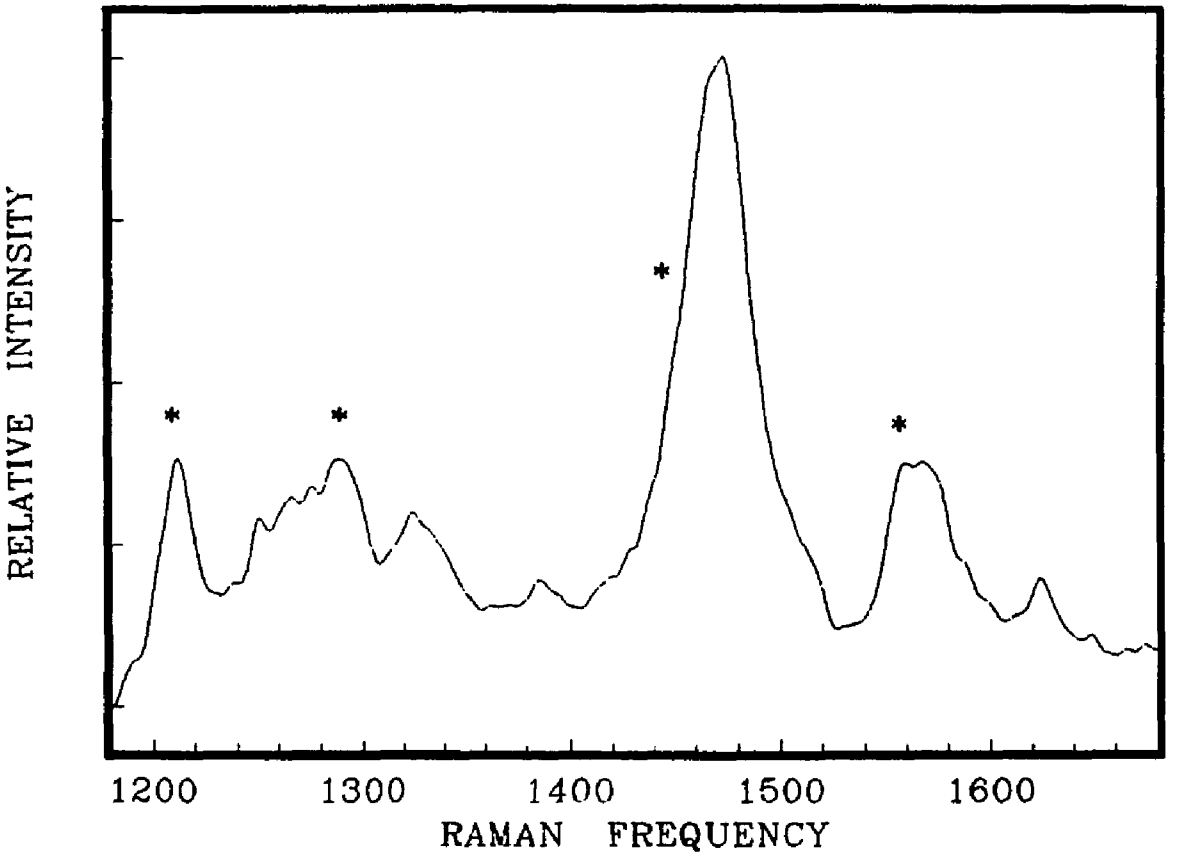

Figure 17. One color transient Raman spectrum of $Ru(Me_2\text{-}bpy)_3^{2+}$ in glycerol at 22°C. Excited state bands have been labeled with an asterisk.

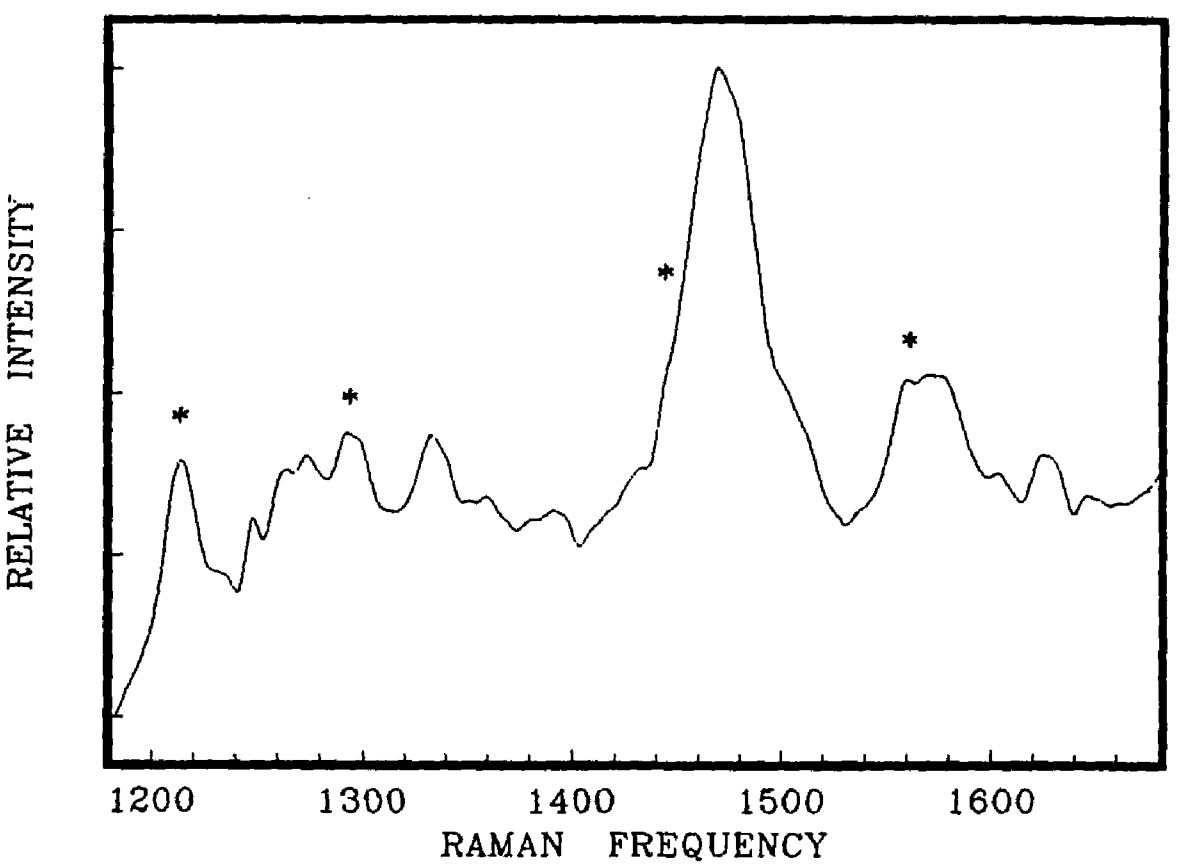

Figure 18. One color transient Raman spectrum of $Ru(Me_2\text{-}bpy)_3^{2+}$ in glycerol at -15°C. Excited state bands have been labeled with an asterisk.

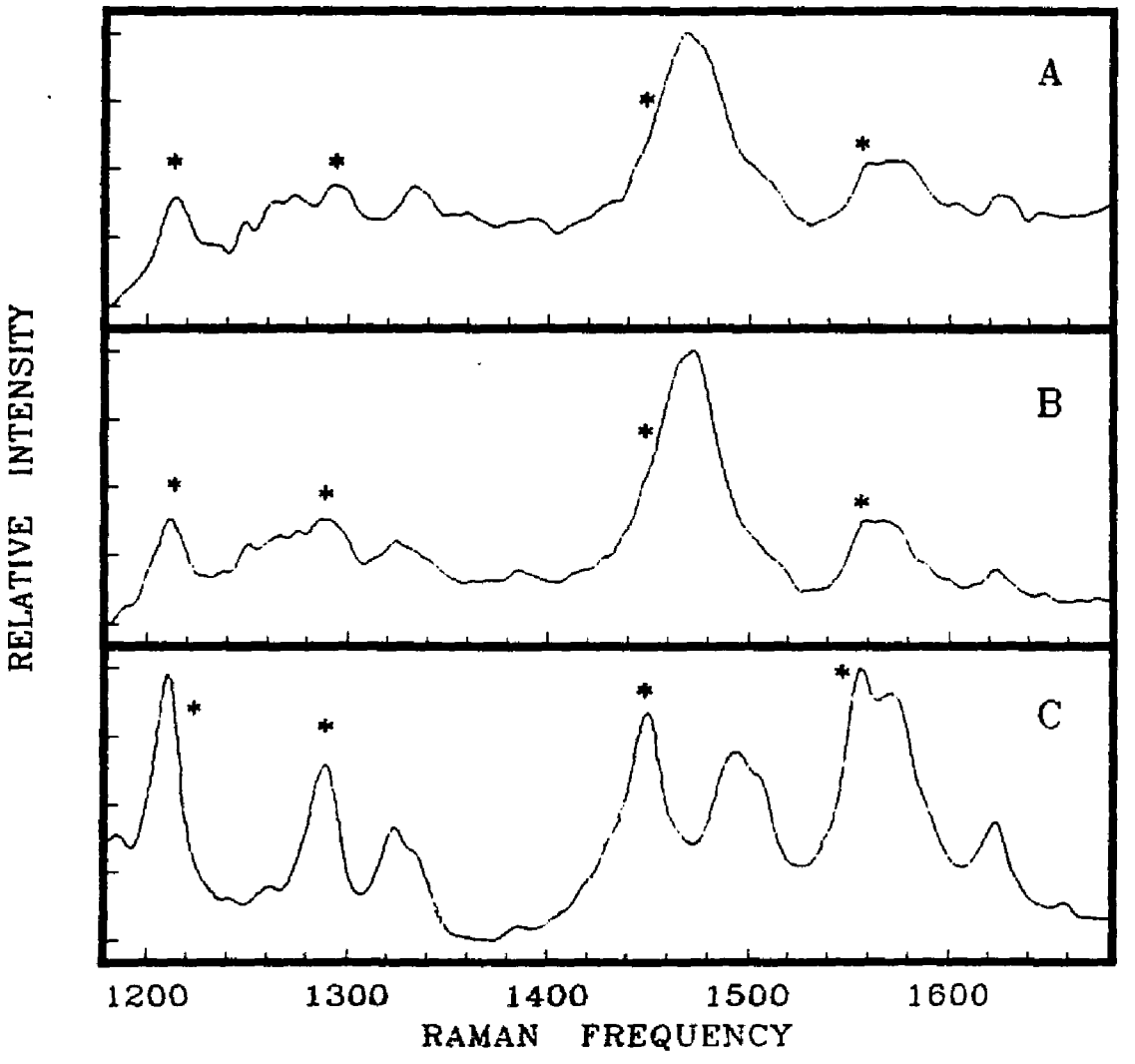

Figure 19. One color transient Raman spectrum of $Ru(Me_2\text{-}bpy)_3^{2+}$. (A) glycerol solution below the glass point at -15°C, (B) glycerol solution above the glass point at 22°C, and (C) water solution at 22°C.

power. By varying the laser intensity, signal strength of the excited state Raman bands can be made to vary by a factor of 20 with respect to the ground state bands. Moreover, the assignments were checked with two color Raman spectrum. Therefore, there is little doubt as to accuracy of the assignments. Bands corresponding to the localized excited MLCT state have been marked in the figure with an asterisk. In this complex, also, the transient Raman spectrum in glycerol appears to be a simple combination of the solvent and transition metal complex spectra. Again, in a fashion similar to the $Ru(bpy)_3^{2+}$ spectra, no bands associated with the complex change significantly in frequency or intensity between the two solvents. It appears, again, that the solvent has not significantly perturbed the MLCT state under interrogation. The transient Raman spectra in glycerol above and below the glass temperature in Figure 19 indicates that the excited state MLCT spectra associated with the localized configuration is invariant to the solvent environment since these bands persist in both spectra. It would appear that solvent motions have a minor contribution to the formation of the localized configuration for $Ru(Me_2\text{-}bpy)_3^{2+}$.

Figure 20, Figure 21, and Figure 22 show the transient Raman spectrum of $Ru(bpym)_3^{2+}$ in water at room temperature, in glycerol at room temperatue, and in glycerol at -15°C, respectively. The assignments of the bands of the ground and excited MLCT state have been previously published(18-19, 24, 42-43). The assignments of the bands of ground and excited MLCT state have been checked by using the laser power dependence of the ground and excited state bands and by two color probe and pump experiments(44-48). There is, therefore,

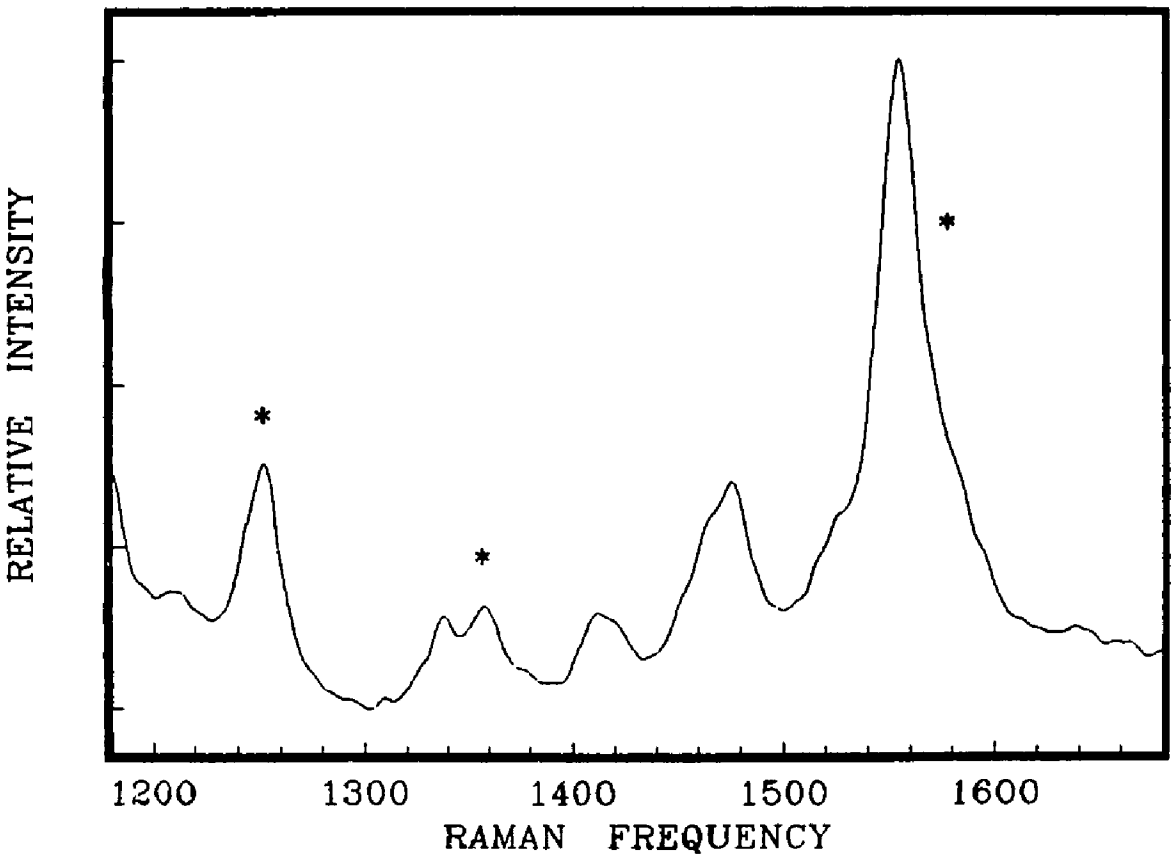

Figure 20. One color transient Raman spectrum of $Ru(bpym)_3^{2+}$ in water at 22°C. Excited state bands have been labeled with an asterisk.

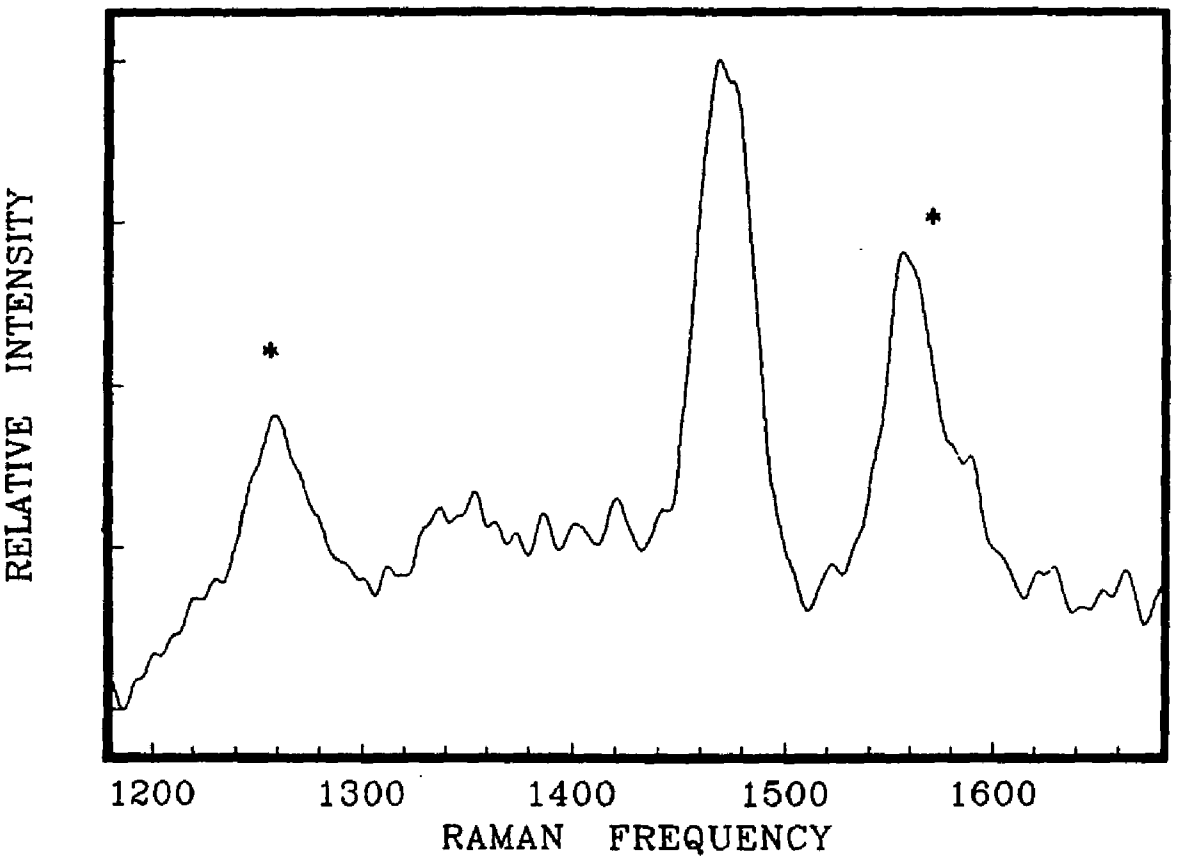

Figure 21. One color transient Raman spectrum of $Ru(bpym)_3^{2+}$ in glycerol at 22°C. Excited state bands have been labeled with an asterisk.

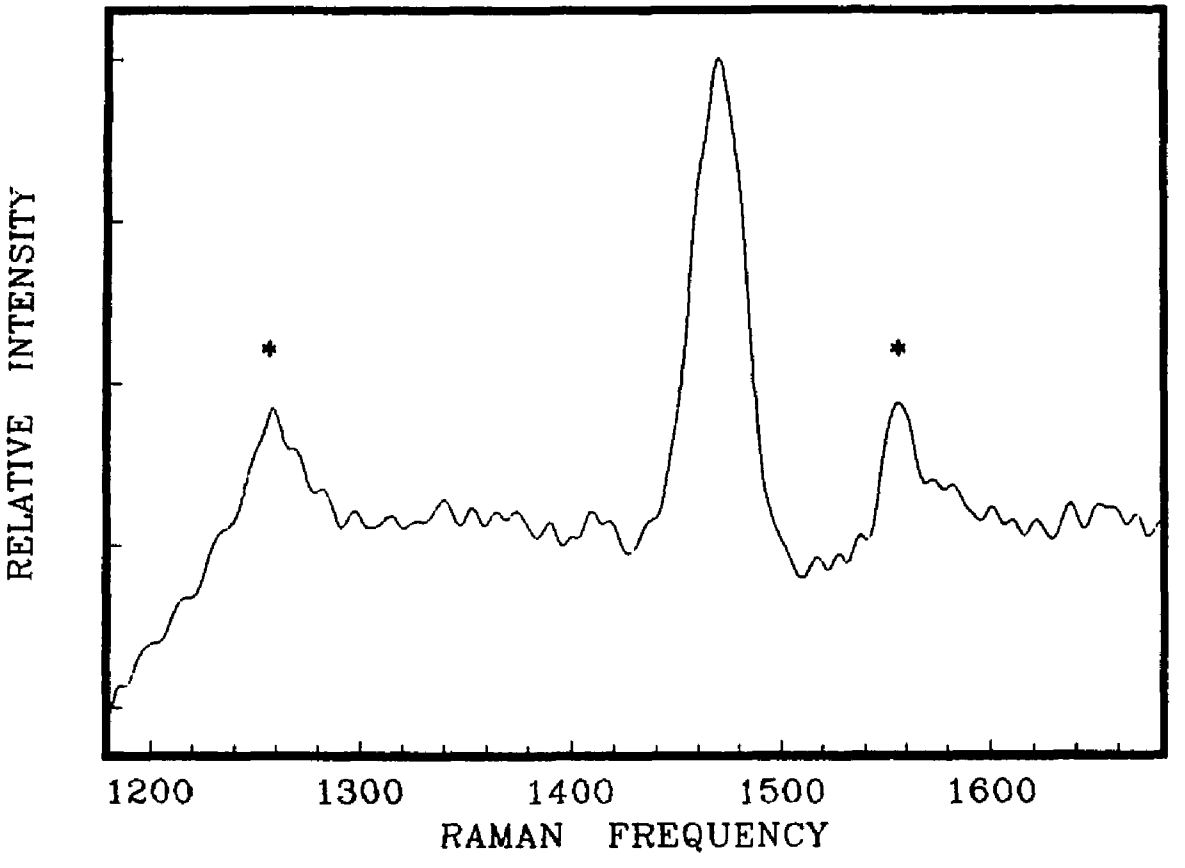

Figure 22. One color transient Raman spectrum of $Ru(bpym)_3^{2+}$ in glycerol at -15°C. Excited state bands have been labeled with an asterisk.

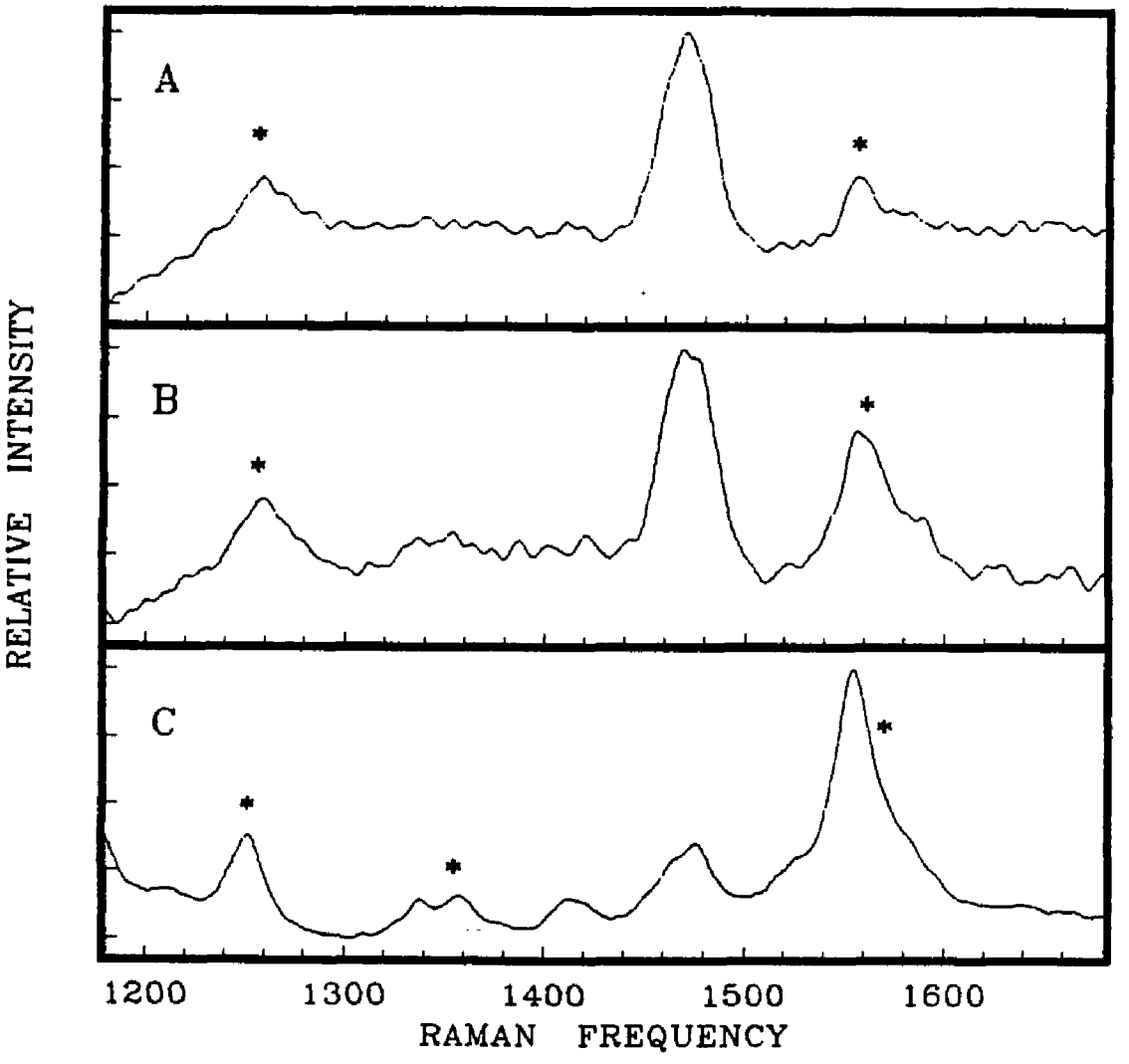

Figure 23. One color transient Raman spectrum of $Ru(bpym)_3^{2+}$. (A) glycerol solution below the glass point at -15°C, (B) glycerol solution above the glass point at 22°C, and (C) water solution at 22°C.

little doubt as to accuracy of the assignments. Bands corresponding to the localized excited MLCT state have been marked in the figure with an asterisk. In this complex, also, the transient Raman spectrum in glycerol appears to be a simple combination of the solvent and transition metal complex spectra. Again, in a fashion similar to the $Ru(bpy)_3^{2+}$ and $Ru(Me_2\text{-}bpy)_3^{2+}$ spectra, no bands associated with the complex change significantly in frequency or intensity between the two solvents. It appears, again, that the solvent has not significantly perturbed the MLCT state under interrogation. The transient Raman spectra in glycerol above and below the glass temperature in Figure 23 indicates that the excited state MLCT spectra associated with the localized configuration are invariant to the solvent environment since these bands persist in both spectra. It would appear that solvent motions have a minor contribution to the formation of the localized configuration for $Ru(bpym)_3^{2+}$. From these three experiments, it is a common occurrence that electron is delocalized within 30ps and there is a minor solvent contribution in the excited MLCT state of D_3 symmetric ruthenium-polypyridine complexes(46,48).

The picosecond high viscosity solution results indicate that there is no solvent influence on the rate of appearance of the localized configuration. By observing the excited MLCT state on a time scale fast compared to solvent reorganization, E_λ(solvent) is practically zero on the observation time scale of the experiment. This is expected to be true as a result of the D_3 symmetry required in the ground electronic state. The dipole structure surrounding the ground state is the same as that around the initially formed Franck-Condon excited state. As a

result, the solvent structure in the excited state is initially characteristic of what is expected for an electron delocalized over all three ligands. Even in this circumstance, the localized configuration is the only one observed. From this result it can be concluded that the vibrational reorganization energy is so much larger than H_{ab}^2 that a localized state is observed on a time scale of 10^{-11}s. It is important to note that vibrational trapping is not the sole mechanism producing an electron-localized configuration but rather that the competition between electronic coupling and vibrational reorganization energy results in a localized configuration. In this case it is obvious that the electron coupling is much less than 375cm^{-1}.

It should be noted that the Raman experiment could only be used to sample the lower 1600 cm^{-1} of the potential well, although the initial level of photo excitation is 12000cm^{-1} above the zero point(49). It is conceivable that at some energy electron delocalization may occur. At this level of excitation, electron transfer can be an important process only if it can effectively compete with vibrational relaxation. The vibrational relaxation can be seen with the decrease of the intensity of anti-Stokes Raman bands. We have searched, without sucess, for evidence of vibrational relaxation in the picosecond anti-Stokes Raman spectrum of $Ru(bpy)_3^{2+}$. It would appear that all vibrational cooling occurs on a time scale much faster than the 30ps laser pulse. This result is consistent with other picosecond experiments which estimate the rate of vibrational decay to be $>10^{11}s^{-1}$ (50). That is not to say that electron transfer cannot occur before vibrational

cooling is complete. However, vibrational relaxation is a dominant mechanism leading to population of the lower lying vibrational state.

MIXED LIGAND COMPLEXES

It is known that interligand electron transfer in hetero-ligand complexes occurs and electrons funnel to the lower energy lying ligands(23,24). Many studies have been reported in mixed ligand ruthenium complexes including bpym and Me_2-bpy ligand(23-24,45). The solvent dependence of this phenomena is an interesting topic. In order to investigate the solvent dependence of ILET we chose two mixed ligand complexes. One is $Ru(bpym)_2(bpy)^{2+}$ which has a fast interligand electron transfer rate $(>(30ps)^{-1})$, and the other is $Ru(Me_2\text{-}bpy)_2(bpy)^{2+}$ which has a slow interligand electron transfer rate $(<(500ns)^{-1})$. In these two mixed ligand complexes interligand electron transfer occurs from the bpy to the bpym ligand, and from the Me_2-bpy to the bpy ligand, respectively. If these interligand electron transfers are solvent dependent, excited state bpy bands in $Ru(bpym)_2(bpy)^{2+}$/glycerol spectrum and more intense excited Me_2-bpy bands in $Ru(Me_2\text{-}bpy)_2(bpy)^{2+}$/glycerol than aqueous solution can be observed, by changing the viscosities. Because solvation reorganization time for high viscosity solvent is longer than that for low viscosity solvent. Solvents were water and glycerol at room temperature whose viscosities are 1cP and 1487cP, respectively.

Figure 24 and Figure 25 are one color transient spectra of $Ru(bpym)_2(bpy)^{2+}$ in water and glycerol at room temperature, respectively. As shown in Figure 24, there is no bpy excited state band found in the spectrum. Excited state electrons are already localized on

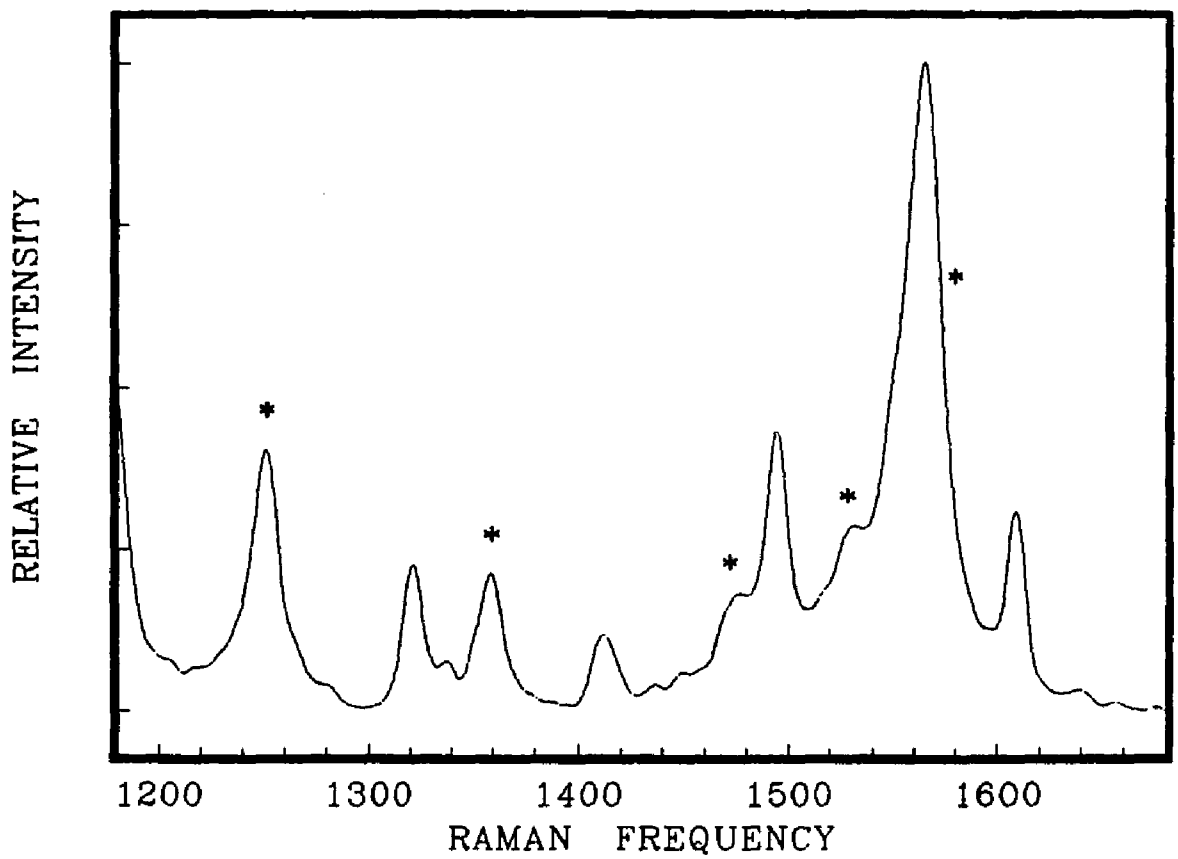

Figure 24. One color transient Raman spectrum of $Ru(bpym)_2(bpy)^{2+}$ in water at room temperature. Excited state bands have been labeled with an asterisk.

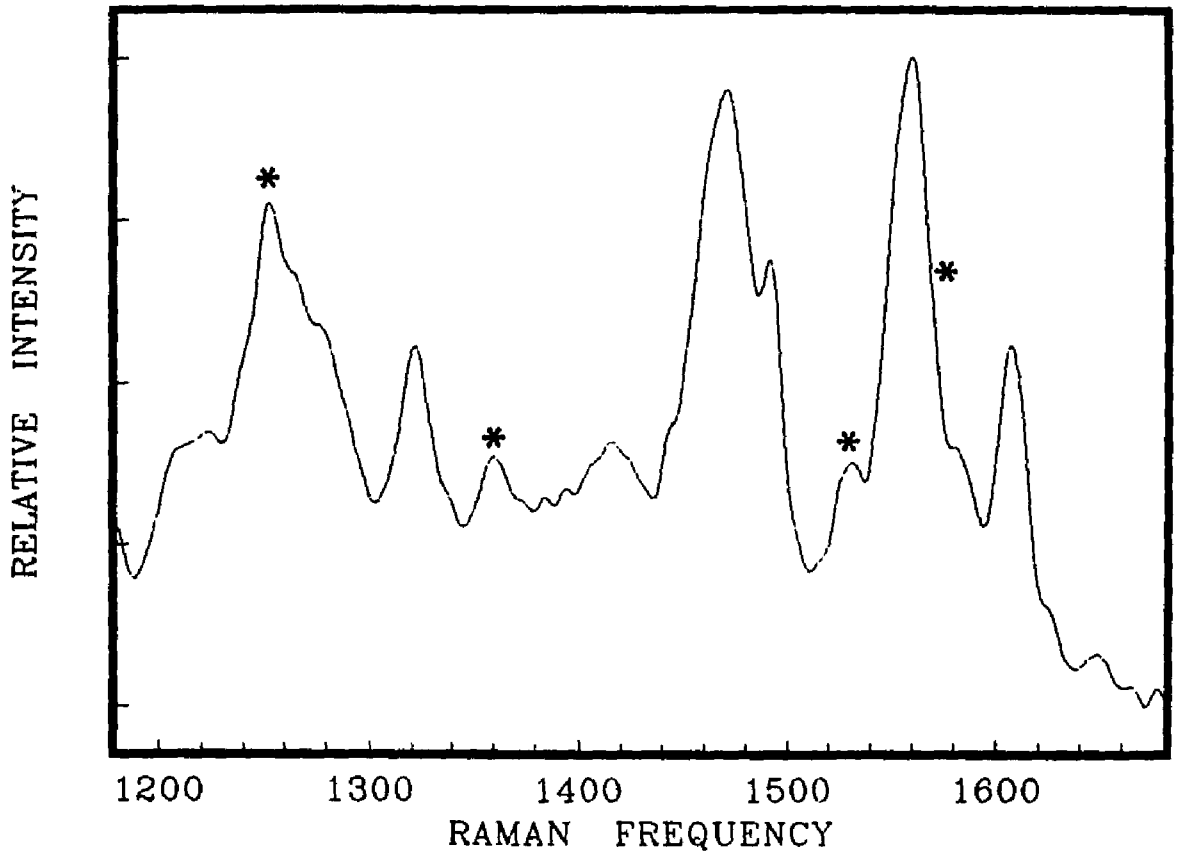

Figure 25. One color transient Raman spectrum of $Ru(bpym)_2(bpy)^{2+}$ in glycerol at room temperature. Excited state bands have been labeled with an asterisk.

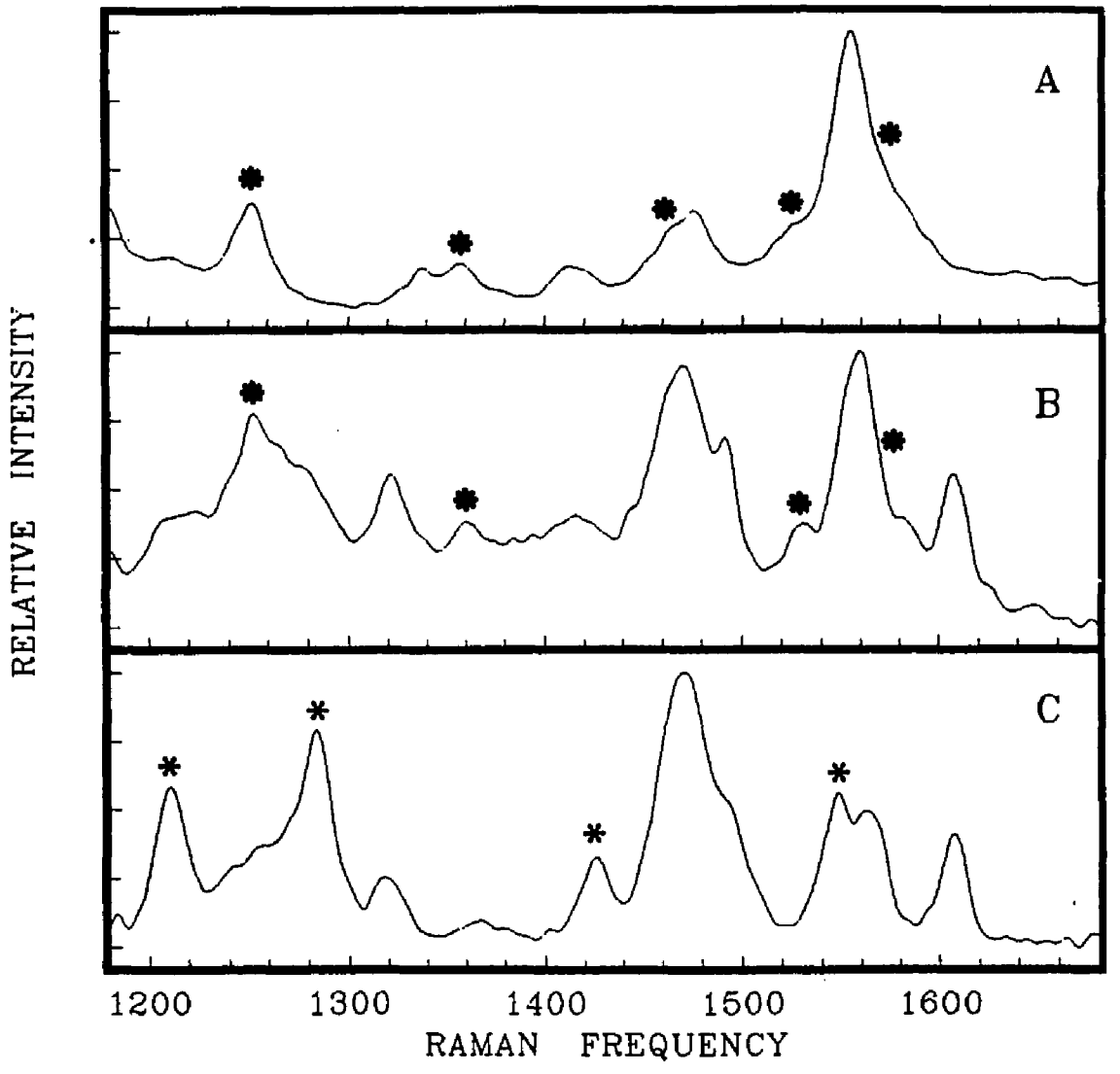

Figure 26. (A) $Ru(bpym)_3^{2+}$ in water, (B) $Ru(bpym)_2(bpy)^{2+}$ in glycerol, and (C) $Ru(bpy)_3^{2+}$ in glycerol.

bpym ligands within the time scale of the laser pulse width. The details are in chapter II. A similar interpretation applies to glycerol. Figure 25 shows no bpy excited state bands in this spectrum. This spectrum, as shown in Figure 26, can be described as the sum of glycerol bands, bpym ground state bands, bpym excited state and bpy ground state bands. Therefore, interligand electron transfer from bpy ligand to bpym ligands is also completed in this viscous solution within the time scale of the laser pulse width. This implies that the solvent has not influenced the MLCT state under interrogation.

One color transient Raman spectra of $Ru(Me_2\text{-}bpy)_2(bpy)^{2+}$ in water and in glycerol at room temperature are shown in Figure 27 and Figure 28 respectively. In this complex we can see both excited state ligands bands from Me_2-bpy and bpy as observed in Figure 27. This Me_2-bpy excited state band is somehow overlapping with the big glycerol band but it is possible to distinguish between the glycerol band with Me_2-bpy band and without it. The shaded part in the glycerol band is the Me_2-bpy excited state band in Figure 28. If this spectrum is compared to the other spectra like Figure 29, it is obvious that there are Me_2-bpy excited state bands in glycerol solution. The shaded bands only appear in $Ru(Me\text{-}bpy)_3^{2+}$ and $Ru(Me_2\text{-}bpy)_2(bpy)^{2+}$ spectra not in $Ru(bpy)_3^{2+}$ spectrum. This indicates that ILET is not influenced by solvent in our time scale.

For the case of mixed ligand complexes the potential surface can be described in a similar fashion to that illustrated in Figure 9. This scheme also illustrates the difference between a nonadiabatic process and adiabatic process like that occuring in the symmetric complexes.

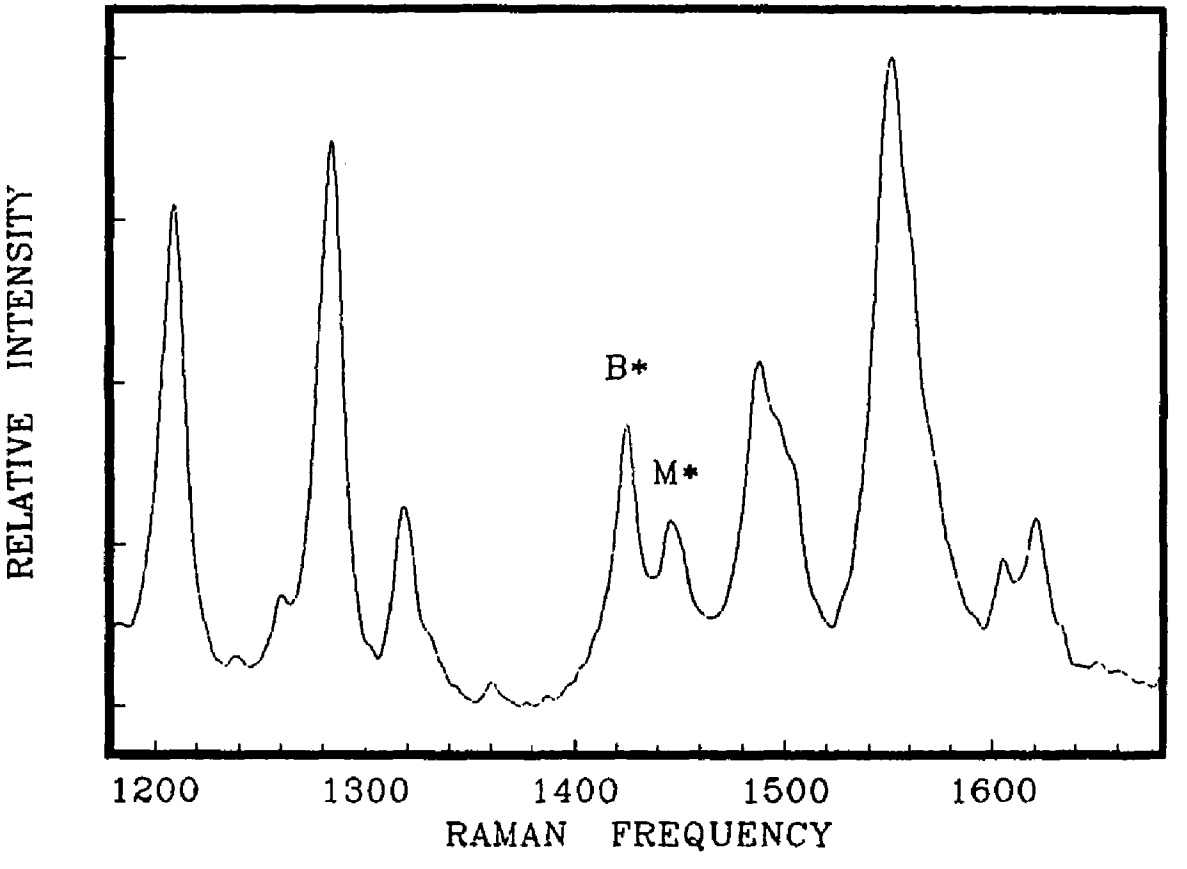

Figure 27. One color transient Raman spectrum of $Ru(Me_2\text{-}bpy)_2(bpy)^{2+}$ in water at room temperature. Excited state bands have been labeled with an asterisk.

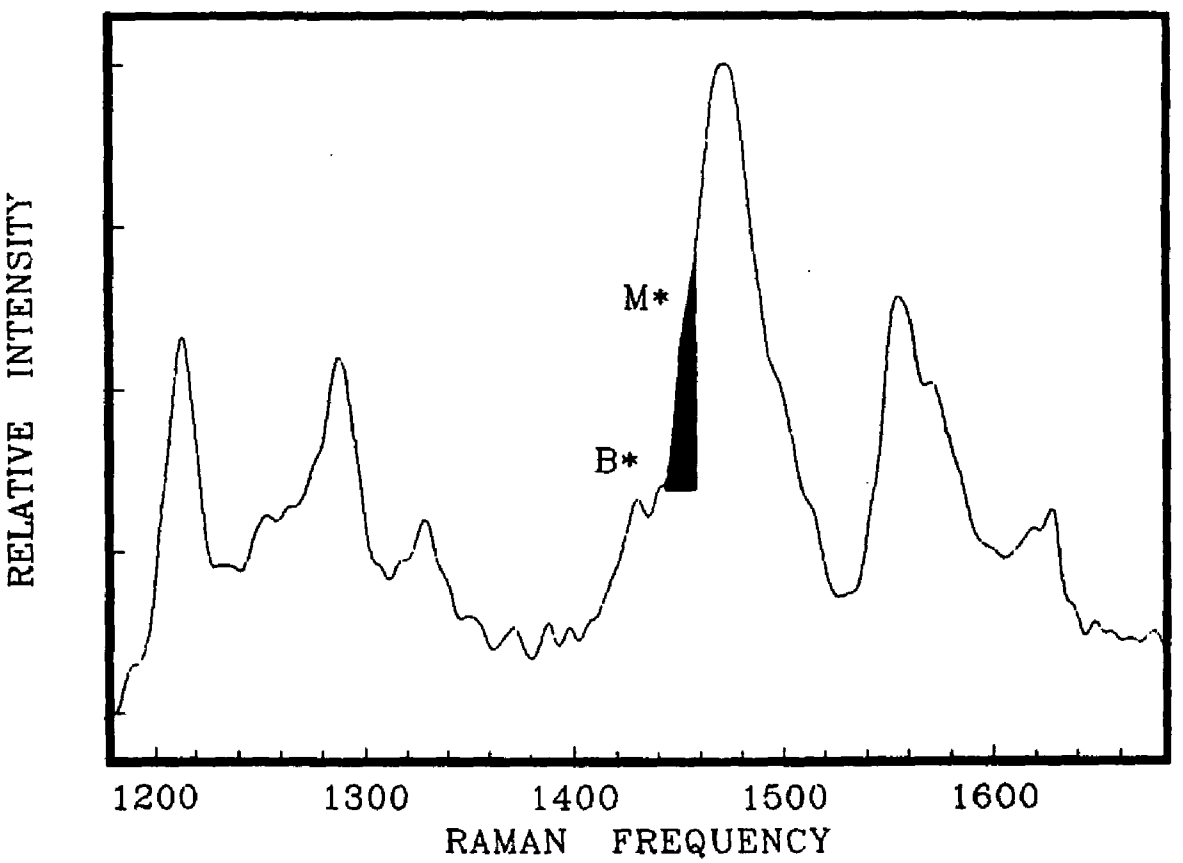

Figure 28. One color transient Raman spectrum of $Ru(Me_2\text{-}bpy)_2(bpy)^{2+}$ in glycerol at room temperature. Excited state bands have been labeled with an asterisk.

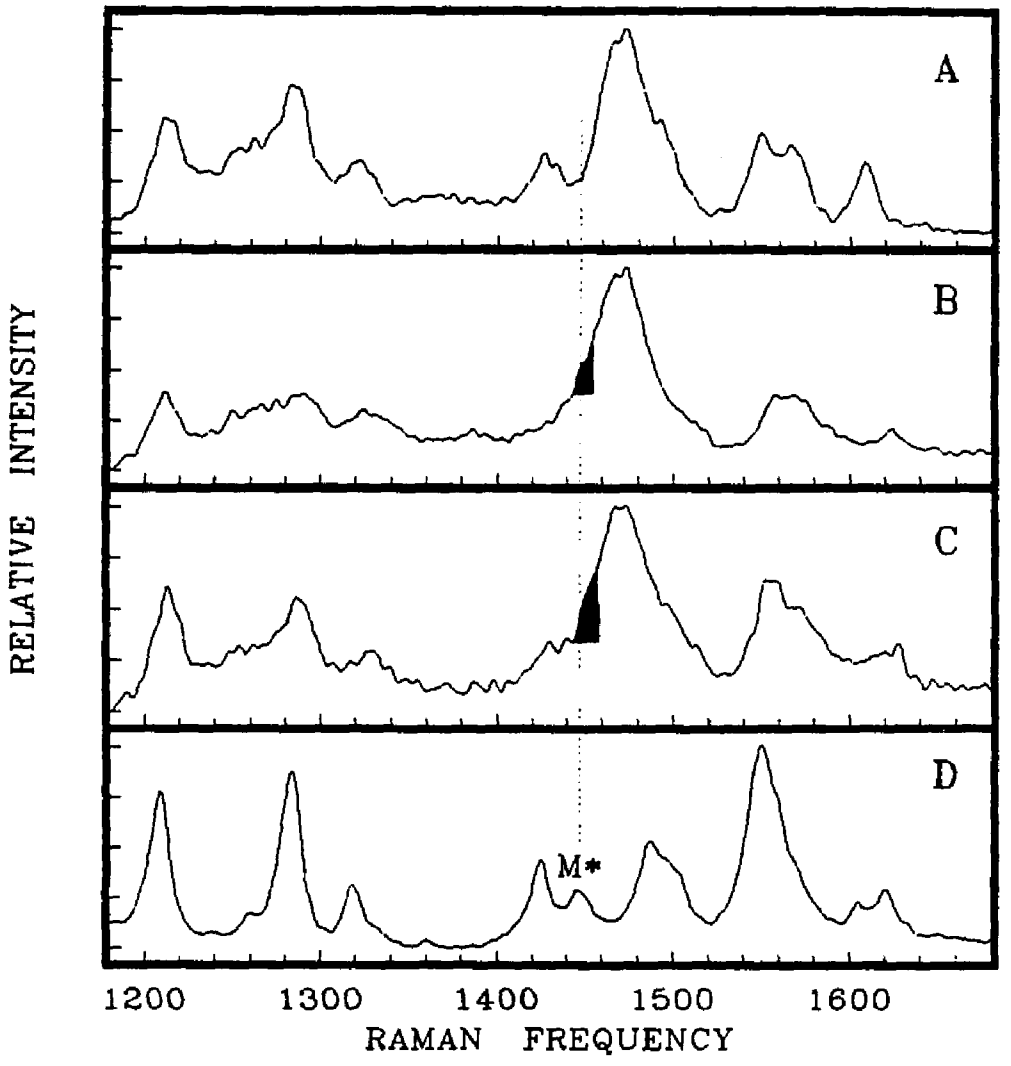

Figure 29. (A) $Ru(bpy)_3^{2+}$ in glycerol, (B) $Ru(Me_2\text{-}bpy)_3^{2+}$ in glycerol, (C) $Ru(bpy)(Me_2\text{-}bpy)_2^{2+}$ in glycerol, and (D) $Ru(bpy)(Me_2\text{-}bpy)_2^{2+}$ in water.

Nonadiabatic potentials correspond to the case of weak interaction between the ligand potentials, while adiabatic potentials corresponds to strong interaction. The energy gap between bpy and bpym ligands is 3240 cm^{-1} (52) and between bpy and Me_2-bpy ligands is 890 cm^{-1} (53). There is no energy gap dependence for ILET found in ruthenium-polypyridine asymmetric complexes by two color time resolved Raman spectroscopy(45). Therefore, the interaction between heteroligands is very weak as in the non-adiabatic limit illustrated in Figure 9. In this case interligand electron transfer has taken place on the upper singlet MLCT state surface. The Me_2-bpy excited state Raman band which we observed was obviously some fraction of electrons on triplet Me_2-bpy ligand surface which were intersystem crossing to the triplet MLCT wells before ILET on the singlet surface is complete.

We observed no new bands in mixed ligand complexes in glycerol. The interpretaion of this result is that the electron coupling is too weak to produce delocalized states. Moreover the viscosity of the solvent does not perturb the potential surface of these metal complexes. From this result it can be inferred that electron localization and interligand electron transfer are not influenced by solvent in ruthenium-polypyridine complexes.

CONCLUSION

By measuring the vibrational spectrum of the transient MLCT state on a time scale fast compared to solvent motions in viscous solution, it has been determined that this electronic state is representative of an intrinsically localized configuration. Furthermore, this behavior appears to be common in all of the complexes investigated in this study. It was also found that vibrational relaxation appears to be much faster than the 30ps laser pulse width and is therefore a dominant mechanism in populating the lower vibrational states. Following vibrational cooling, interligand electron transfer can only occur by a slow electron transfer process involving tunneling from the lower vibrational levels. No information regarding electron transfer from the upper region of the potential surface was presented. As a result, conclusions can be made concerning only the bottom of the potential well. The data clearly show that the interligand electron coupling is too small to produce an electron-delocalized state with a barrier to electron transfer lower than $1400cm^{-1}$.

In principle, the electron transfer rates in the upper region of the potential could be significantly different from those at the bottom of the well due to more favorable Franck-Condon factors, a higher density of states, or change in the electronic coupling from mixing with nearby electronic states. Given this, the vibrational relaxation process could be considered as contributing to electron trapping by reducing electron transfer rates to those characteristics of tunneling from the bottom of the potential.

RATE OF INTERLIGAND ELECTRON TRANSFER

In order to estimate the rate of interligand electron transfer through barrier by tunneling, the band width is examined. If there is a difference between the bandwidth of tris ligand complex and mixed ligand complex, interligand electron transfer rate can be deduced by using uncertainty principles. If there is a resonance between symmetric potential wells in ruthenium tris ligand complexes, there will be level splitting observed. This Raman spectrum is not a high resolution spectrum, therefore we cannot observe this splitting but it will be reflected in the band width. Broadening of bands is expected to be observed.

CONCEPT OF TUNNELING(54)

1. SYMMETRIC POTENTIAL SYSTEM

Assuming that there are two independent potential wells like Figure 30, then the degenerate wave functions can be described as

$$\psi_1(x) = \frac{1}{\sqrt{2}}(\psi_0(x) + \psi_0(-x))$$

$$\psi_2(x) = \frac{1}{\sqrt{2}}(\psi_0(x) - \psi_0(-x))$$

If there is no overlap between $\psi_0(x)$ and $\psi_0(-x)$, both wavefunctions have the same energy. Eo. But if there is overlap between $\psi_0(x)$ and $\psi_0(-x)$, they have different energies. E_1 and E_2 where $E_1<E_0<E_2$. Therefore energy difference $\Delta E=E_2-E_1$ can be obtained as follows. Schrödinger equations for ψ_0 and ψ_1 are

$$\psi_0'' + \frac{2m}{\hbar^2}\{Eo-V(x)\}\psi_0=0 \qquad (1)$$

$$\psi_1'' + \frac{2m}{\hbar^2}\{E_1-V(x)\}\psi_1=0 \qquad (2)$$

multiply eq. (1) by ψ_1 - eq. (2) by ψ_0

$$\psi''_o\psi_1 - \psi_o\psi_1'' + \frac{2m}{\hbar^2}\{E_o-E_1\}\psi_o\psi_1 = 0$$

Integrate this equation

$$(\psi_o'\psi_1 - \psi_o\psi_1')_0^\infty + \frac{2m}{\hbar^2}\{Eo - E1\}\int_o^\infty \psi_o\psi_1\,dx = o$$

$$\therefore E_1 - E_o = -\frac{\hbar^2}{m}\psi_{o(o)}\psi_o'(o)$$

Apply the same procedure to obtain E_2

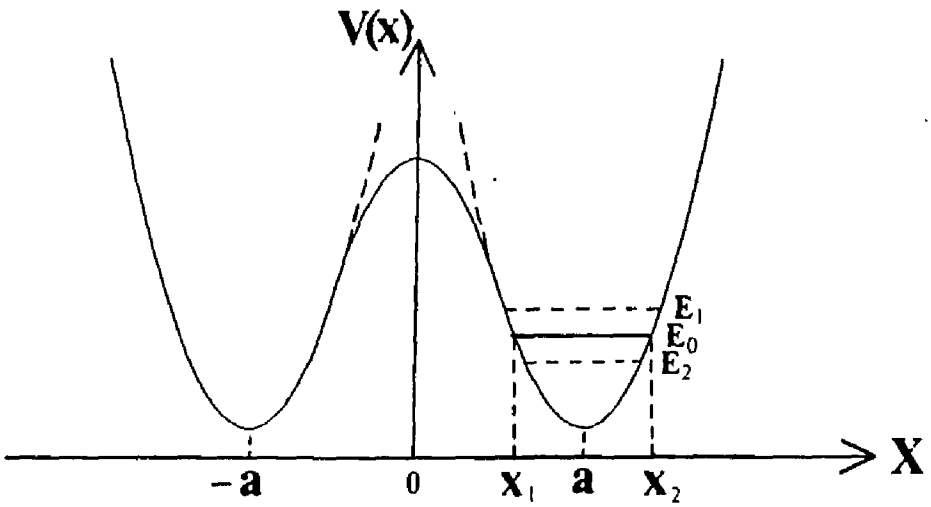

Figure 30. Schematic diagram of potential - symmetric case.

$$E_2 - E_o = + \frac{\hbar^2}{m} \psi_o(o)\psi_o'(o)$$

$$\therefore \quad \Delta E = E_2 - E_1 = \frac{2m}{\hbar^2} \psi_o(o)\psi_o'(o)$$

Therefore by using WKB approximation

$$\psi_o(o) = \frac{\{mv\}^{1/2}}{[2m[Vo - Eo]^{1/4}} \exp\left[-\frac{\sqrt{2m}}{\hbar} \int_0^{x_1} (V-E_o)^{1/2}dx\right]$$

$$\psi_o'(o) = \frac{\{2m[Vo - Eo]^{1/2}\}}{\hbar} \psi_0(o)$$

$$\Delta E = E_2 - E_1$$

$$= 2\,hv \exp\left[-\frac{\sqrt{2m}}{\hbar} \int_0^{x1} (V-Eo)^{1/2}dx\right]$$

$$= 2\,hv \exp\left[-\frac{2\sqrt{2m}}{\hbar} \int_{-x1}^{x1} (V-Eo)^{1/2}dx\right]$$

Moreover, consider the time dependent term in Schrodinger equation where $\Psi(x,t)$ is time dependent wavefunction. The probability is described as

$$\Psi\Psi^* = \psi_0^2(x) \sin^2\left(\frac{1}{2}\, t\, \frac{\Delta E}{\hbar}\right) + \psi_0^2(-x) \cos^2\left(\frac{1}{2} t \frac{\Delta E}{\hbar}\right)$$

This equation includes the term which describes a cycle going back and forth between two wells through tunneling

$$t\, \frac{\Delta E}{\hbar} = \pi \qquad (3)$$

Therefore, tunneling frequency νt is

$$\nu t = 2\frac{\Delta E}{h}$$

$$= \frac{2\nu}{\pi} \exp\left[-\frac{2\sqrt{2m}}{\hbar}\int_{-x1}^{x1}(V-Eo)^{1/2}dx\right]$$

2. ANTI-SYMMETRIC POTENTIAL SYSTEM

There is a large decrease in tunneling frequency when the shape of two wells are different. This is because of the lack of resonance between the two wells. Assuming the following potential wells shown in Figure 31. When the left well is lower in energy than the right well, most of lower state Ψ_0 exists in the left well and most of the next lowest well Ψ_1 is in right well. Wavefunction in right well can be approximated as

$$\Psi_1 + C\,\Psi_0 \quad , \quad \text{where } C<<1.$$

This can also apply to the potential wells that have same minima but different shape. The general conclusion of tunneling for antisymmetric potential wells is that :

1. Tunneling frequency decreases when potential wells are antisymmetric.

2. If the energy gap between two minima is about several % of barrier height, tunneling probability drops several power of ten.

This is a relation called Harmony approximation

$$\frac{\nu t}{\nu t^o} = \frac{2\,h\,\nu t^o}{[\{h\nu_t{}^o\}^2 + 16(\Delta V)^2]^{1/2}} \qquad (4)$$

Where

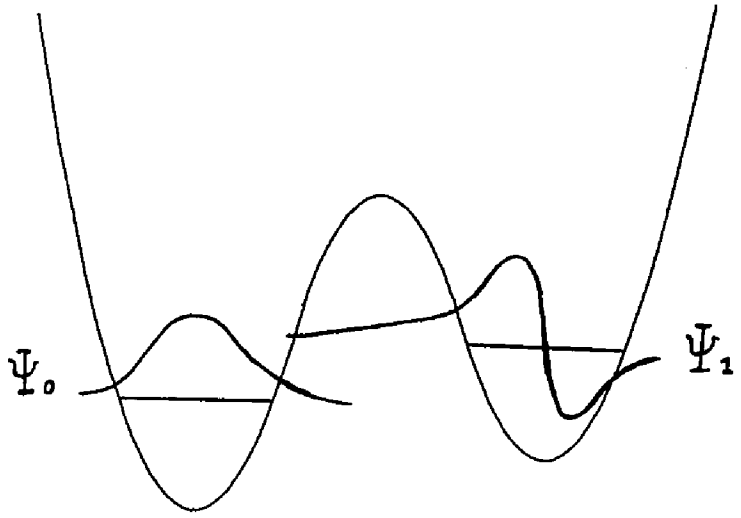

Figure 31. Schematic diagram of potential - antisymmetric case.

νt^{o} = symmetric frequency

νt = antisymmetric frequency

ΔV = energy difference between two minima.

SELECTION RULE FOR RESONANCE RAMAN(55)

The electron is assumed to be in its vibrational ground state |1> at the beginning of the scattering and is left in some vibrational state |f> at the end of the scattering. The differential cross-section is

$$\frac{d\sigma}{d\Omega} = \sum_{f}^{w_f<w} \frac{e^4 w(w-w_f)^3}{16\pi^2\varepsilon_o{}^2 h^2 C^4} \left| \sum_i \left(\frac{\varepsilon s D_{fi} \varepsilon D_{i1}}{w_i - w} + \frac{\varepsilon D_{fi} \varepsilon s D_{i1}}{w_i - w + w} \right) \right|^2$$

Here ε and εs are the unit polarization vectors. |i> is intermediate state. D is density matrix elements.

Given that $w_s = w - w_f$

Since the initial and final state are connected by a pair of electric-dipole matrix elements. Dfi and Di1, Dfi and Di1 can be non-zero only if |f> and |i> have opposite parity and |i> and |1> have opposite parity. This means |f> and |1> have the same parity. Therefore if we apply this selection rule to the problem of excited state resonance Raman spectra of D_3 symmetric Ruthenium complexes, the selection rule will be like as follows

$$\psi_+(x) = \frac{1}{\sqrt{2}} (\psi_n(x) + \psi_n(-x))$$

$$\psi_-(x) = \frac{1}{\sqrt{2}} (\psi_n(x) - \psi_n(-x))$$

$$\psi_+(-x) = \psi_+(x)$$

$$\psi_-(-x) = -\psi_-(x)$$

Since $\psi+$ has even parity and $\psi-$ has odd parity, resonance Raman bands originated from ψ_+ go to ψ_+ and originated from $\psi-$ go to $\psi-$

$\psi_+ \rightarrow \psi_+$

$\psi- \rightarrow \psi-$

$\psi_+ \not\rightarrow \psi-$

$\psi- \not\rightarrow \psi_+$

This result is shown in Figure 32.

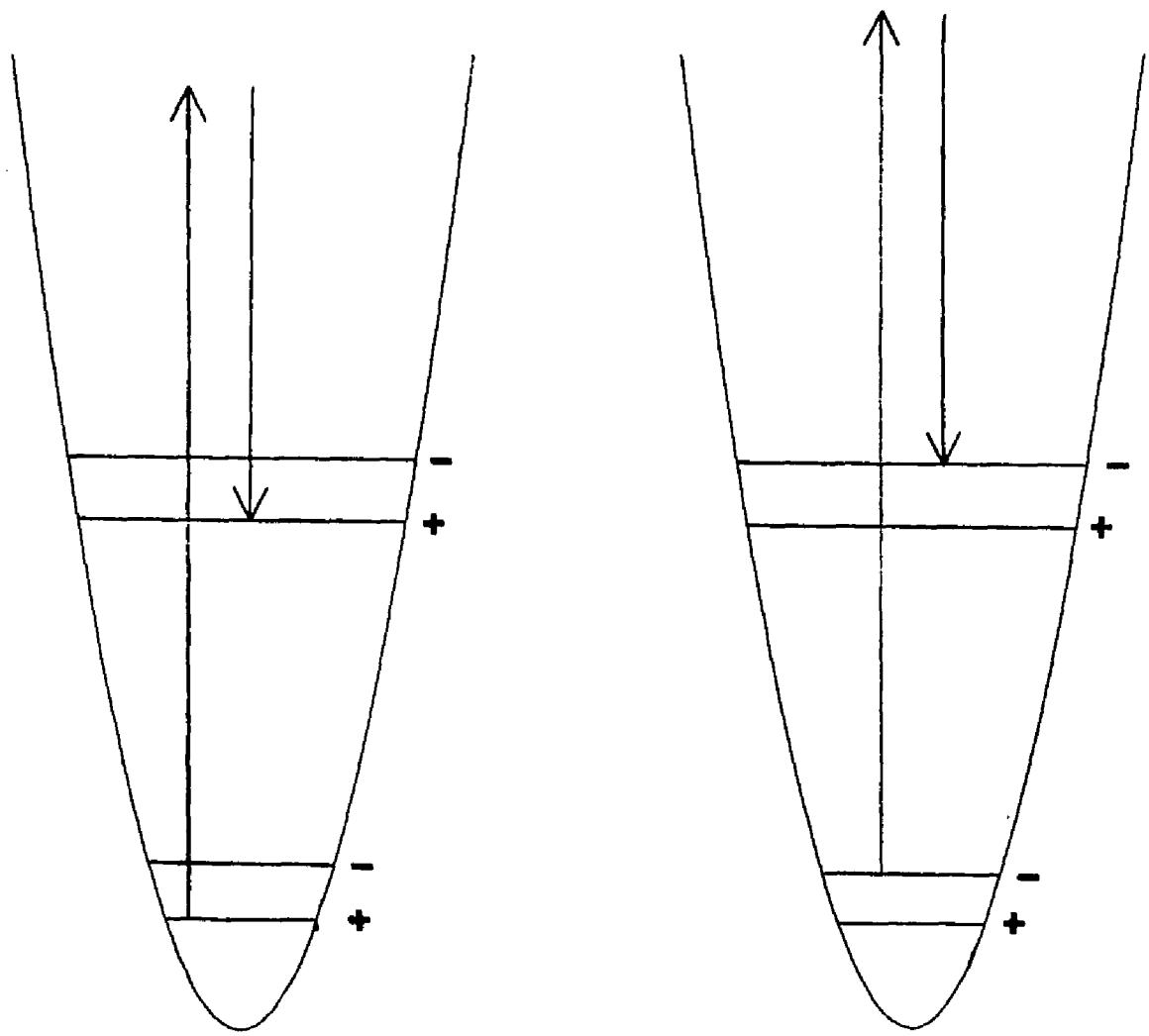

Figure 32. Selection rule for resonance Raman.

ANALYSIS OF BANDWIDTH

The tunneling analysis will now be applied to the ruthenium-polypyridine complexes. As mentioned before, the energy gap between the lower ligand bpym and higher ligand bpy is 3240cm^{-1}. Therefore the band width of the bpym excited state in Ru(bpym)(bpy)$_2^{2+}$ corresponds to the uncoupled energy level. In Figure 33, there are increases in the bandwidth of the bpym excited state 1251cm^{-1} band. This band was chosen because it does not overlap with bpy excited state bands - as the substitution of bpy ligand by bpym ligand increases. Choosing this 1251cm^{-1} band as a standard band we can estimate the tunneling splitting by comparing the increase of bandwidth. If the 1251cm^{-1} band in Ru(bpym)$_2$(bpy)$^{2+}$ or Ru(bpym)$_3^{2+}$ consists of two standard bands, the increase of the band width corresponds to the splitting. The observed band widths of Ru(bpym)(bpy)$_2^{2+}$, and Ru(bpym)$_3^{2+}$ are 11cm^{-1}, 13cm^{-1}, and 14cm^{-1}, respectively. Therefore the splittings are 2cm^{-1} for Ru(bpym)$_2$(bpy)$^{2+}$ and 3cm^{-1} for Ru(bpym)$_3^{2+}$. From this result the time required to tunnel to the other bpym potential well is calculated by using the equation (3), and tunneling times are 8ps for Ru(bpym)$_2$(bpy)$^{2+}$ and 6ps for Ru(bpym)$_3^{2+}$. This increase of speed is because Ru(bpym)$_3^{2+}$ has one more path open to tunneling to bpym than Ru(bpym)$_2$(bpy)$^{2+}$. That means three bpym potential wells are coupled stronger than two bpym potential wells in Ru(bpym)$_2$(bpy)$^{2+}$.

In Figure 34, there is the increase of bandwidth in bpy excited state 1425cm^{-1} - this band was chosen because there is no overlap

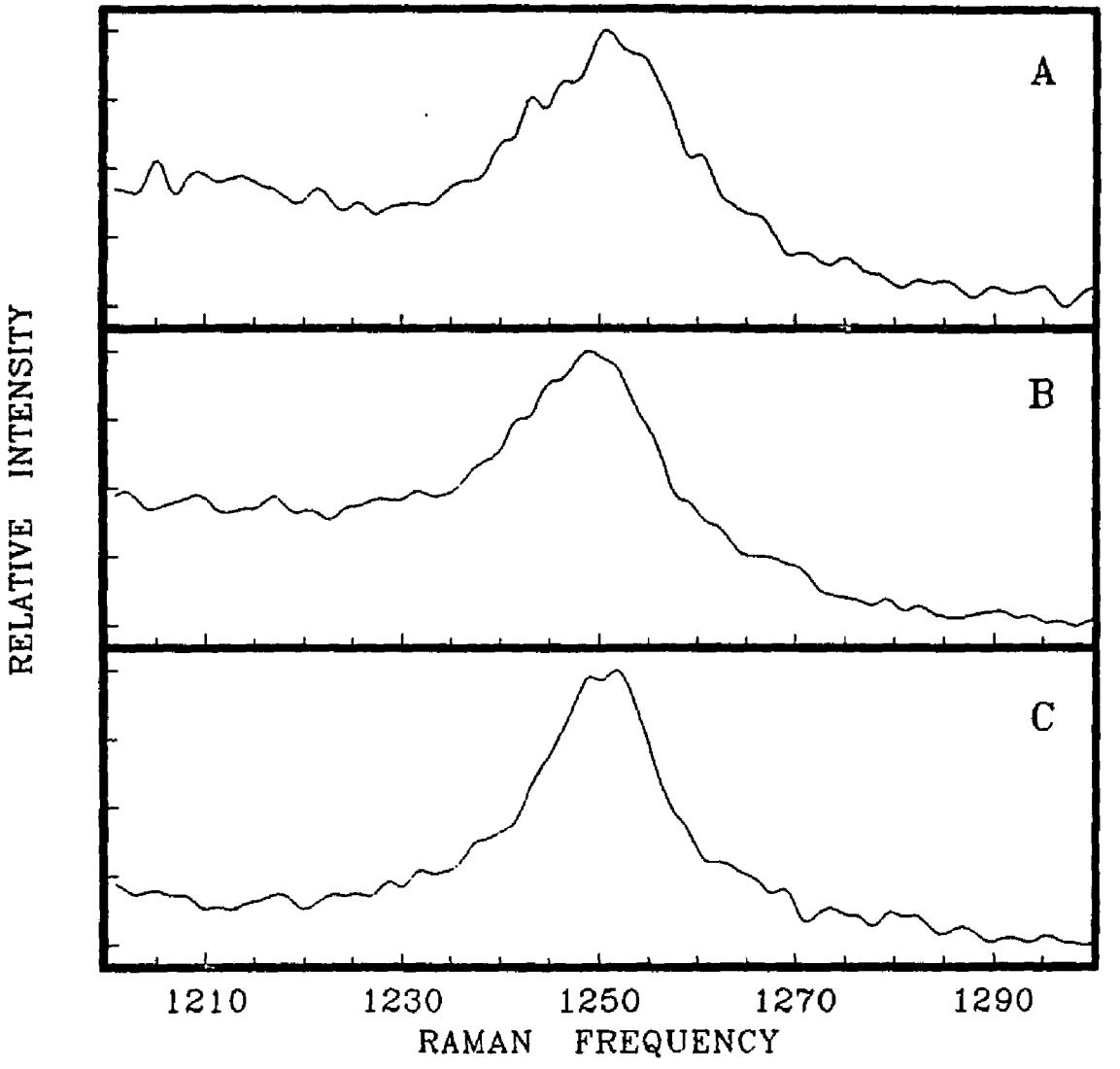

Figure 33. Comparison of 1251cm^{-1} bpym bandwidth. (A) $Ru(bpym)_3^{2+}$ in water, (B) $Ru(bpym)_2(bpy)^{2+}$ in water, and (C) $Ru(bpym)(bpy)_2^{2+}$ in water.

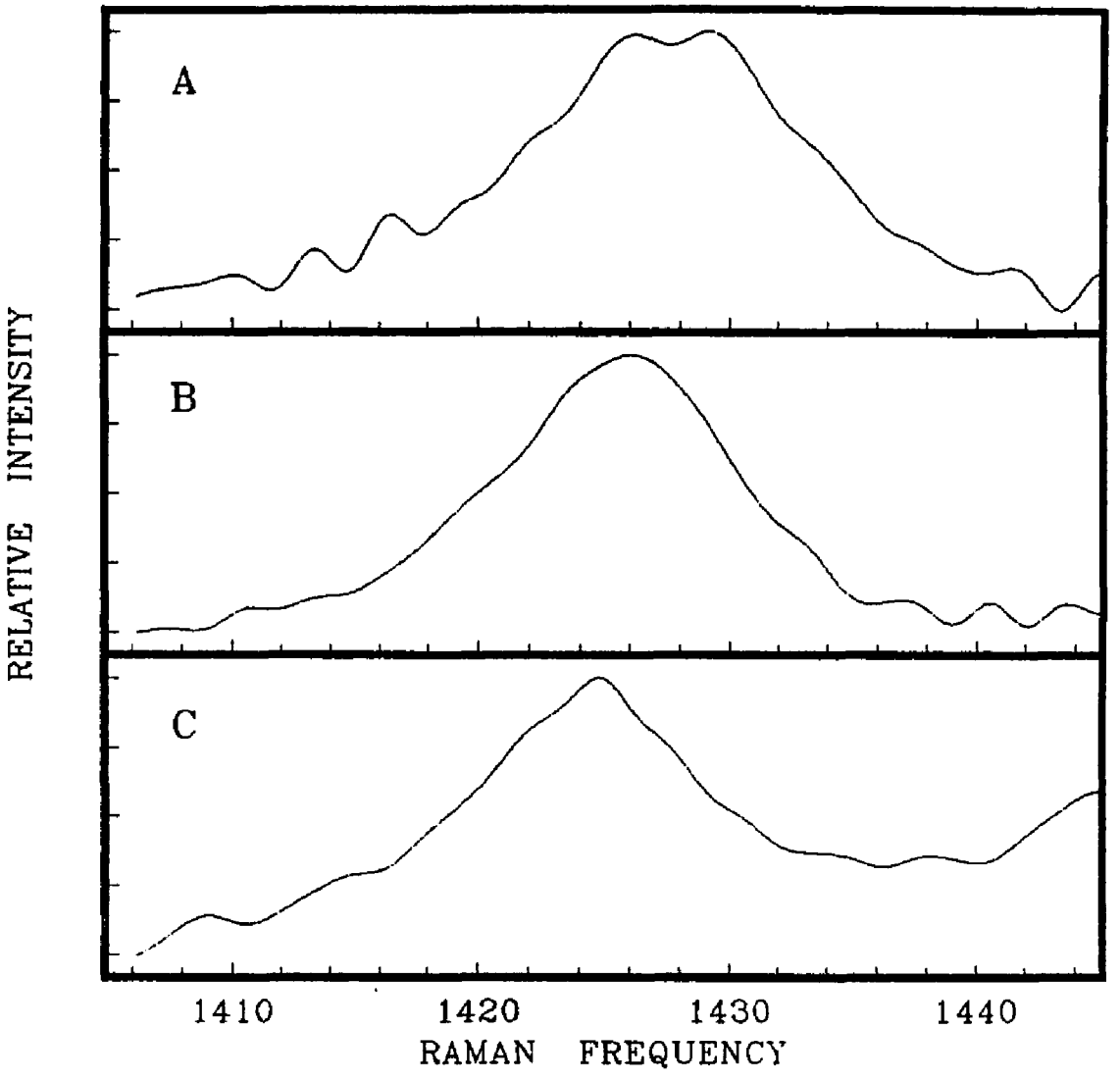

Figure 34. Comparison of 1425cm^{-1} bpy bandwidth. (A) $Ru(bpy)_3^{2+}$ in water, (B) $Ru(bpy)_2(Me_2\text{-}bpy)^{2+}$ in water, and (C) $Ru(bpy)(Me_2\text{-}bpy)_2^{2+}$ in water.

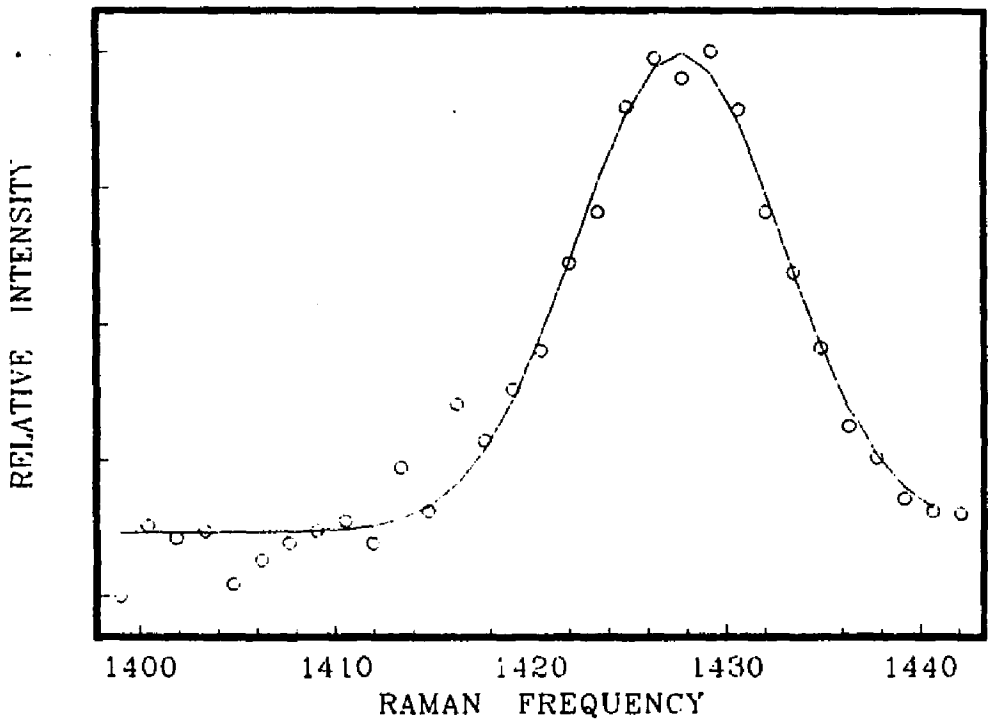

Figure 35. Gaussian fitting for bpy excited state band in $Ru(bpy)_3^{2+}$ in water.

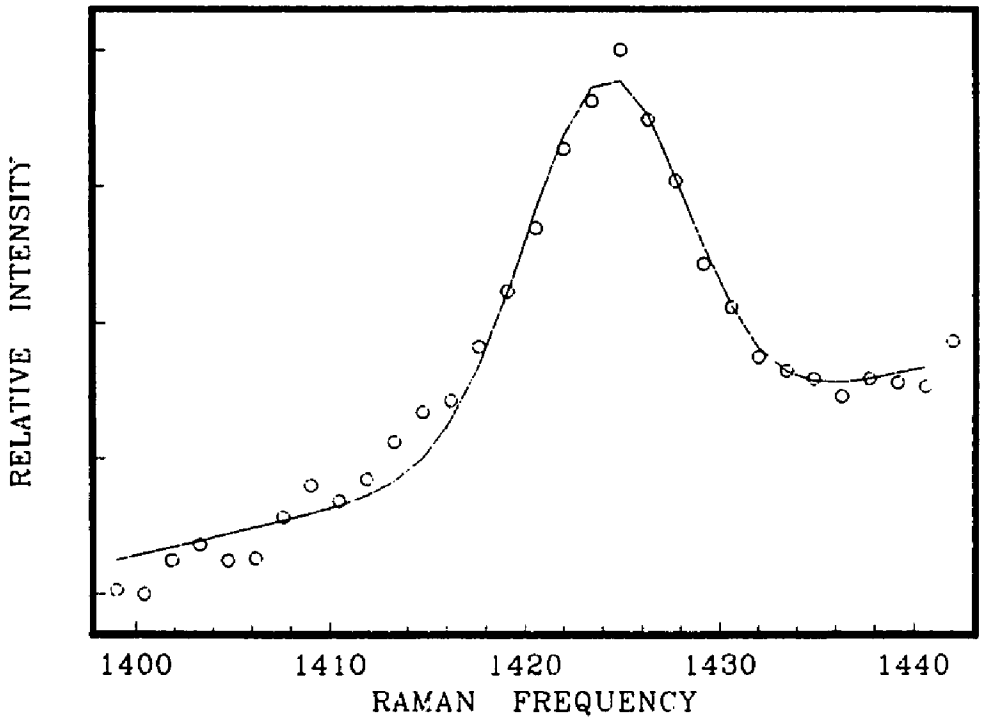

Figure 36. Gaussian fitting for bpy excited state band in $Ru(Me_2\text{-}bpy)_2(bpy)^{2+}$ in water.

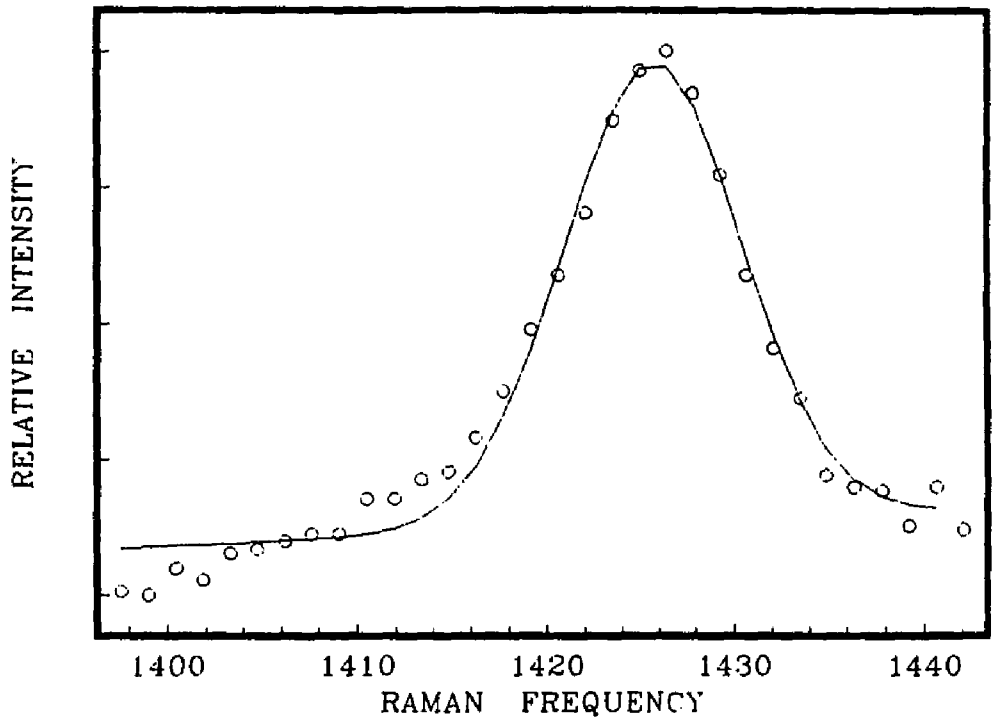

Figure 37. Gaussian fitting for bpy excited state band in $Ru(Me_2\text{-}bpy)(bpy)_2^{2+}$ in water.

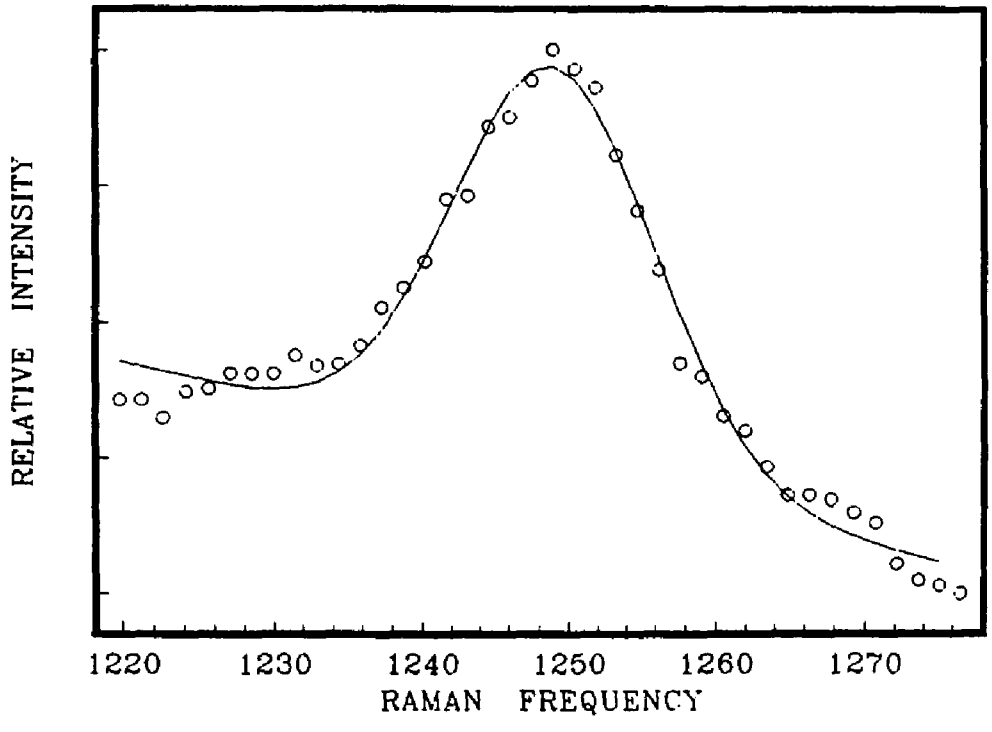

Figure 38. Gaussian fitting for bpym excited state band in $Ru(bpym)_2(bpy)^{2+}$ in water.

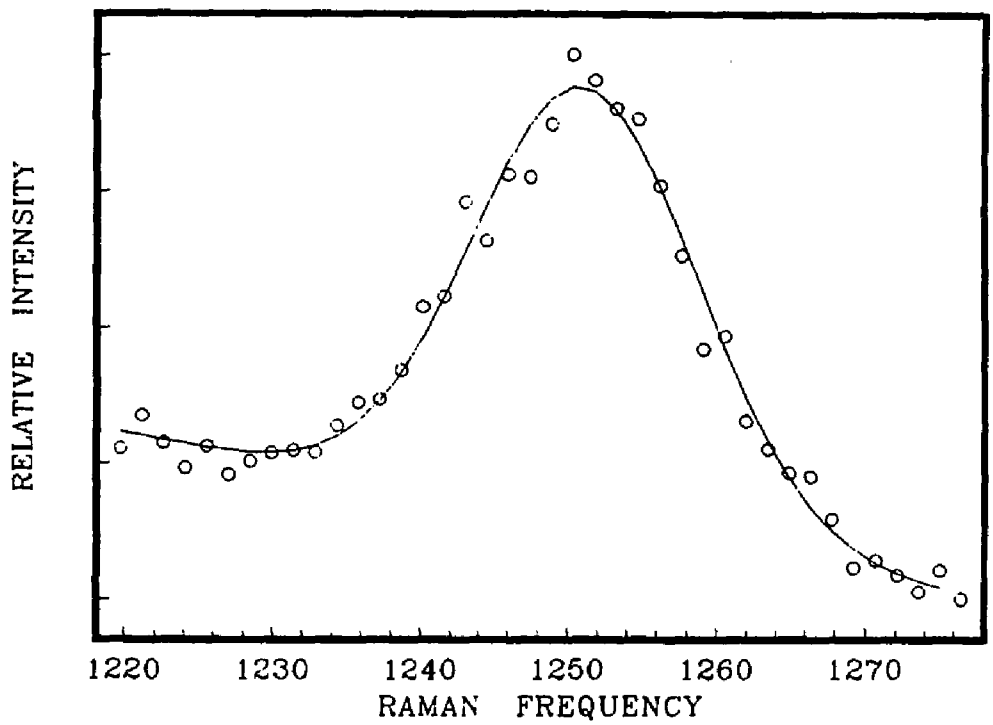

Figure 39. Gaussian fitting for bpym excited state band in $Ru(bpym)_3^{2+}$ in water.

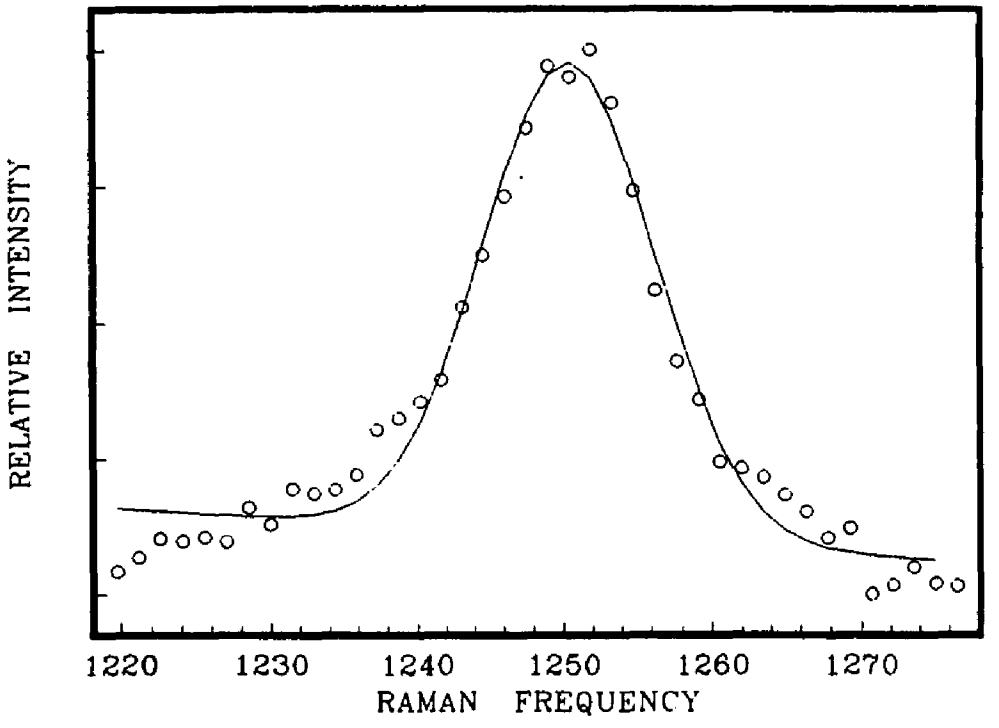

Figure 40. Gaussian fitting for bpym excited state band in $Ru(bpym)(bpy)_2^{2+}$ in water.

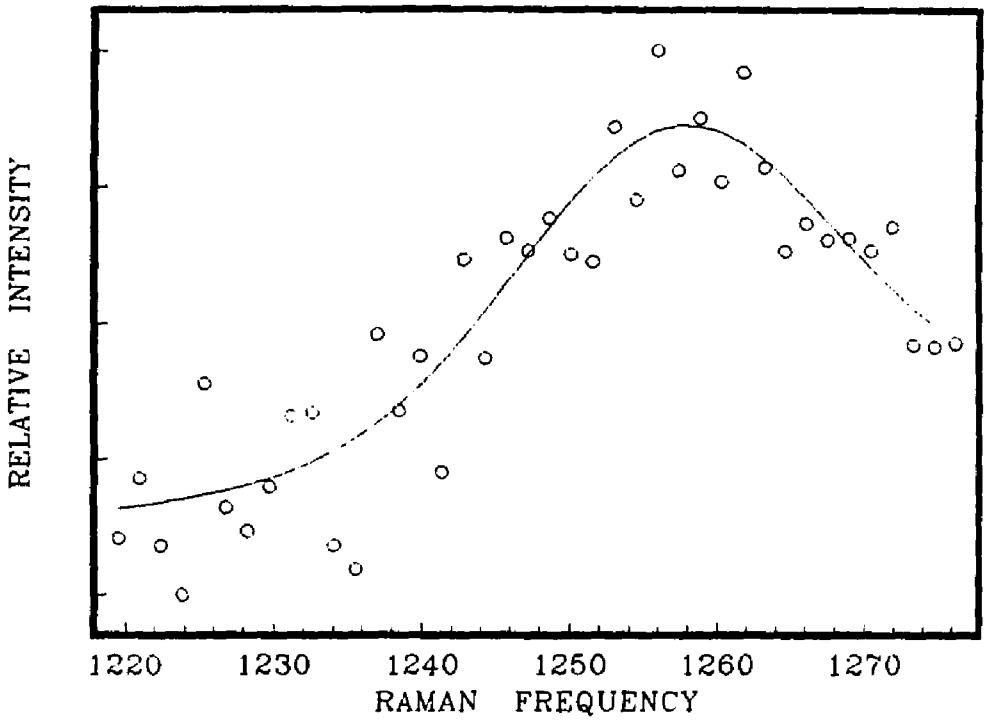

Figure 41. Gaussian fitting for bpym excited state band in $Ru(bpym)_3^{2+}$ in glycerol at 22°C.

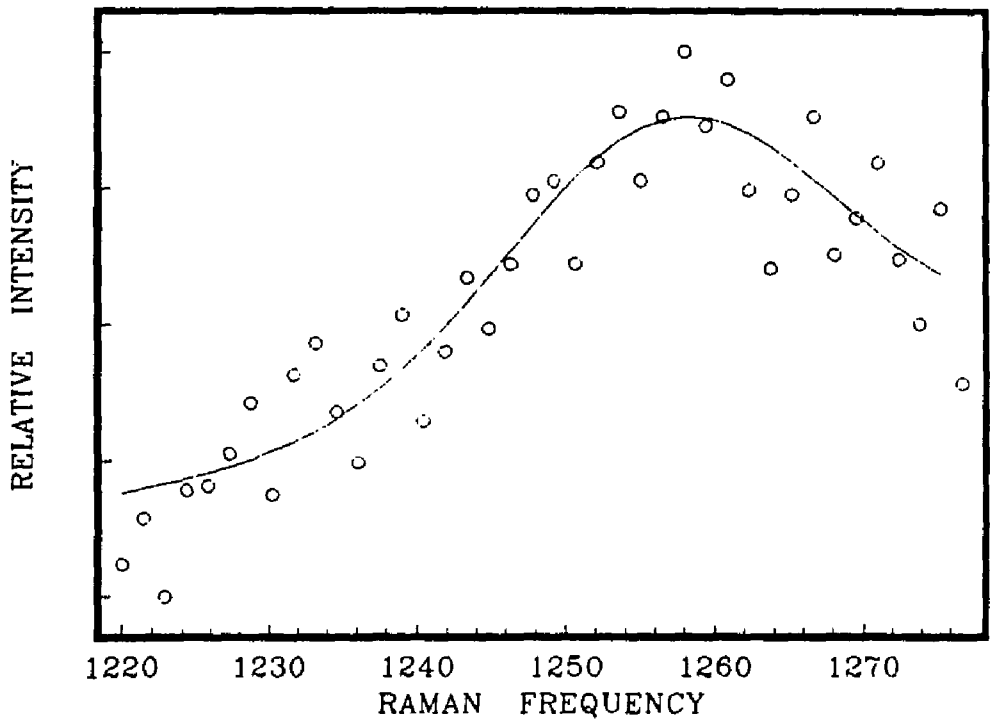

Figure 42. Gaussian fitting for bpym excited state band in $Ru(bpym)_3^{2+}$ in glycerol at -15°C.

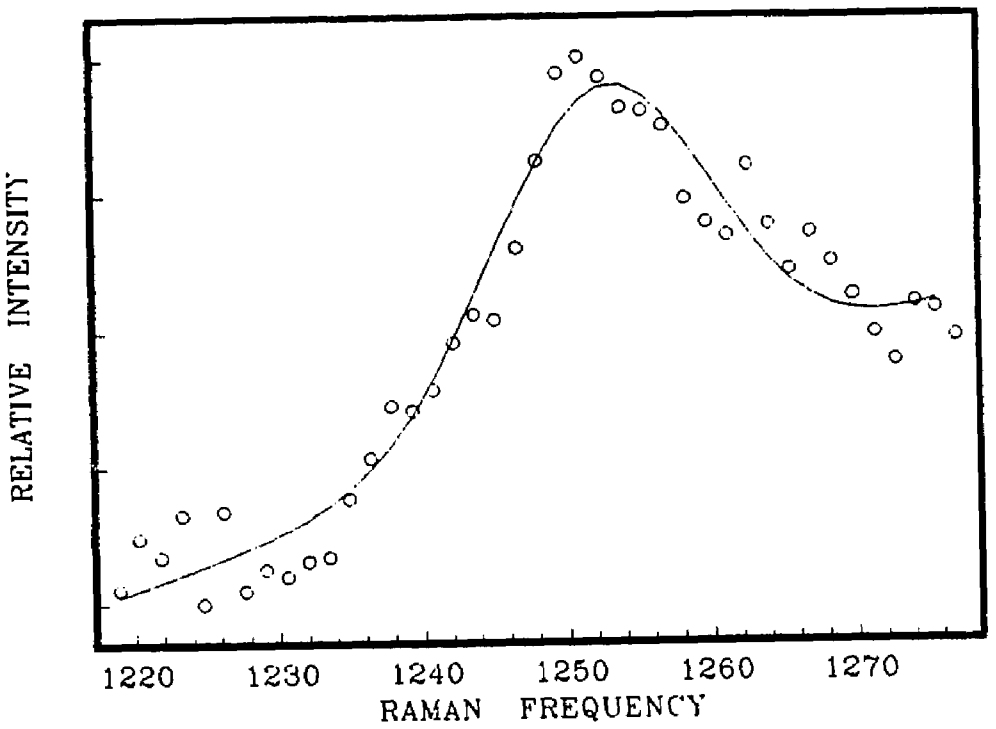

Figure 43. Gaussian fitting for bpym excited state band in $Ru(bpy)(bpym)_2^{2+}$ in glycerol at 22°C.

with Me_2-bpy excited state bands - as the increase of substitution of bpy ligand by Me_2-bpy ligand. The observed band widths of Ru(bpy)$(Me_2\text{-bpy})_2^{2+}$, Ru(bpy)$_2(Me_2\text{-bpy})^{2+}$, and Ru(bpy)$_3^{2+}$ are $8cm^{-1}$, $9cm^{-1}$, and $11cm^{-1}$, respectively. Therefore the splittings are $1cm^{-1}$, for Ru(bpy)$_2(Me_2\text{-bpy})^{2+}$ and $3cm^{-1}$ for Ru(bpy)$_3^{2+}$. The time required to tunnel to the other bpy potential well is calculated by using the equation (3), and tunneling times are 17ps for Ru(bpy)$_2Me_2$-bpy)$^{2+}$ and 6ps for Ru(bpy)$_3^{2+}$. This increase of speed is because of Ru(bpy)$_3^{2+}$ has one more path open to tunneling to bpy than Ru(bpy)$_2(Me_2\text{-bpy})^{2+}$. It is obvious that three bpy ligands couple stronger than two bpy ligands.

The observed band widths of Ru(bpym)(bpy)$_2^{2+}$ and Ru(bpym)$_3^{2+}$ in glycerol are $14cm^{-1}$ and $17cm^{-1}$, respectively. Therefore the splittings are $3cm^{-1}$ for Ru(bpym)$_3^{2+}$ in glycerol. The time required to tunnel to the other bpym potential well is calculated by using the equation(3), and tunneling times are 6ps for Ru(bpym)$_3^{2+}$. This is as fast as the tunneling speed in water. Therefore the solvent is not a major factor for interligand electron transfer through tunneling. The comparison of bpy excited state $1425cm^{-1}$ band in glycerol was not possible because of the overlap of this band with big glycerol band.

The calculated splitting of Ru(bpym)$_3^{2+}$ in water, Ru(bpym)$_3^{2+}$ in glycerol at room temperature, and Ru(bpym)$_3^{2+}$ in glycerol at -15 ° C are $3cm^{-1}$, $3cm^{-1}$, and $3cm^{-1}$, respectively. Therefore the time required to tunnel to the other bpym potential well is calculated by using the equation (3), and tunneling times are 6ps for all cases. This

constant tunneling rate also supports the idea that solvent plays a minor roll in interligand electron transfer reaction.

SUMMARY

Our study was the first direct evidence for localization in ruthenium-polypyridine complexes on the picosecond time scale. Picosecond resonance Raman spectra in viscous solvents clearly show that solvent plays a minor role in creating a localized configuration in the MLCT state.

From the analysis of bandwith, the rate of interligand electron transfer between homoligands by tunneling is several picoseconds.

REFERENCES

1. K. Kalyanasundaram, Coord. Chem. Rev., 46,139,1982
2. G. A. Crosby, R. G. Highland, and K. A. Truesdell, Coord. Chem. Rev., 64,41,1985
3. A. Juris, V. Balzani, F. Barigelletti, S. Campagna, P.Belser, and A. von Zelewski, Coord, Chem. Rev., 84,85,1988
4. E. Krausz and J. Ferguson, Prog. Inorg. Chem, 37,1989,293.
5. M.K. DeArmond, and M.L. Myrick, Acc. Chem. Res., 1989,22,364.
6. W. Halper and M.K. DeArmond, J. Lumin, 5, 225, 1972.
7. W. Halper and M.K. DeArmond, Chem. Phys. Lett., 24, 114, 1974.
8. M.K. DeArmond and C.M. Carline, Coord. Chem. Rev., 36, 325, 1981.
9. C.M. Carline and M.K. DeArmond, Chem. Phys. Lett, 89, 297, 1982.
10. R.F. Dallinger and W. H. Woodruff, J. Am. Chem. Soc., 101, 4391, 1979.
11. P.G. Bradley, N. Kress, B.A. Hornberger, R.F. Dallinger, W.H. Woodruff, J.Am. Chem. Soc., 103, 7441, 1981.
12. J. Ferguson, E.R. Krausz, and M. Maeder, J. Phys. Chem., 89, 1852, 1985.
13. J. Ferguson and E.R. Krausz, Inorg. Chem. 26, 1383, 1987.
14. J. Ferguson and E.R. Krausz, Chem. Phys. Lett, 93, 21, 1982.
15. E. Krausz, Chem, Phys. Lett., 116, 501, 1985
16. Y.J.Chang, C. Veas, and J.B. Hopokins, Appl. Phys. Lett., 49, 1758, 1986
17. Y.J.Chang, D.R. Anderson, and J.B. Hopkins, International Conference on Lasers 1986, edited by R.W. McMillan (STS,

McLean, Va., 1987),p. 169

18. M. Hunziker and A. Ludi, J.Am. Chem. Soc., 99,, 7370, 1977
19. G.H. Allen, R.P. White, D.P. Rillema, and T.J. Meyer, J. Am. Chem. Soc., 106, 2613, 1984
20. M.J. Cook, A.P. Lewis, G.S.G. McAuliffe, V. Skarda, A.J. Thomson, J.L. Glasper, and D.J. Robbins, J. Chem. Soc., Perkins Trans. 2, 1293, 1984
21. G.A. Crosby and W.H. Elfring, Jr., J. Phys. Chem., 80, 2206, 1976
22. S. Anderson, and K.R. Seddon, J.Chem. Research(S). 74, 1979
23. P.A. Mabrouk, and M.S. Wrighton, Inorg. Chem., 25, 526, 1986
24. G.H. Allen, R.P. White, D.P. Rillema, and T.J. Meyer, J. Am. Chem. Soc., 106, 2613, 1984
25. D. A. Long, Raman Spectroscopy (McGraw-Hill, New York, 1977)
26. D.P. Strommen and K. Nakamoto, J. Chem. Educ., 54, 474, 1977
27. W.H. Woodruff and S. Fabquharson, ACS Symposium series 85, 215, 1978
28. W. Keifer and H.J. Bernstein, J. Appl. Specrosc., 25, 609, 1971
29. N. Mataga, Denki Kagaku, 57, 1025, 1989
30. T.J. Meyer, Prog. Ingor. Chem., 30, 389, 1984
31. N. Sutin, Prog. Inorg. Chem., 30, 441, 1984
32. C. Creutz, Prog. Inorg. Chem., 30, 1, 1983
33. R.A. Marcus, J. Chem. Phys., 43, 679, 1965
34. N.S.. Hush, Trans. Faraday Soc., 57, 155, 1961
35. N.R. Kestner, J. Logan, and J. Jortner, J. Phys. Chem., 78, 2148, 1974
36. B.S. Brunschwig, J. Logan, M.D. Newton, and N. Sntin, J. Am. Chem. Soc., 102, 5798, 1980

37. J.J. Hopfield, Proc. Natl. Acad. Sci. U.S.A., 71, 3640, 1974

38. A.G. Motten, K. Hanck, and M.K. DeArmond, Chem. Phys. Lett., 79, 541, 1981

39. J.V. Casper, T.D. Westmoreland, G.H. Allen, P.G. Bradley, T.J. Meyer, and W.H. Woodruff, J. Am. Chem. Soc., 106, 3492, 1984

40. M. Forester and R.E. Hester, Chem. Phys. Lett., 81, 42, 1981

41. L.K. Orman and J.B. Hopkins, Chem. Phys. Lett., 149, 375, 1988

42. M.J. Cook, A.P. Lewis, G.S.G. McAulitte, V. Skarda, A.J. Thomson, J.L. Glasper, and D.J. Robbins, J. Chem. Soc., Perkin Trans. 2, 1293, 1984

43. G.A. Crosby and W.H. Elfring, Jr., J. Phys. Chem., 80, 2206, 1976

44. Y.J. Chang, L.K. Orman, D.R. Anderson, T. Yabe, and J.B. Hopkins, J. Chem. Phys., 87, 3249, 1987

45. L.K. Orman, Y.J. Chang, D.R. Anderson, T. Yabe, X. Xu, S. Yu, and J.B. Hopkins, J. Chem. Phys., 90, 1496, 1989

46. T. Yabe, D.R. Anderson, L.K. Orman, Y.J. Chang, and J.B. Hopkins, J. Phys. Chem, 93, 2302, 1989

47. Y.J. Chang, X. Xu, T. Yabe., S. Yu, D.R. Anderson, L.K. Orman, and J.B. Hopkins, J. Phys. Chem. 94, 729, 1990

48. L.K. Orman, D.R. Anderson, T. Yabe, and J.B.Hopkins, Advances in Chemistry Series No. 226: Inorganic Compounds with Unusual Properties, In Press.

49. J.V. Casper and T.J. Meyer, J. Am. Chem. Soc., 105, 5583, 1983

50. J.B. Hopkins and P.M. Rentzepis, Chem. Phys. Lett., 142, 503, 1987

51. P.J. Carroll and L.E. Brus, J.Am.Chem.Soc., 109,7613,1987

52. D.P. Rillema, G. Allen, T.J. Meyer, and D. Conrad, Inorg. Chem., 22, 1617, 1983

53. P.A. Mabrouk and M.S. Wrighton, Inorg. Chem., 25, 526, 1986

54. R.P. Bell, The Tunnel Effect in Chemistry, 1980, Chapman and Hill

55. R. Loudon, The Quantum Theory of Light, 1983, Oxford University Press.

CHAPTER II

INTRODUCTION

This chapter is based on our paper submitted to Journal of Physical Chemistry in January 1990. What follows is a modified version of this paper.

Picosecond two color Raman spectroscopy is applied to measure ILET in mixed ligand complexes of 2, 2'-bipyridine (bpy) with 2,2'-bipyrimidine (bpym) or 4,4'-dicarboxy-2,2'-bipyridine (carboxy-bpy). This two color Raman technique not only increases the confidence of the spectroscopic assignments but also significantly reduces the spectral congestion by removing ground state bands from the spectrum. Conclusions regarding ILET dynamics are therefore much more straightforward.

SPECTROSCOPIC ANALYSIS OF BPYM COMPLEXES

In order to extract ILET dynamics from the vibrational spectrum, assignments must be established for both the electronic state and ligand parentage of the observed vibrational bands. Figure 1 shows the one color Raman spectrum of $[Ru(bpym)_3]^{2+}$ at 354.7nm. Excitation at this wavelength produces the excited MLCT state. In addition 354.7nm is also in resonance with an electronic absorption of the excited MLCT state. As a result, one color Raman spectra obtained at this wavelength will exhibit vibrational bands from both the ground and excited electronic states. The electronic state parentage of the vibrational bands is determined by observing the laser power dependence of the spectrum. The low laser power spectrum is shown in Figure 1A and the high laser power spectrum in Figure 1B. Bands assigned to the ground state are connected by dashed lines. Bands which appear to be enhanced in the high power spectrum are assigned to the excited MLCT state and these bands are indicated by asterisks. It is worth noting that the strong ground state doublet at 1553 and 1581 cm^{-1} becomes unresolved in Figure 1B due to the growth of an excited state band at 1560 cm^{-1}. The assignments are confirmed in the two color spectrum discussed later where ground state bands are removed by a spectrum differencing technique. These results agree qualitatively with earlier(1) one color transient Raman results on $[Ru(bpym)_3]^{2+}$ with the exception that there are many more resolved features in the present experiment.

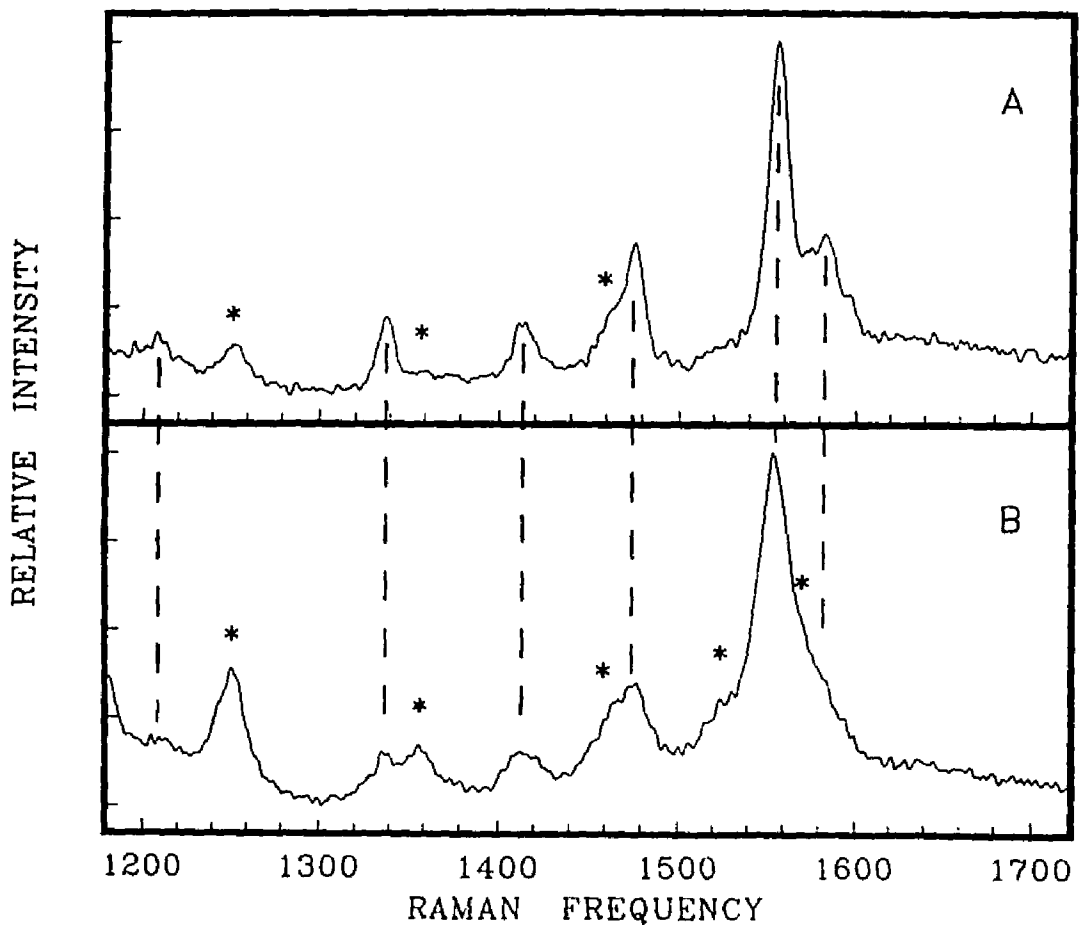

Figure 1: One color picosecond Raman spectrum obtained by excitation at 354.7nm for $Ru(bpym)_3^{2+}$. The two spectra are produced under different laser energy densities. The relative difference in laser fluence is $\approx 5\times10^3$. Dashed lines are drawn at the frequencies corresponding to bands assigned to the ground electronic state. Asterisks denote excited state bands. Spectra were obtained in a rotating quartz cell.

a) Ground state spectrum obtained under low power excitation.
b) Excited state and ground state spectra obtained under high power excitation. 25μJ/pulse in a 0.1mm diameter beam waist.

The one color Raman spectra for the series of mixed ligand $[Ru(bpym)_{3-n}(bpy)n]^{2+}$ are shown in Figure 2 where n = 0,1,2,3 in spectra A through D respectively. The mixed ligand complexes in spectra B and C show a mixture of ground state bands from each ligand. The ground state bands assigned to the bpy ligand are easy to identify in the spectra because the frequencies are very similar to those found in $[Ru(bpy)_3]^{2+}$ which has been fully characterized.(2-4) These bands are connected by solid lines in Figure 2. This method of assigning the ligand parentage of Raman bands depends on the invariance of the vibrational frequencies of a particular ligand to chemical substitution at another coordination site of the complex. For the complexes discussed in this paper most frequencies remain constant within the resolution of the apparatus as summarized in Table 1 and Table 2. As a result, this method provides extremely high confidence in the assignments.

The filled in bands in Figure 2 are assigned to the excited MLCT state localized on the bpym ligand. These bands are identical to those identified in the $[Ru(bpym)_3]^{2+}$ spectra shown in Figure 1. The excited state bands due to bpy appear to be absent in the mixed ligand spectra shown in Figure 2B and 2C. Dashed lines indicate the *expected* position of the bpy excited state bands. In the $[Ru(bpy)_3]^{2+}$ spectrum shown in Figure 2D these excited state bands are the dominate features observed. However, they are clearly absent in the mixed ligand spectra shown in Figure 2B and 2C. For completeness, it should be noted that the bpy band at 1491 cm^{-1} was once assigned(2-3) as an excited state band but later reassigned(4) as a ground state band.

TABLE 1

Assignment	$[Ru(bpym)_3]^{2+}$	$[Ru(bpym)_2(bpy)]^{2+}$	$[Ru(bpym)(bpy)_2]^{2+}$	$[Ru(bpy)_3]^{2+}$
Bpym*	669.	669.	669.	–
Bpym	1013.	1014.	1013.	–
Bpym*	1040.	1039.	1040.	–
Bpym*	1179.	1179.	1177.	–
Bpy*	–	–	–	1209.
Bpym*	1252.	1247.	1247	–
Bpy*	–	–	–	1283.
Bpy	–	1321.	1317.	1316.
Bpym*	1322.	–	1320.†	–
Bpym	1338.	1337.	1333.	–
Bpym*	1356.	1357.	1356.	–
Bpym	1412.	1413.	1409.	–
Bpy*	–	–	–	1426.
Bpym	1474.	1473.	1469.	–
Bpym*	–	–	1474.†	–
Bpy*	–	–	–	1480.
Bpy	–	1494.	1491.	1489.
Bpym*	1486.	–	1493.†	–
Bpy*	–	–	–	1502.
Bpym*	1524.	1524.	1526.	–
Bpy*	–	–	–	1546.
Bpy	–	–	–	1560.
Bpym	1553.	(1556.)	(1561.)	–
Bpym*	–	–	1560.†	–
Bpym	1581.	–	–	–
Bpy	–	1607.	1605.	1605.

Assignments and Stokes frequencies for the ground and excited states. Bands in parenthesis are believed to be partially overlapped. In this case the assignment is given to the band with the largest contribution to the peak intensity. First column gives ligand parentage. Excited state bands are identified by asterisks. Vibrational frequencies were obtained using a calibration procedure which included the attenuated Rayleigh line in the Raman spectrum. Frequencies are in units of cm^{-1} and are believed to be accurate to $\pm 1.5\ cm^{-1}$. †Frequencies determined from the pure two color spectrum shown in Figure 3C.

TABLE 2

Assignment	$[Ru(carboxy\text{-}bpy)_3]^{2+}$	$[Ru(carboxy\text{-}bpy)(bpy)_2]^{2+}$	$[Ru(bpy)_3]^{2+}$
Bpy*	–	–	1209.
Carboxy-bpy*	1216.	1214.	–
Carboxy-bpy	1276.	1272.	–
Carboxy-bpy*	1283.	1278.	–
Bpy*	–	–	1282.
Carboxy-bpy	1298.	–	–
Carboxy-bpy*	1310.	1307.	–
Bpy	–	1317.	1316.
Carboxy-bpy*	1364.	1363.	–
Carboxy-bpy	1373.	1375.	–
Bpy*	–	–	1426.
Carboxy-bpy	1433.	–	–
Carboxy-bpy*	1449.	1447.	–
Carboxy-bpy	1480.	–	–
Bpy*	–	–	1480.
Bpy	–	(1491.)	1489.
Bpy*	–	–	1502.
Bpy*	–	–	1546.
Carboxy-bpy	1546.	1542.	–
Bpy	–	(1561.)	1560.
Bpy	–	(1605.)	1605.
Carboxy-bpy	1618.	–	–

Assignments and Stokes frequencies for the ground and excited states. Bands in parenthesis are believed to be partially overlapped. In this case the assignment is given to the band with the largest contribution to the peak intensity. First column gives ligand parentage. Excited state bands are identified by asterisks. Vibrational frequencies were obtained using a calibration procedure which included the attenuated Rayleigh line in the Raman spectrum. Frequencies are in units of cm^{-1} and are believed to be accurate to $\pm 1.5\ cm^{-1}$.

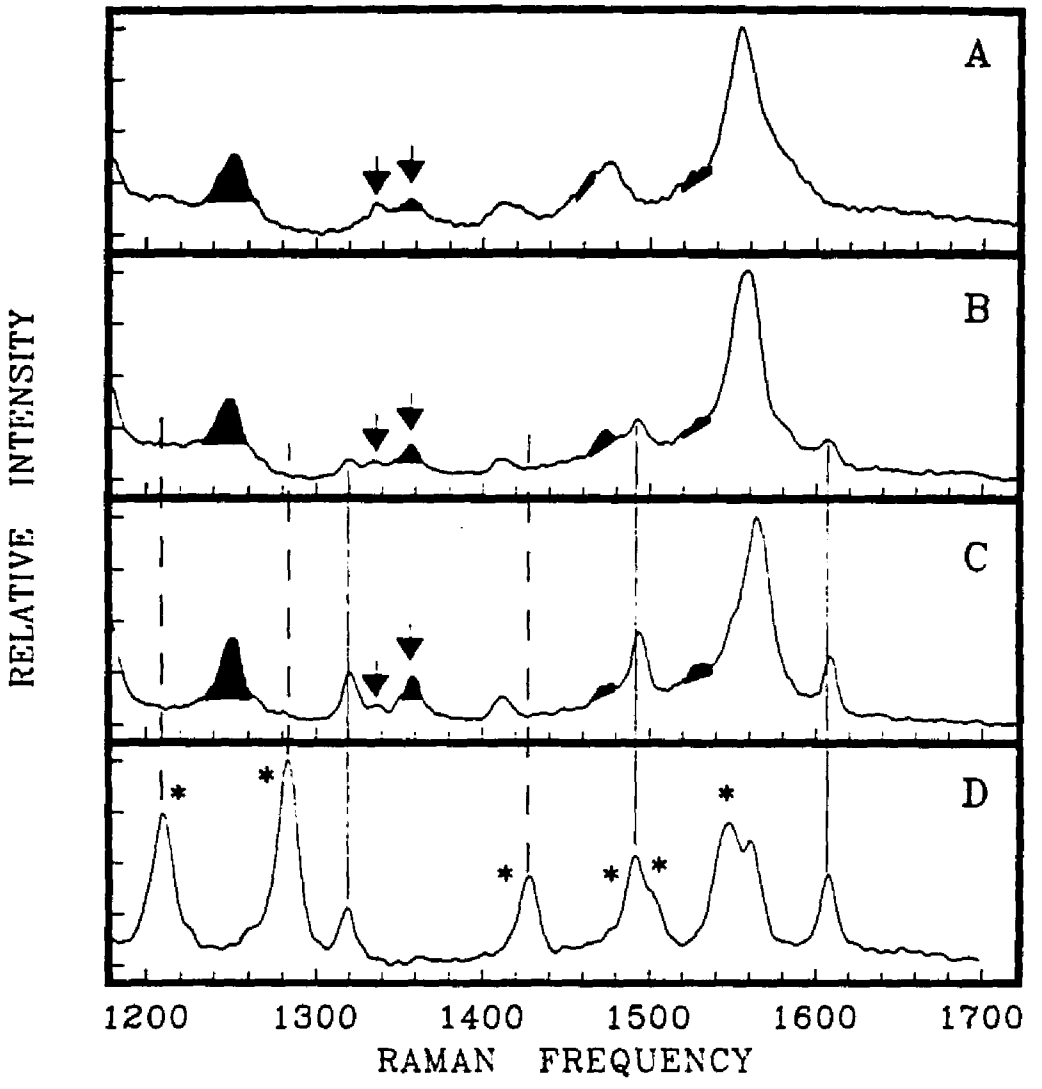

Figure 2: One color picosecond Raman spectrum obtained at 354.7nm. Concentration is 1mM. Laser fluence is 25μJ/pulse in a 0.1mm diameter beam waist. Dashed lines are drawn at the frequencies corresponding to excited state bpy bands. Solid lines indicate ground state bpy bands. The filled in peaks are excited state bpym bands. Asterisks denote excited state bpy bands. Arrows are explained in the text. Spectra were obtained in a rotating quartz cell.

a) $Ru(bpym)_3^{2+}$
b) $Ru(bpym)_2(bpy)^{2+}$
c) $Ru(bpym)(bpy)_2^{2+}$
d) $Ru(bpy)_3^{2+}$

Confirmation of excited state band assignments is demonstrated in the two color spectrum shown in Figure 3. In this figure the spectra are obtained under conditions where the excited MLCT state is produced by excitation at 532nm and probed by a low fluence laser pulse at 354.7nm. The raw two color spectrum is presented in frame A and the one color spectrum in frame B. The pure transient spectrum in frame C is calculated as the difference spectrum A-B. In figure 3C ground state bands have completely subtracted out. This transient spectrum contains bands due entirely to the excited MLCT state. The bands are denoted by asterisks in the spectrum. The assignments obtained from the two color data agree completely with those resulting the *one color* spectra discussed in Figure 1. Several new bands which were obscured in the one color data are now apparent in Figure 3C. In particular, the excited state bands at 1560cm^{-1} which was overlapped by ground state bands in the one color spectrum is now clearly visible. The existance of this excited state band is responsible for the apparent frequency shift of the cluster of unresolved bands near 1553 cm^{-1} in Figures 2A-2C. As the ground state bpym bands become less intense in Figure 2B and 2C, the excited state bpym band at 1560cm^{-1} begins to dominate.

The result of ILET on the relative population of electrons localized on the bpy and bpym ligand are shown in Figure 4. The top frames is a pure two color transient spectrum of a 50% mixture of $[Ru(bpy)_3]^{2+}$ and $[Ru(bpym)_3]^{2+}$. The bottom frame is the pure two color transient spectrum of the mixed ligand complex $[Ru(bpym)(bpy)_2]^{2+}$. The filled in peaks correspond to the excited

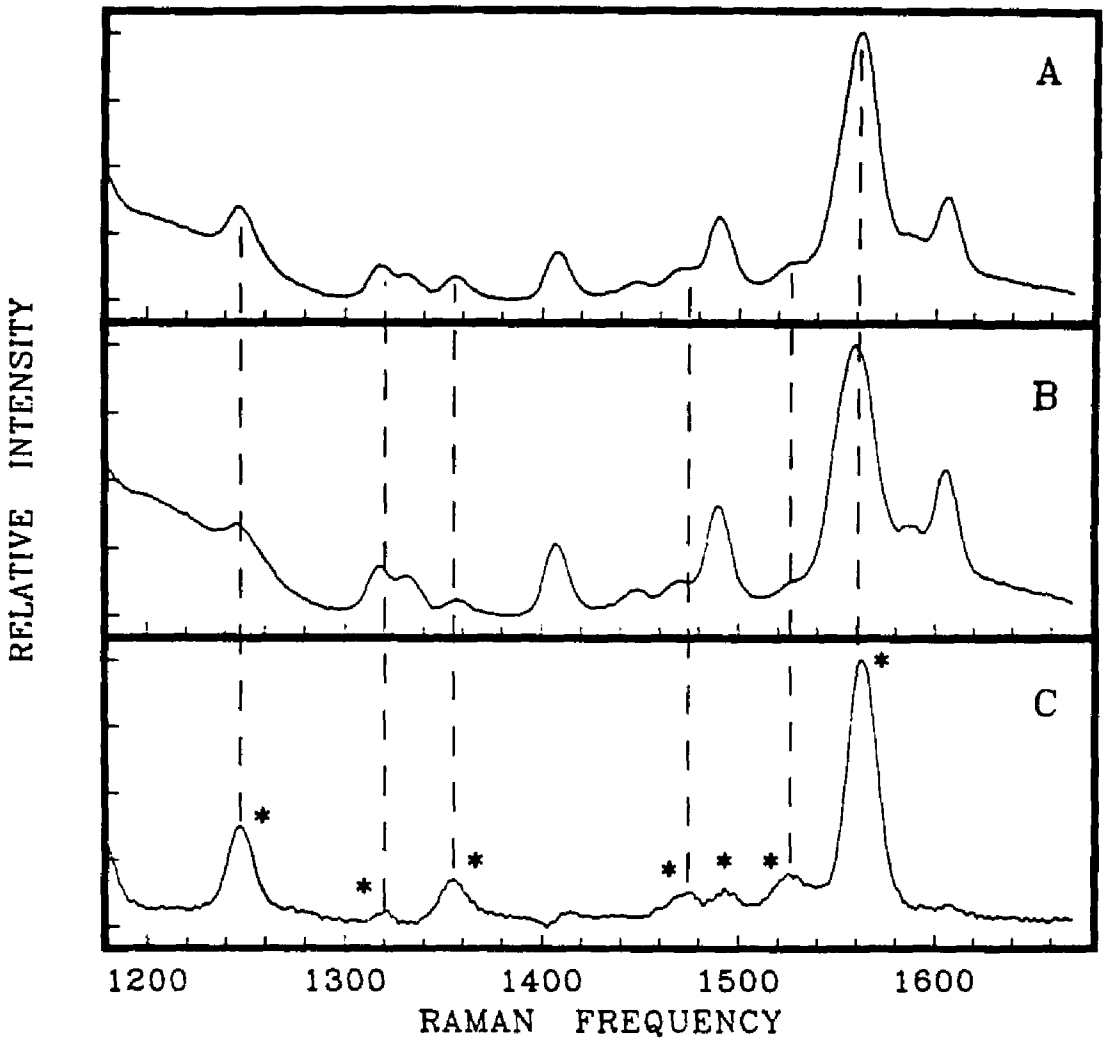

Figure 3: Comparison of one color and two color picosecond Raman spectra of $Ru(bpy)_2(bpym)$. Concentration is 2mM. Dashed lines are drawn at some of the frequencies of excited state bpym bands. Asterisks also indicate excited state bpym bands. Time delay between pump and probe pulses is 0ps. Spectra were obtained in a flowing quartz cell.

a) Total raw two color spectrum obtained at 354.7nm with 532nm excitation.
b) One color spectrum obtained at 354.7nm.
c) Pure two color spectrum obtained by subtracting spectrum (b) from spectrum (a).

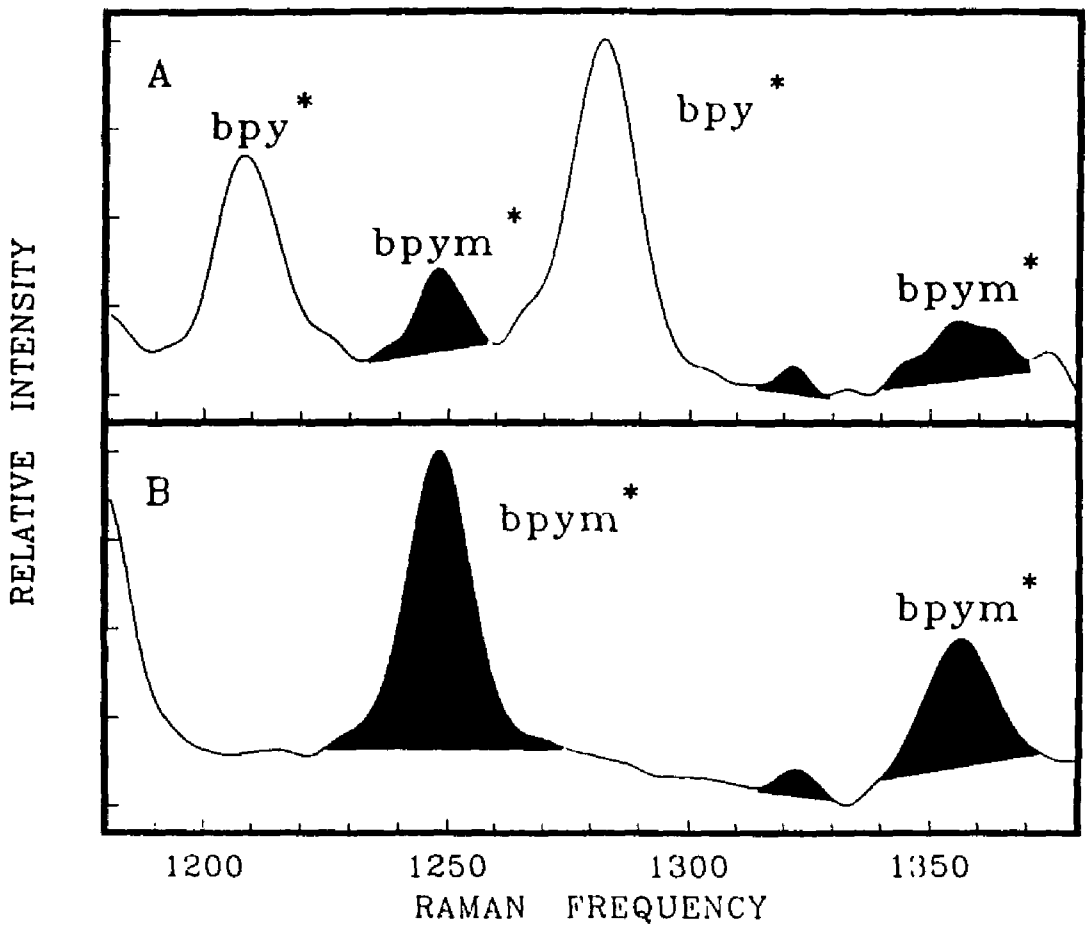

Figure 4: Pure two color picosecond Raman spectra of $Ru(bpy)_2(bpym)$ obtained by excitation at 532nm and probing at 354.7nm concentration is 2mM. All three spectra have been corrected for one color background signal using the procedure described in the text. Filled in bands correspond to the excited state of bpym. Time delay between pump and probe pulses is 0ps. Spectra were obtained in a free flowing jet.

a) Expanded spectrum of 50:50 mixture of $Ru(bpy)_3^{2+}$ and $Ru(bpym)_3^{2+}$.

b) Expanded spectrum of $Ru(bpy)_2(bpym)^{2+}$ with the time delay between the pump and probe of 0ps.

MLCT state localized on the bpym ligand. The data in this figure confirm the conclusion that no bands are observed in the mixed ligand complex due to the excited MLCT state localized on the bpy ligand. In fact, the limited spectral congestion provided by the two color technique allows us to state that the fraction of the excited state which is localized on the bpy ligand must be less than 1% compared to that localized on the bpym ligand in the first 30ps. Time delay spectra were obtained out to 20ns by optically delaying the pump and probe lasers. No further time evolution of the excited state was observed.

SPECTROSCOPIC ANALYSIS OF CARBOXY COMPLEXES

The vibrational analysis of the spectra corresponding to the carboxy-bpy complexes is similar to that discussed above. For this series of complexes the spectra are quite congested. However, the analysis can be simplified using two color spectroscopy. Figure 5 shows the raw two color, one color and pure transient spectra of $[Ru(carboxy\text{-}bpy)_3]^{2+}$ in frames A-C respectively. Transient bands assigned to the excited MLCT state localized on the carboxy-bpy ligand are indicated by asterisks in Figure 5C. Ground state bands appear as negative-going peaks due to a combination of population bleaching and a change in optical density of the solution which results from the absorption of the transient.(4-6)

Pure transient spectra for the mixed ligand complexes $[Ru(carboxy\text{-}bpy)_{3-n}(bpy)_n]^{2+}$ are shown in Figure 6 where n = 0,2,3 in frames A through C respectively. The filled in peaks are the excited state bands assigned to carboxy-bpy from Figure 5. Dashed lines indicate the expected position of the bpy excited state bands. Ground state bands from bpy and carboxy-bpy are connected by solid lines. It is apparent from the data in Figure 6 that bpy excited state bands are *not* observed in the spectrum of the mixed ligand complex. It should be noted that the largest bpy excited state band at 1282 cm^{-1} is *near*, but clearly shifted in frequency, from the carboxy-bpy excited state band at 1274 cm^{-1}. The bpy excited state bands at 1426, 1480, and 1502cm^{-1} are absent from the spectrum. At 1546cm^{-1} there is an apparent 'peak' in the pure two color spectrum (Figure 6B) which

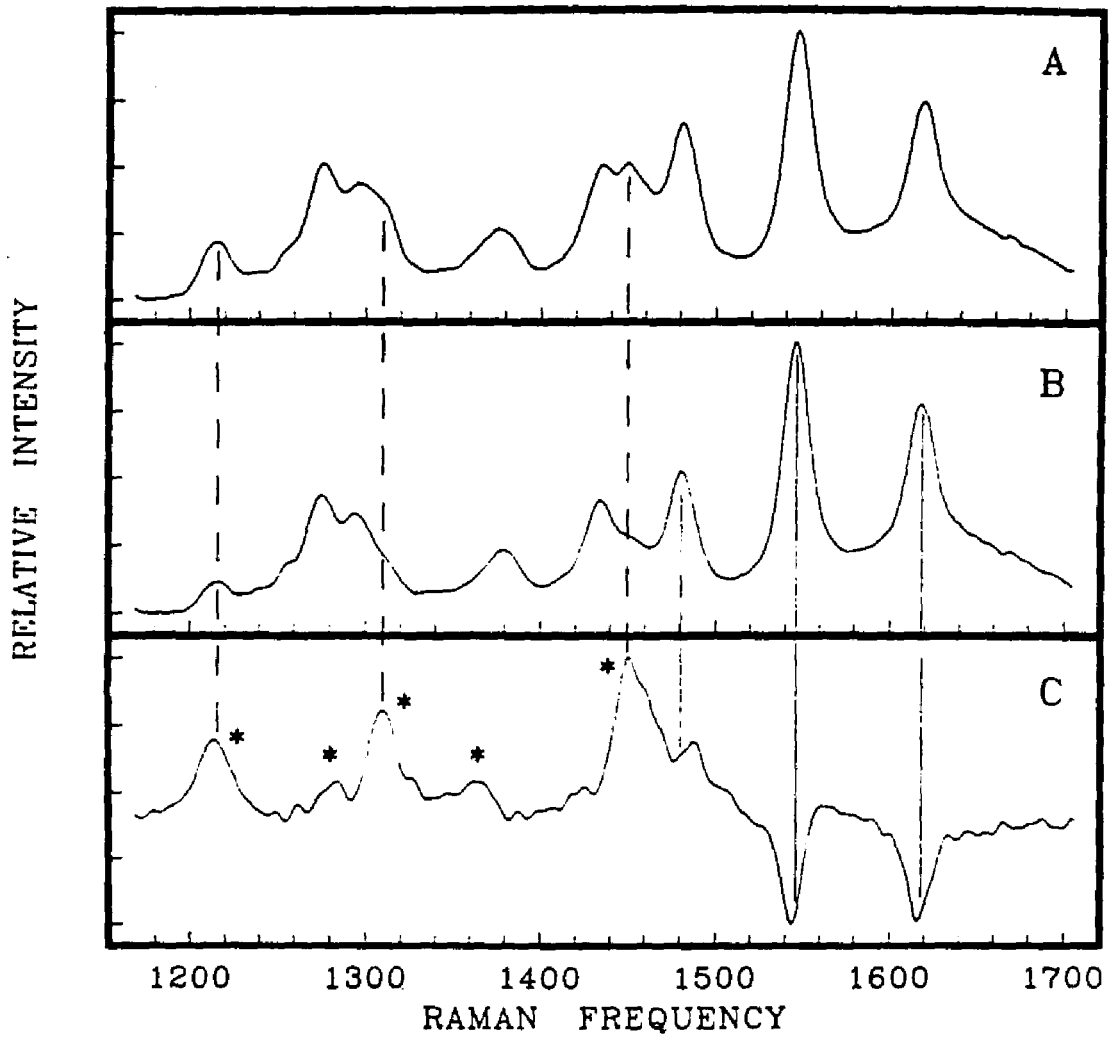

Figure 5: Comparison of one color and two color picosecond Raman spectra of $[Ru(carboxy\text{-}bpy)_3]^{2+}$. Concentration is 2mM. Dashed lines are drawn at some of the frequencies of excited state carboxy-bpy bands. Asterisks also indicate excited state carboxy-bpy bands. Solid lines denote ground state bands. Time delay between pump and probe pulses is 0ps. Spectra were obtained in a free flowing jet.

a) Total raw two color spectrum obtained at 354.7nm with 532nm excitation.
b) One color spectrum obtained at 354.7nm.
c) Pure two color spectrum obtained by subtracting spectrum (b) from spectrum (a).

might be mistakenly assigned as a bpy excited state band. This 'peak' is not an excited state band. It appears as a result of the two adjacent ground state bands (indicated by solid lines) which are undergoing depletion.

The signal-to-noise in these spectra allow a limit of less than 3% to be placed on the excited state population which could be localized on the bpy ligand after the first 30ps. Time delay spectra were obtained out to 20ns with no further time evolution of the excited state observed.

RATES OF INTERLIGAND ELECTRON TRANSFER

One of the problems with abstracting interligand electron transfer rates from the Raman data presented in this paper is that no dynamics are actually observed--the growth of one transient at the same rate as the decay of another is not observed. It might be argued that Raman scattering from the higher energy ligand is not observed because the resonance Raman enhancement for this ligand is reduced in the mixed ligand complexes. This possibility cannot be entirely ruled out. However, there is one piece of experimental data which suggests that this is not the case. Consider the lower energy ligand which is thought to be the final acceptor of MLCT excitation (bpym or carboxy-bpy). In both the bpym and the carboxy-bpy series of complexes, there is a very dramatic change in the ratio of the intensities of the ground to excited state Raman bands. In particular, consider the bpym series of complexes shown in Figure 2 and compare the bpym ground and excited state band at 1338 and 1356cm^{-1} respectively. These two bands are marked by arrows in Figures 2A to 2C. As more *bpy* is substituted into the complex, (Figure 2B and 2C) the ground state *bpym* band decreases in intensity by a factor of three compared to the excited state band. In other words, as the concentration of bpym in the complex is reduced, the ground state bpym band decreases in intensity much faster than the excited state bpym band. This result is interpreted to indicate that there is another route to excitation of the bpym ligand, namely through the bpy ligand. If this is true the intensity of excited state bpym will remain invariant to ligand subsitution since in every case $[Ru(bpym)_3]^{2+}$,

$[Ru(bpym)_2(bpy)]^{2+}$, and $[Ru(bpym)(bpy)_2]^{2+}$ one bpym excited state is produced regardless of which ligand is initially excited. This same result is found for the carboxy-bpy series of complexes shown in Figure 6. The transient Raman results presented in this paper therefore suggest that fast ILET is occurring and is largely complete during the time window sampled by the laser pulsewidth. This conclusion suggest a rate significantly faster than $\geq 3x10^{10}s^{-1}$.

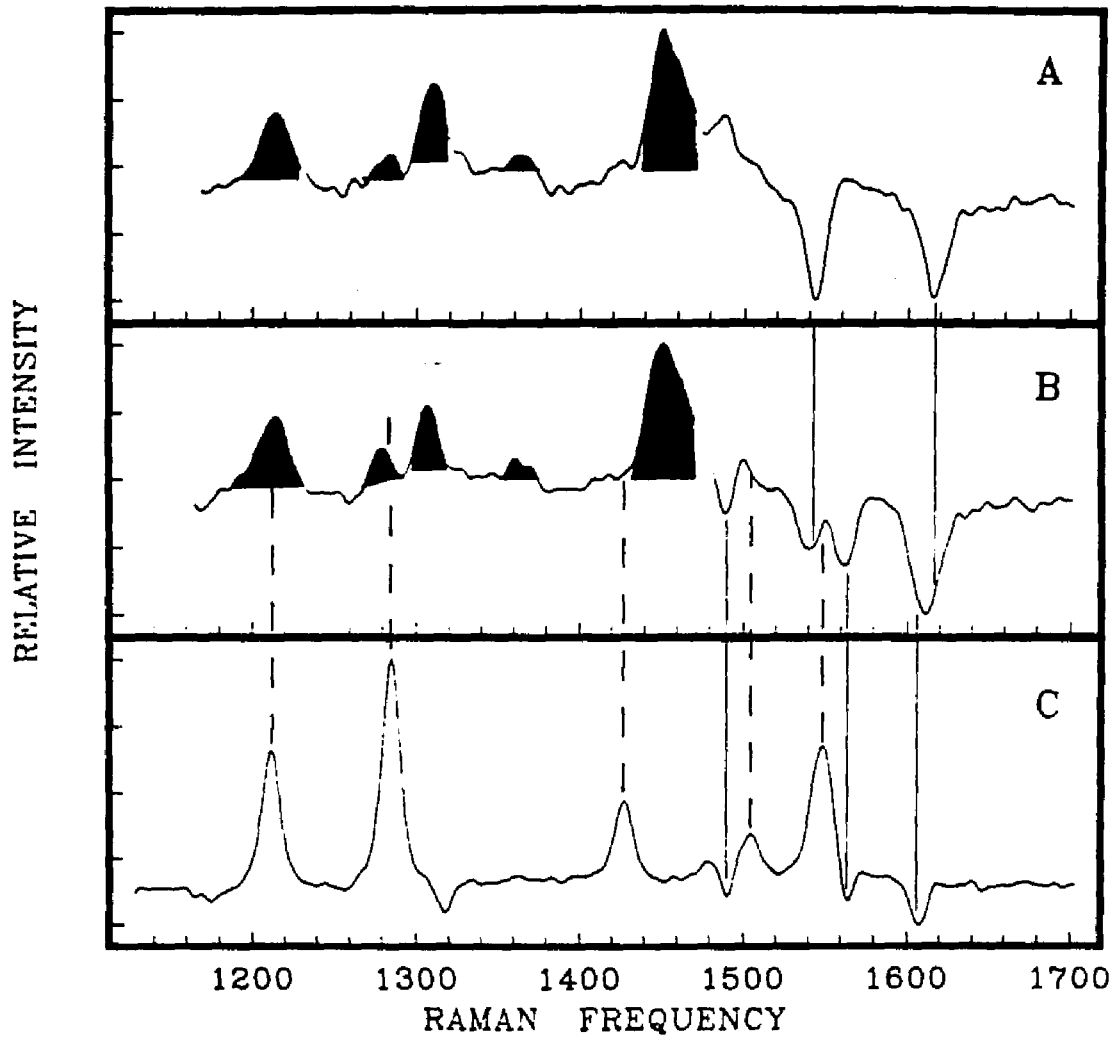

Figure 6: Pure two color picosecond Raman spectra. Pump is 532nm and probe wavelength is 354.7nm. Concentration is 2mM. Dashed lines are drawn at some of the frequencies of excited state carboxy-bpy bands. Asterisks also indicate excited state carboxy-bpy bands. Solid lines denote ground state bands. Time delay between pump and probe pulses is 0ps. Spectra were obtained in a flowing quartz cell.

a) $[Ru(carboxy\text{-}bpy)_3]^{2+}$.
b) $[Ru(carboxy\text{-}bpy)(bpy)_2]^{2+}$.
c) $[Ru(bpy)_3]^{2+}$.

CONCLSUIONS

The picosecond Raman spectra of mixed ligand complexes of bpy with bpym and carboxy-bpy indicate that the major fraction of the electrons in the excited MLCT state are localized on the lower energy ligand on a 30ps or faster time scale. The signal-to-noise characteristic of these data allow a limit of $\leq$ 1% and $\leq$3% to be placed on the population which remains on the higher energy bpy ligand in the bpym and carobxy-bpy complexes respectively. The energy gaps which separate the dissimilar ligands on the electron transfer reaction coordinate can be estimated from ground state electrochemistry. This is a result of the fact that the electrochemically reduced complex is thought to mimic excited state behavior with the added electron residing on the ligand(7). For the mixed ligand complexes discussed in this paper the energy gaps(8-9) are 3240 cm^{-1} and 3080 cm^{-1} between the higher energy ligand (bpy) and the lower energy ligand (bpym and carboxy-bpy) respectively. It has been suggested(10) that in mixed ligand complexes it might be possible to utilize the chemical energy stored in the higher energy ligand in the MLCT excited state. The present results indicate that electron transfer is largely complete on a 30ps or faster time scale for rather modest energy gaps. These results suggest that the chemical potential of the higher energy (less reducing) ligand in mixed ligand complexes cannot be effciently utilized in a chemical reaction.

REFERENCES

1. Y.C.Chung, N.Leventis, P.J.Wagner, and G.E.Leroi, Inorg. Chem., 24,1966, 1985
2. P.B.Bradley, B.A.Hornberger, R.F.Dallinger, and W.H.Woodfuff, J. Am. Chem. Soc.,103,7441,1981
3. C.M.Carlin and M.K.DeArmond, Chem. Phys. Lett., 89,297,1982
4. L.K.Orman and J.B.Hopkins, Chem. Phys. Lett., 149, 375, 1988
5. L.K.Orman, Y.J.Chang, D.R.Anderson, T.Yabe, X.Xu, S.Yu, and J.B.Hopkins, J. Chem. Phys., 90, 1469, 1989
6. Y.J.Chang, X.Xu, T.Yabe, S.Yu, D.R.Anderson, L.K.Orman, and J.B.Hopkins, J. Phys. Chem., 94,729, 1990
7. A.G.Motten, K.Hanck, and M.K.DeArmond, Chem. Phys. Lett., 79, 541, 1981
8. D.P.Rillema, G.Allen, T.J.Meyer, and D.Conrad, Inorg. Chem., 22,1617,1983
9. C.M.Elliot and E.J.Hershenhart, J. Am. Chem. Soc., 104, 7519,1982
10. C.V.Kumar, J.K.Barton, I.R.Gould, N.J.Turro, and J.V.Houten, Inorg. Chem. , 27, 648, 1988

CHAPTER III.

INTRODUCTION

This chapter is based on our paper that is being submitted to Chemical Physics Letter. The contents are specially modified to the dissertation.

This chapter discusses the use of picosecond Raman spectroscopy to measure ILET in mixed ligand complexes of 2,2'-bipyridine (bpy) and 4,4'-diphenyl -2,2'-bipyridine (Ph_2-bpy). The nanosecond resonance Raman and luminescence data show that the excited state is localized on the Ph_2-bpy ligand in mixed ligand complexes.(1-2)

SPECTROSCOPIC ANALYSIS OF PHENYL-BPY

In pure two-color time-resolved Raman spectra the excited state bands appear as positive-going peaks while the ground state peaks show as negative-going peaks.(3) The existence of negative-going peaks is interpreted as the result of two factors; depletion of ground state population and a change of optical density of the solvent.

Figure 1A shows the raw two-color Raman spectrum of $Ru(Ph_2\text{-}bpy)_3$ which contains both ground and excited state MLCT bands. Existense of both bands is due to the fact that both states are in resonance with 354.7nm probe pulses. Figure 1B is the one-color background spectrum excited by low power probe pulses; this spectrum contains mostly ground state bands. Figure 1C is the subtracted specrum Figure 1A - Figure 1B. In Figure 1C, apparent excited state bands are marked with asterisks. The peak positions are denoted by the dashed line which illustrates the corresponding peak assignment in the raw two color spectrum. The $1288cm^{-1}$ excited state band is extended to the shoulders of the $1280cm^{-1}$ band in Figure 1A. In this spectrum the $1280cm^{-1}$ band is a ground state band and the $1288cm^{-1}$ band is the excited state band. As a result of the $1280cm^{-1}$ band depletion the left shoulder of the $1288cm^{-1}$ band is cut off in Figure 1C. In other words, skewed lineshape is due to depletion of a band on the left side. Solid lines connect ground state peaks from Figure 1C depletion. Ground state peaks at $1610cm^{-1}$ and $1538cm^{-1}$ do not appear to be line up with Figure 1A peaks. The reason for this is that these peaks may also

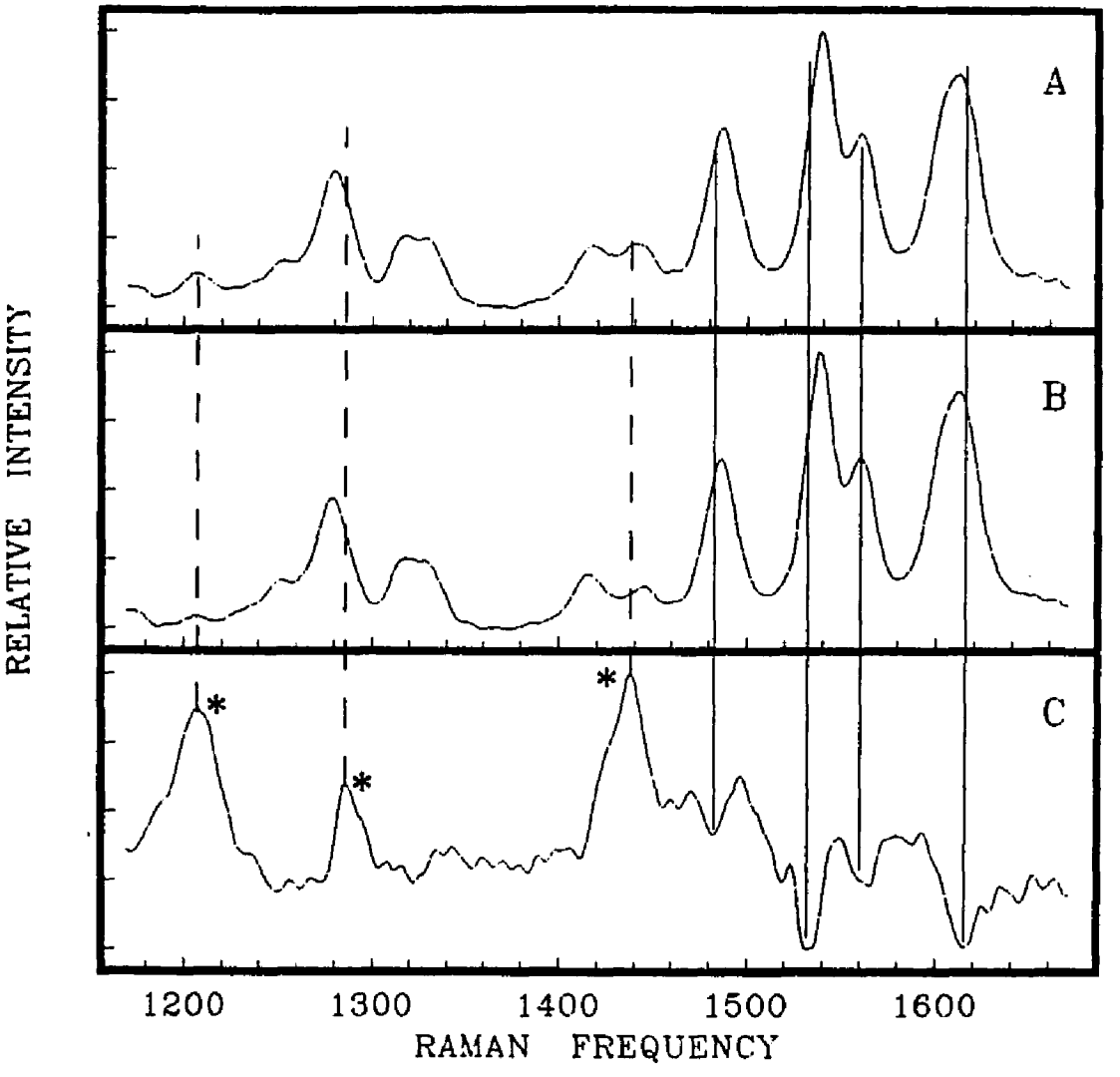

Figure 1. Two color transient Raman spectra of $Ru(Ph_2\text{-}bpy)_3^{2+}$. (A) Total raw two color spectrum obtained at 354.7nm with 532nm excitation. (B) One color background spectrum obtained at 354.7nm. (C) Pure two color sprectrum obtained by subtracting spectrum (B) from (A).

consist of overlapping ground state and excited state bands. Consequently it is very hard to tell whether peaks are ground state or excited state by the one color resonance Raman technique.(4)

The two-color Raman spectra for the series of mixed ligand $Ru(bpy)_{3-n}(Ph_2\text{-}bpy)_n$ are shown in Figure 2 where n=0,1,2,3 in spectra A through D respectively. Mixed ligand complex spectra can be interpreted as the combination of ground and excited state bands from the $Ru(Ph_2\text{-}bpy)_3$ ligand and ground state bands alone from the $Ru(bpy)_3$ ligand. In Figure 2A, all excited state $Ru(bpy)_3$ bands do not line up with any excited state bands in Figure 2B and 2C indicating that there are no excited state bands from this ligand. Excited state bands only line up with excited state $Ru(Ph_2\text{-}bpy)_3$ band from Figure 2D. On the other hand there is depletion from $Ru(bpy)_3$ shown in Figure 2B and 2C. Also, there is depletion from $Ru(Ph_2\text{-}bpy)_3$ found in mixed ligand complexes. Considering the signal-to-noise ratio in the mixed ligand background spectrum, the bpy ligand excited state band, if present at all, is less than 7%. This number comes from a comparison between the intensities of bpy bands in the mixed ligand spectra to those in $Ru(bpy)_3^{2+}$. In the latter the ratio is about 0.3 for the $1316cm^{-1}$ and $1425cm^{-1}$ ground and excited state band. In the mixed ligand complex the excited state band is not observed. A limiting ratio of 0.02 can be established for the ground to excited state bpy band ratio. Therefore the limiting value of bpy excited state band in the mixed ligand complex is 7%. It might be argued that Raman scattering from the higher energy ligand is not observed because the

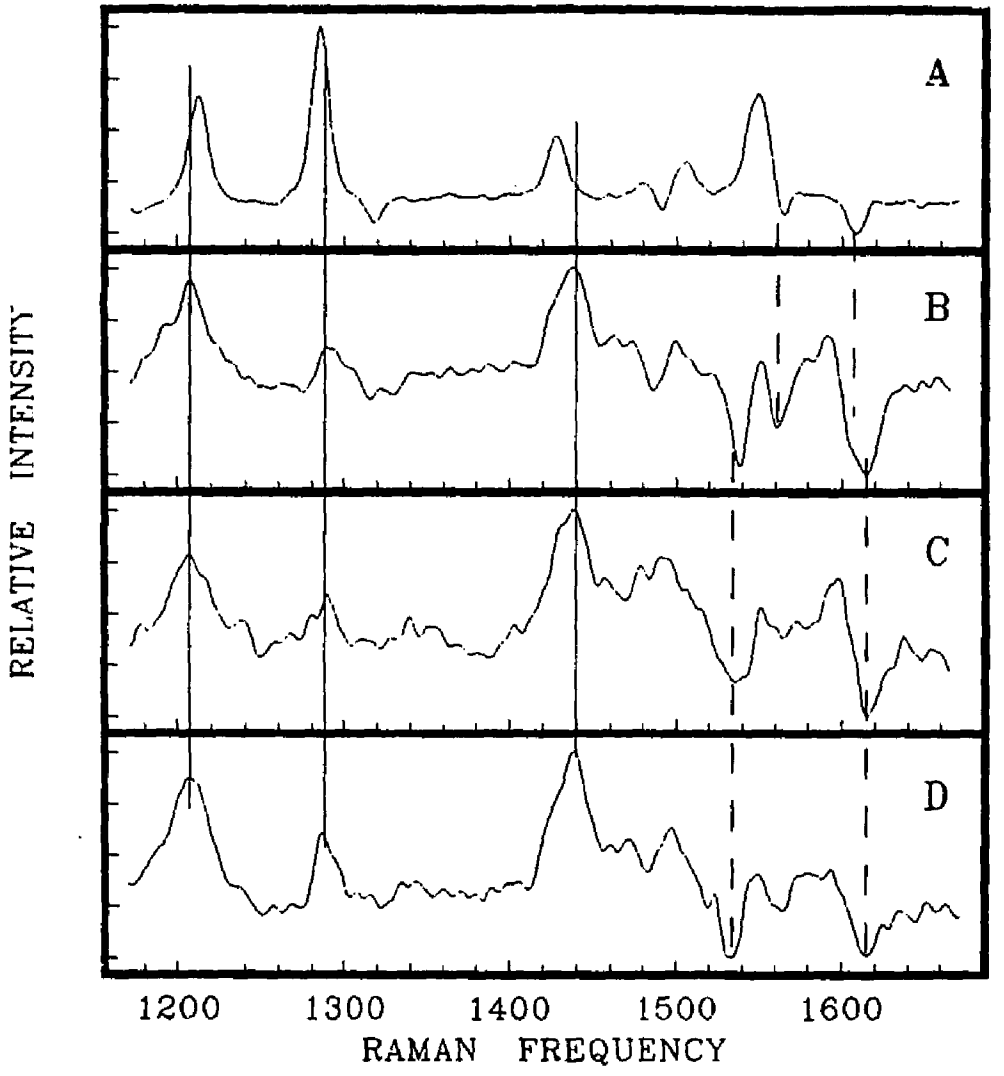

Figure 2. Comparison of pure two color spectra. (A) $Ru(bpy)_3^{2+}$ (B) $Ru(bpy)_2(Ph_2\text{-}bpy)^{2+}$ (C) $Ru(bpy)(Ph_2\text{-}bpy)_2^{2+}$ (D) $Ru(Ph_2\text{-}bpy)_3^{2+}$.

resonance Raman enhancement for this ligand is reduced in the mixed ligand complexes. This possibility cannot be entirely ruled out. However, there is the evidence which suggests that this not the case. Consider the lower energy ligand which is thought to be the final acceptor of MLCT excitation. In Ph_2-bpy mixed ligand complexes, there is a dramatic change in the ratio of the intensities of the ground to excited state Raman bands. In particular, if we compare the Ph_2-bpy ground and excited state bands at 1253cm^{-1} and 1207cm^{-1} respectively in Figure 2, the change is obvious. As more bpy is substituted into the complex (Figure 3B and 3C), the ground state Ph_2-bpy band decreases in intensity by a factor of three compared to the excited state Ph_2-bpy band. In other words, as the concentration of Ph_2-bpy in the complex is reduced, the ground state band decreases in intensity much faster than the excited state Ph_2-bpy band. This result is interpreted to indicate that there is another route to excitation of the Ph_2-bpy ligand, namely through the bpy ligand. If this is true the intensity of excited state Ph_2-bpy will remain invariant to ligand substitution since in every case $Ru(Ph_2\text{-bpy})_3$, $Ru(Ph_2\text{-bpy})_2(bpy)$, and $Ru(Ph_2\text{-bpy})(bpy)_2$ one Ph_2-bpy excited state is produced regardless of which ligand is initially excited. The transient Raman results therefore suggest that fast ILET is occuring and is largely complete during the laser pulsewidth. This conclusion suggests a rate significantly faster than $3x10^{10}$ s^{-1}.

The nanosecond laser excitation resonance Raman spectra for $Ru(Ph_2\text{-bpy})_2(bpy)$ and $Ru(Ph_2\text{-bpy})(bpy)_2$ by Turro et al. also

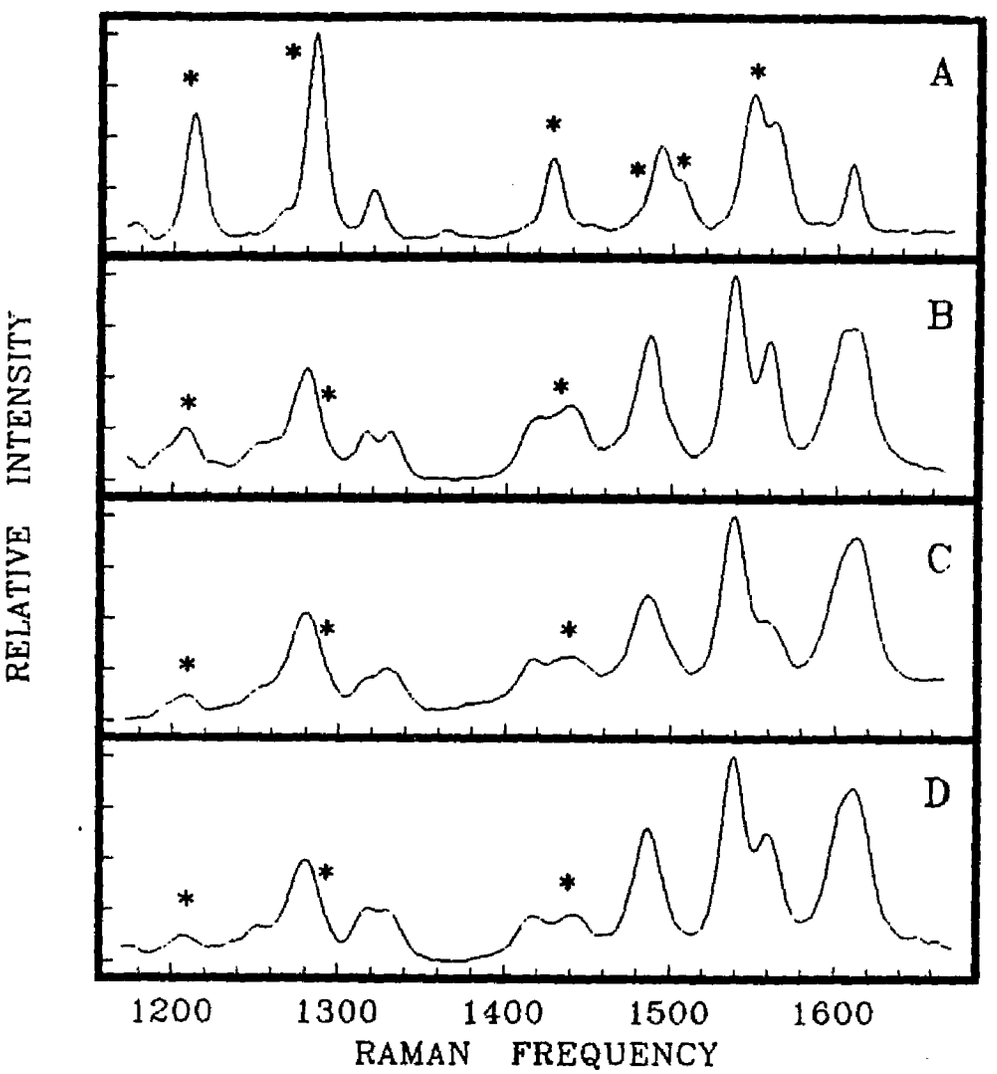

Figure 3. Comparison of total raw two color spectra. (A) $Ru(bpy)_3^{2+}$ (B) $Ru(bpy)_2(Ph_2\text{-}bpy)^{2+}$ (C) $Ru(bpy)(Ph_2\text{-}bpy)_2^{2+}$ (D) $Ru(Ph_2\text{-}bpy)_3^{2+}$.

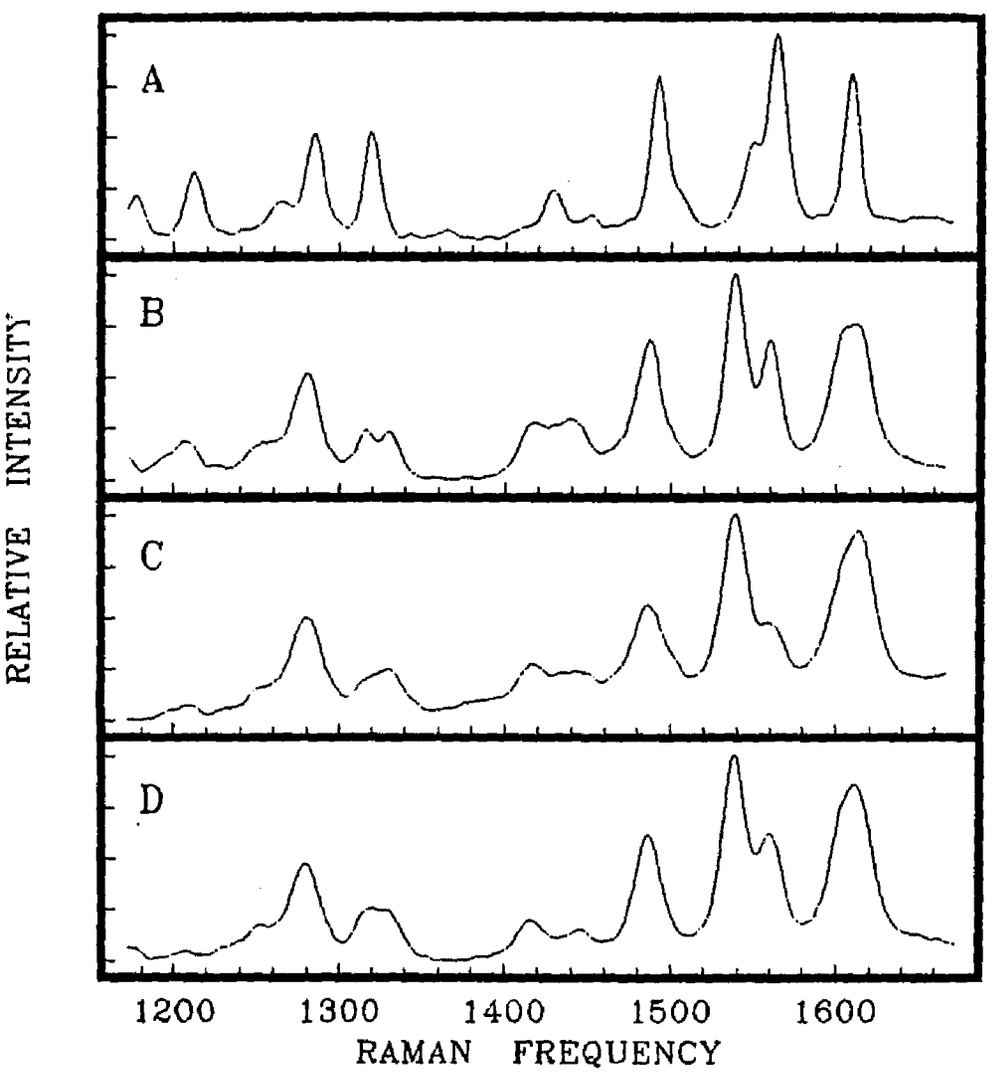

Figure 4. Comparison of one color background spectra. (A) $Ru(bpy)_3^{2+}$ (B) $Ru(bpy)_2(Ph_2\text{-}bpy)^{2+}$ (C) $Ru(bpy)(Ph_2\text{-}bpy)_2^{2+}$ (D) $Ru(Ph_2\text{-}bpy)_3^{2+}$.

concluded that the excited states were localized in the Ph_2-bpy ligand in these complexes.(1) Their conclusion was based on incorrect assignments. They claimed that the 1251cm^{-1} bpy excited state band was dramatically reduced in its intensity as replacing bpy ligand by Ph_2-bpy ligand and 1605cm^{-1} Ph_2-bpy excited state band was dramatically increased by substituting bpy ligand by Ph_2-bpy ligand. The problem of their interpretation was that they assumed all the Raman bands in their spectra were excited state bands, or they could not distinguish the ground state bands from excited state bands. Contrary to their results, the result in Figure 2 clearly shows that most of the bands observed in the mixed ligand spectra are ground state. Therefore it is not appropriate to use the 1605cm^{-1} vibrational band for the localization argument. The big advantage of our two-color technique is that it is possible to separate ground and excited state bands. This result is illustrated in Figure 2 and clearly shows that excited state electrons are localized on a favored ligand - the lower energy lying ligand within the 30ps laser pulse width time scale.

CONCLUSIONS

The picosecond Raman spectra of mixed ligand complexes of bpy with Ph_2-bpy indicate that the major fraction of the electrons in the excited MLCT state are localized on the lower energy ligand on a 30 ps or faster time scale. The signal-to-noise characteristics of these data allows a limit of < 7% of the population to remain in the higher energy bpy ligand. The energy gaps which separate the dissimilar ligands on the electron transfer reaction coordinate can be estimated from electrochemistry. For the mixed ligand complexes discussed in this paper the energy gap is $1300cm^{-1}$ between the higher energy ligand bpy and the lower energy ligand Ph_2-bpy.(5) The present result and previous results in similar complexes indicate that electron transfer is largely complete on a 30 ps or faster time scale when energy gaps are larger than $1300cm^{-1}$ up to $3240cm^{-1}$.(6)

REFERENCES

1. C,V,Kumar, J.K.Barton, I.R.Gould, N.J.Turro, and J. Van Houten, Inorg. Chem., 27,648,1988
2. W.E.Jones, Jr., R.A.Smith, M.T.Abramo, M.D.Williams, and J. Van Houten, Inorg. Chem.,28, 2281,1989
3. L.K.Orman and J.B.Hopkins, Chem. Phys. Lett., 149, 375, 1988
4. Y.J.Chang, X.Xu, T.Yabe, S.Yu, D.R.Anderson, L.K.Orman, and J.B.Hopkins, J.Phys.Chem., 94,729,1990
5. Y.Ohsawa, K.W.Hanck, and M.K.DeArmond, J. Electroanal. Chem.,175,229,1984
6. L.K.Orman, Y.J.Chang, D.R.Anderson, T.Yabe, X.Xu, S.Yu, and J.B.Hopkins, J. Chem. Phys., 90, 1469, 1989

VITA

Takahiro Yabe was born in Japan in 1957. He received his B.S. degree in 1984 and M.E. degree in 1986 at Keio University.

He has been studying physical chemistry under Professor J.B. Hopkins since 1986 at Louisiana State University.

DOCTORAL EXAMINATION AND DISSERTATION REPORT

Candidate: Takahiro Yabe

Major Field: Chemistry

Title of Dissertation: Picosecond Resonance Raman Studies of Solvent Effects on Electron Transfer in Ruthenium-polypyridine Complexes.

Approved:

John B Hopkins
Major Professor and Chairman

F. Glenn Kemby
Dean of the Graduate School

EXAMINING COMMITTEE:

George B. Stanley

Richard W Hanson

Jeffrey V. Nel

Mary Quilty Burkley

Neil R. Kestner

Date of Examination:

1/MAY/90